Photocopy and Use Authorization

In presenting this dissertation in partial fulfillment of the requirements for an advanced degree at Idaho State University, I agree that the Library shall make it freely available for inspection. I further state that permission for extensive copying of my thesis for scholarly purposes may be granted by the Dean of the Graduate School, Dean of my academic division, or by the University Librarian. It is understood that any copying or publication of this thesis for financial gain shall not be allowed without my written permission.

Signature _____

Date _____

Oncostatin M Receptor as a Viable Target for Radioimmune Therapy in the Treatment of Synovial Sarcoma

by

Sarah McCollum

A dissertation

submitted in partial fulfillment

of the requirements for the degree of

Doctor of Philosophy in the Department of Biomedical and Pharmaceutical Sciences

Idaho State University

August 2022

Committee Approval

To the Graduate Faculty:

The members of the committee appointed to examine the thesis of Sarah McCollum find it satisfactory and recommend that it be accepted.

_____

Major Advisor

_____

Committee Member

_____

Committee Member

_____

Committee Member

_____

Graduate Faculty Representative

Animal Welfare Approval

Murine experiments were conducted with the approval of the Idaho State University institutional animal care committee, protocol 775, and use committee in accordance with legal and ethical standards.

TABLE OF CONTENTS

List of Figures

List of Tables

List of abbreviations

ADC – Antibody Drug Conjugate

AFC – Antibody- Fluorescence Conjugate

BRD9 - bromodomain-containing protein 9

cBAF – Canonical BAF

DAR – Drug-Antibody ratio

EPO – Erythropoietin

GFP – Green fluorescence protein

GTEx – Genotype-Tissue Expression

HDAC - Histone Deacetylase

IFN – interferon

IL-6 - Interleukin-

IL-6 – Interleukin-6

JAK – Janus Kinase

LIFR – Leukemia Inhibitory Factor Receptor

MB – Megabase

NRTK – Non-receptor Tyrosine Kinase

OSMR – Oncostatin M Receptor

PET – Positron Emission Tomography

PRC2- Polycomb Repressive Complex 2

PRL – prolactin

RIT – Radioimmune Therapy

SCID – Severe Combined Immune Deficiency

SPECT - Single Photon Emission Computed Tomography

SS – Synovial Sarcoma

STAT – Signal Transducer and Activator of Transcription

TCGA – The Cancer Genome Atlas

TMB – Tumor Mutational Burden

TPO – Thrombopoietin

TYK2 – Tyrosine Kinase 2

γc - Common γ chain

Abstract

Synovial sarcoma is a soft tissue malignancy of the muscle that primarily affects adolescents and young adults. Due to its low incidence, little advancement has been made in the treatment of this cancer. With an overall survival rate of roughly 40%, the need for new treatments for synovial sarcoma is evident. Further complicating the development of new therapies for this disease is its low mutational burden. With a median of 1.7 mutations/Mb, there are few phenotypical differences between tumor tissue and normal tissue which can be targeted. However, I have identified the cell surface receptor Oncostatin M Receptor (OSMR) as being overexpressed in synovial sarcoma tissue with low expression in non-malignant tissues, making it an ideal target for therapy. Due to the potential for off-target effects and resistance development with small molecule inhibitors, I elected to develop an anti-OSMR radioimmune therapy (RIT). Here, I describe the investigation of OSMR in SS as a viable therapeutic target, and the synthesis and characterization of a novel anti-OSMR RIT for use in the treatment of synovial sarcoma. I also show that this novel therapeutic agent has potential as an imaging tool, making it a potential theranostic drug in a cancer which currently has no FDA approved targeted therapies.

Key words: Cancer, Sarcoma, Synovial Sarcoma, Targeted Therapy, Immune Therapy, Radiation Therapy, Radioimmune Therapy, Oncostatin M Receptor, Translocation Mutation, Fusion Protein, Oncoprotein, Metastasis, Mutational Burden, SS18-SSX, t(X;18)

1. Background

1.1 History of the Treatment of Synovial Sarcoma

Synovial sarcoma is a pediatric muscle cancer which primarily affects adolescents and young adults. With 800 new cases a year in the US (1), it is a less prevalent malignancy resulting in few advancements in the treatment of this disease. While soft tissue sarcomas represent less than 1% of all cancers (2), and synovial sarcoma (SS) represents 5-10% of all soft tissue sarcomas (3), those affected by this disease have few options for treatment.

In 1959, Crocker and Stout published the first comprehensive study on synovial sarcoma in children (4). Due to the rarity of SS, this study examined 43 reports from multiple institutions over a long period of time. They noted that SS most often occurred in the extremities and that when metastasis occurred, it was most likely to be in the lungs. Prior to this study, the standard treatment for SS had been amputation, however Crocker and Stout concluded that a wide local excision was just as effective.

This remained the standard of care for synovial sarcoma until 1993 when Landenstein et al. published a study of the results of the CWS-81 study performed in Germany between 1981 and 1985 (5). This study included 31 children diagnosed with SS during the time of the study, which received combination chemotherapy with radiation therapy after a wide local excision. Landenstein et al. concluded that irradiation of the surgery site and adjuvant chemotherapy served to increase the rate of event-free survival of patients and recommended this treatment as the standard of care for SS patients.

Unfortunately, little advancements have been made in the field of SS treatment, and the standard of care set by Landenstein et al. remains today despite the passing of three decades (Figure 1.1). The advancements made in other fields of cancer research have shown us what

progress there is to be made in this field. Targeted therapy created to target certain proteins expressed in cancer cells unique to the disease has been extremely successful in directing therapy to the diseased cells, which both improves its effectiveness and reduces the potential for off target effects. And 2018 Nobel prize winners James P Allison and Tasuku Honjo have been recognized for their major contribution of immune checkpoint blockade therapy, which has revolutionized the treatment of cancer directing us to look more at how the immune system can be utilized to treat cancer. Unfortunately, SS patients have demonstrated little benefit from any of these discoveries and are limited to traditional treatments.

1.2 The t(X:18) Translocation Mutation and its Impact on Sarcomagenesis

1.2.1 The Genetics of Synovial Sarcoma and the SS18-SSX Fusion Protein

Synovial sarcoma is part of a group of cancers which are driven by fusion proteins. Fusion proteins, sometimes referred to as fusion oncoproteins, are a form of mutated proteins which are composed of the parts of two fused proteins. These oncoproteins form as a result of chromosomal translocation, where a double strand break occurs in the DNA and is repaired incorrectly, stitching one part of a chromosome with that of another. This chromosomal translocation can result in the transcription and translation of fusion proteins.

In the case of SS, the chromosomal translocation t(X;18) is exhibited in 90% of synovial sarcomas and is sufficient to drive sarcomagenesis (6). This translocation, which occurs between the X chromosome and chromosome 18, results in SS18-SSX fusion proteins (7). The wild-type SS18 protein is known to be a subunit of the BAF complexes, also termed the SWI/SNF complexes (8)(9). These chromatin remodeling complexes, first discovered in yeast (10), are

integral in controlling transcription, and therefore any mutations in the complex have potential to be amplified through altered gene expression throughout the genome.

In 2013, Kadoch and Crabtree proposed a mechanism for how the SS18-SSX fusion protein retargets the BAF complex, suggesting that the presence of the SS18-SSX fusion protein in SS competes with the wild type SS18 protein for the binding site on the BAF complex. When SS18-SSX is bound, it displaces BAF47, a subunit of the BAF complex known to have tumor suppressing characteristics (8). This displacement was proposed to retarget the BAF complex to Polycomb Repressive Complex 2 (PRC2) repressed domains in the genome and activates them (Figure 1.2)(12). McBride et al. further elucidated the mechanism by which the altered BAF complex causes these epigenetic changes and sought to uncouple the effects of BAF47 loss from the effects of fusion protein inclusion into the complex. They determined that loss of BAF47 is a loss of function mutation causing BAF complex targeted genes to no longer be activated. However, the inclusion of the fusion protein creates a gain of function mutation, retargeting the complex to activate genes that it would not before. McBride et al. conclude that synovial sarcoma is unique in this way, having both a gain and loss of function within the complex (12). These theories were largely accepted by the scientific community and believed to be the mechanism by which the fusion protein drives SS.

However, in 2021, Li et al. published data which directly opposed this theory, showing that BAF47 is not displaced by SS18-SSX (11). Instead, they show that the inclusion of the SS18-SSX fusion protein into the canonical BAF complex (cBAF) resulted in degradation of cBAF, rather than retargeting. They instead propose that the decrease in cBAF levels is what results in the altered gene expression characteristic of SS (Figure 1.3).

Despite the consequences of the SS18-SSX fusion protein formation being well understood, this mutation does not result in a protein which could be considered a druggable target. Furthermore, interfering with epigenetic mechanisms with far reaching consequences could cause more harm than good. This, along with the characteristically low Tumor Mutation Burden (TMB) of synovial sarcoma, has made the development of targeted therapies, especially immunotherapies, for synovial sarcoma challenging (13).

The TMB is a measurement which reflects the frequency of mutations within a tumor's genome. This number is an important factor used to predict the response of a malignancy to immunotherapy. Cancers use many mechanisms to avoid the hosts immune system, however when an accumulation of mutations is present, the likelihood of one of those mutations resulting in a cell surface protein which could be recognized as foreign by the immune system increases. For this reason, cancers with a high TMB are considered good candidates for immune therapy treatment, while those with low TMB's likely will not respond. A TMB of at least 10 mutations per megabase (MB) is considered a high-TMB and indicates a high likelihood that the tumor will respond well to immune therapy (14). Unfortunately, synovial sarcomas are among the cancers with the lowest TMB, averaging 1.7 mutations/MB (13). Because of this, SS has historically responded poorly to immune therapy, and this treatment is not clinically approved for SS.

The combination of a low TMB, as well as the few mutations present being non-druggable targets, has served to make the development of new and advanced therapies for SS extremely challenging. However, there are multiple ongoing pre-clinical studies which are targeting the downstream effects of the SS18-SSX fusion protein which aid malignancies in proliferation and metastasis (15)(16)(17). While the chromosomal translocation mutation cannot be targeted directly, there remain other options for the treatment of SS which need to be explored.

1.2.2 The Effects of the SS18-SSX Fusion Protein and the Epigenetics of Synovial Sarcoma

While most targeted therapies focus on unique protein expression or pathway activation as a result of genetic mutations, there is also the possibility of using targeted therapies that target the epigenetic changes that can occur in cancer. Because the SS18-SSX fusion protein is a member of the SWI/SNF complex and results in widespread changes to the epigenetic profile of SS cells, this strategy warrants significant attention. Not only can epigenetic strategies lead us to more options for therapy, but they are also useful in the diagnosis of SS and can serve as prognostic markers predicting patient outcomes. This information can be integral in selecting the most beneficial treatment plan for a patient.

Because many sarcomas arise in overlapping anatomical locations, it is difficult to differentiate sarcomas for an accurate diagnosis based on location. However, an accurate diagnosis is vital for effective treatment and ensuring the patient has the best possible outcome. In an effort to improve the ability to more accurately diagnose and differentiate between synovial sarcoma, Ewing sarcoma, and OS, Wu et al. established a methylation profile unique to each sarcoma which can be referenced to aid in diagnosis. They discovered that each sarcoma had a distinct gene enrichment pattern, and they were able to correctly diagnose 36 clinical samples of sarcomas based only on their methylation profiles. While Wu et al. only documented enrichment patterns for these three sarcomas, they hypothesize that many more sarcomas have unique methylation patterns that could be used to aid in diagnosis and differentiation from other sarcoma types (18).

Epigenetic markers have also been shown to be a useful tool for prognosis. The enzymatically active subunit of PRC2, EZH2, has been implicated in cancer development and

metastasis (19). Its role is to methylate lysine 27 of histone 3 (H3K27) and thus repress gene expression. In an analysis of 55 clinical cases of synovial sarcoma, Changchien et al. concluded that cases with high EZH2 expression were more likely to have larger tumor size, along with metastasis and an overall poor prognosis (20). Changchien et al. also suggested that EZH2 levels could be useful in identifying subtypes of synovial sarcoma, with the poorly differentiated subtype having higher levels of EZH2 than monophasic or biphasic subtypes. A meta-analysis performed by Jiang et al. not only found that EZH2 plays an important role in many types of cancer, but also helped to elucidate the mechanism by which this subunit of PRC2 propagates malignancies. They suggest that PRC2 has a role in inhibiting cell cycle suppressor proteins, and aberrant or overactive EZH2 can cause uncontrolled cell growth in this manner. Jiang et al. also present evidence that EZH2 can facilitate epithelial-mesenchymal transition (EMT), thus promoting cancer metastasis (21).

In addition to its potential as a prognostic marker, EZH2 has potential as a therapeutic target. In January of 2020, the FDA approved the first EZH2 small molecule inhibitor, tazemetostat, for the treatment of epithelioid sarcoma (22). Many other clinical trials are ongoing, evaluating the efficacy of tazemetostat in many other malignancies including synovial sarcoma. A study performed by Kawano et al. tested tazemetostat in vivo with synovial sarcoma xenografted mice and found that the drug was able to suppress tumor growth (23). Further evidence of the effect of EZH2 inhibition in synovial sarcoma is presented by Shen et al. Using shRNA and siRNA, they were able to suppress cell growth and migration in vitro. Furthermore, they showed the same effect as a result of using an EZH2 inhibitor which has yet to be FDA approved (24). While there may be no FDA approved EZH2 inhibitors for synovial sarcoma

currently, pre-clinical experiments would suggest that the results in epithelioid sarcoma will be translated into synovial sarcoma as well.

Similar to many other sarcomas, HDAC (Histone Deacetylase) inhibition is a therapeutic strategy being investigated in synovial sarcoma. Having a single translocation mutation which largely drives synovial sarcoma leaves the malignancy vulnerable to epigenetic silencing. Pre-clinical trials have shown that HDAC inhibitors are effective at inducing apoptosis in synovial sarcoma cells by decreasing the expression of the SS18-SSX fusion protein. Ito et al. first discovered in their study that the HDAC inhibitor depsipeptide (Romidepsin) was highly effective at suppressing tumor growth in synovial sarcoma cell lines. They also found that Romidepsin was able to inhibit tumor growth and reduce rates of metastasis with in vivo mouse models (25). Since that time, clinical trials investigating the effects of depsipeptide on multiple sarcomas have begun (26). To investigate the mechanism by which HDAC inhibitors are able to induce apoptosis in synovial sarcoma, Laporte et al. analyzed RNA-seq gene expression data and determined that treatment with Quisinostat induced expression changes in pathways related to apoptosis and antigen presentation as well as other pathways important to tumorigenesis. They showed that HDAC inhibition was able to activate CDKN2A, a known tumor suppressor gene, allowing proapoptotic pathways to be activated. Furthermore, they show that gene expression related to antigen presentation was increased by treatment with an HDAC inhibitor and suggest that this may indicate potential for increased antigenicity of synovial sarcoma allowing for treatment with immunotherapy (27).

The histone demethylase, KDM2B, has been identified as another potential target of treatment in synovial sarcoma. This subunit of Polycomb Repressive Complex 1 (PRC1) is responsible for histone demethylation and has been implicated in multiple types of malignancies.

Banito et al. discovered that, not only was KDM2B expressed at high levels in synovial sarcoma cells, but that KDM2B knockdown was able to inhibit cell growth and induce cell differentiation almost as well as SS18-SSX knock-down (28). While Banito et al. was able to inhibit KDM2B through use of shRNAs, there are currently no small molecule inhibitors targeting this enzyme.

1.3 Current Clinical trials and Pre-Clinical Strategies in the Treatment of Synovial Sarcoma

The combination of synovial sarcoma being a rare malignancy along with having an extremely low number of mutations which drive the cancer has led to stagnation in the field of novel SS treatments. However, there are a number of strategies currently being researched in this field, as well as multiple clinical trials currently underway.

A phase III trial is exploring the potential of the drug Anlotinib in the treatment of SS (29). Anlotinib is an orally administered Receptor Tyrosine Kinase (RTK) inhibitor which inhibits PDGFR, FGFR and VEGFR (30). While the role of Receptor Tyrosine Kinases is well known in cancer, and inhibition of this class of receptors has proven effective in other cancer types, attempts to treat sarcomas with this class of pharmaceuticals has proven ineffective in the past (31)(32). One hypothesis for why this may be, is that sarcomas use many RTK's to support proliferation and growth, causing them to be drug resistant to a single RTK inhibitor. However, by using an RTK inhibitor which can inhibit RTK's across three axes, the possibility of the malignancy becoming resistant to treatment is reduced. Preliminary reports of the study results show that patients responded well to treatment initially, however only 26% of patients remained progression free after a year (33). Anlotinib shows promise as a potential therapy for SS patients, but also highlights the difficulty of overcoming drug resistance in cancer treatment. While, in the case of RTK's, there may be pharmaceutical agents which can target multiple pathways at once,

this is rarely the case, and preventing malignancies from developing resistance and growing through other means is one of the greatest challenges to the field.

Patwardhan et al. have found that a drug similar to Anlotinib, Nintedanib, is showing potential in the treatment of SS (34). Nintedanib is an orally administered tri-RTK inhibitor which is FDA approved for the treatment of idiopathic pulmonary fibrosis (IPF) (35) and has also shown efficacy in the treatment of non-small-cell lung cancer when given in combination with docetaxel (36). Patwardhan et al. propose the use of Nintedanib which inhibits the same three RTK receptors as Anlotinib for use in SS treatment. In their study, they show that SS cell lines express the target receptors of this drug, and that the drug effectively suppresses tumor growth. Nintedanib shows promise as a potential therapy for SS patients but is likely to share the same struggles as Anlotinib with development of drug resistance.

Another attempt to treat SS through RTK inhibition is the CAMPFIRE clinical trial, which is exploring the treatment of SS in both children and adults with Ramucirumab in combination with gemcitabine and docetaxel (37). Ramucirumab is a monoclonal antibody which blocks the VEGFR2 receptor and prevents signaling. While this study is still underway and no results are available as of yet, there are some preclinical studies of Ramucirumab in the treatment of SS which have been published. Lowery et al. studied the effects of Ramucirumab in multiple pediatric solid tumor models and found that Ramucirumab alone was not able to suppress tumor growth, but showed benefit when administered in combination with a cytotoxic chemotherapy (38). While the FDA approval of Ramucirumab would greatly benefit many patients, this treatment strategy does not serve to reduce the need for cytotoxic chemotherapy treatment and, in fact, highlights the fact that the field of SS treatment is dependent on them. Cytotoxic chemotherapies such as vincristine, gemcitabine and cisplatin are known to be poorly

tolerated in the clinic, causing hair loss, nausea, vomiting, diarrhea, weight loss and failure to thrive. The complications these drugs can cause can lead to a disruption or premature halt to therapy, resulting in poor outcomes for patients. Furthermore, cancer is often able to become resistant to these therapies and monotherapy is often insufficient to achieve complete remission (39). Another undesirable effect these therapies have is that of decreasing the patient's quality of life. In a disease such as SS, where up to 20% of patients present with metastasis at their diagnosis and are considered incurable (40), a large consideration of treatment should be the effect on a patients quality of life. Because they do not have what is currently considered a curable disease, the aim becomes to improve and lengthen their life, rather to irradicate their disease. Cytotoxic chemotherapies are not the tool of choice for this goal, highlighting the need for the development of targeted therapy for this disease.

The SPEARHEAD-1 phase II trial (41) is taking another approach for the treatment of synovial sarcoma. Using CAR-T therapy, an innovative technique which has rapidly gained attention in the field of oncology, the group hopes to treat SS through genetically altered T-cells which are obtained from the patient and engineered to express a receptor which binds to the testis antigen MAGE-A4, which is often overexpressed in cancers. Research has shown MAGE-A4 to be overexpressed in up to 82% of synovial sarcomas (42), making it an ideal target for therapy. While this clinical trial is ongoing and no articles have been published, the results were presented at the American Society of Clinical Oncology's (ASCO) 2021 annual meeting and showed promising results (43). They state that out of 25 SS patients, 2 achieved a complete response to therapy, 8 patients experienced a partial response, and 11 patients achieved lasting stable disease. These results are extremely promising and the addition of CAR-T therapy to the field of SS treatment would greatly improve our ability to treat this disease.

Yet another strategy for the treatment of SS currently in clinical trials is the use of the drug FHD-609 (44). FHD-609 is a bromodomain-containing protein 9 (BRD9) degrader and has high specificity for its target, inhibiting BRG1 and BRM (45). These proteins are essential components to the SWI/SNF complex, which is affected by the SS18-SSX fusion protein (46). By inhibiting this complex, the effects of the malfunctioning SWI/SNF complex can be mitigated and SS growth and progression slowed. This Phase I trial is in its early phases, and while there are no results to comment on at this time, this innovative treatment technique has promise in the treatment of SS. However, the SWI/SNF complex has many roles outside of those which lead to SS and the inhibition of this complex could prove to have high toxicities.

Table 1.1 Summary of Current Pharmaceutical Research in SS

Therapy	Target	Status
Tazemetostat	EZH2 Inhibitor	Trial Ongoing
EPZ005687	EZH2 Inhibitor	Pre-Clinical
Depsipeptide	HDAC Inhibitor	Trial Ongoing
Anlotinib	RTK Inhibitor	Trial Ongoing
Nintedanib	RTK Inhibitor	Preclinical
Ramucirumab	RTK Inhibitor	Trial Ongoing
CAR-T	MAGE-A4	Trial Ongoing
FHD-609	Bromodomain Inhibitor	Trial Ongoing

1.4 Receptor Tyrosine Kinases and Their Role in Cancer Development

As discussed in chapter 1.3, RTK's have been implicated in many cancers, and their inhibition has been a strategy for treatment of many malignancies, including SS (29)(34)(37).

Both RTK's and Jak proteins belong to the class of tyrosine kinases, however, whereas Jaks are Non-Receptor Tyrosine Kinases (NRTK's) and must be associated with a receptor to aid in signaling, RTK's are a receptor themselves and are able to function as kinases intrinsically and without the need for extra proteins such as Jaks. There are 58 known RTK's (47) which can be divided into 20 sub-families (48) and serve a wide range of functions in the body (Figure 1.4). While each subfamily has an essential function in the human body, each subfamily has been associated with at least one type of cancer (48) highlighting the potential for this family of receptors to contribute to development of malignancy.

A number of these subfamilies have been implicated in synovial sarcoma genesis, including the VEGFR (49), PDGFR (50) and FGFR (51) subfamilies, each of which act as a signaling pathway for different growth factors. There are multiple ways in which these pathways can become overactive, such as increased receptor concentration, constitutive receptor activation, or overexpression of ligands.

Vascular Endothelial Growth Factor Receptor (VEGFR) is responsible for development of vascular structures and angiogenesis (52). In many malignancies, VEGF becomes upregulated through the activation of other oncogenes, resulting in increased vascularization of the tumor tissues and allowing them to have increased access to blood flow (53). This can occur in SS as well, and increased VEGF expression has been associated with a poor prognosis in SS patients (49). Another RTK implicated in synovial sarcoma is Platelet Derived Growth Factor Receptor (PDGFR). This receptor and its corresponding growth factor are important for development, vasculature formation and wound healing, but when acting aberrantly can lead to increased tumorigenesis (54). Fibroblast Growth Factor Receptor (FGFR) is another RTK associated with synovial sarcoma progression, and has a wide range of roles ranging from development to

metabolism to homeostasis (55). Multiple attempts have been made to inhibit these RTK's in synovial sarcoma as described in chapter 1.3. While some of them have met with success, an overarching problem to the field of RTK inhibition has been the development of resistance. Because there are multiple subfamilies of RTK's, cancers can quickly adapt to the loss of function of one subfamily and continue to grow through the use of another. This has spurred efforts to develop treatments which can target multiple RTK receptor subfamilies at once, such as Anlotinib (33), so that this development of resistance may be avoided.

1.5 The Interleukin-6 Cytokine Receptor Family

1.5.1 The JAK/STAT Pathway and its Role in Cancer Development

The Janus Kinase (JAK) – signal transducer and activator of transcription (STAT) pathway is an important signaling cascade in cytokine and growth factor signaling and has been implicated in many cancers (56)(57)(58). When functioning normally, the pathway plays an integral role in processes such as immune cell signaling (59), cell proliferation, differentiation, apoptosis and migration (60). This pathway is responsible for relaying signals from cytokines, growth factors and interleukins outside of the cell to elicit a response inside the nucleus (58). Understanding this signaling cascade and how it can contribute to cancer progression has potential for leading to new therapeutic strategies in SS.

The JAK's were discovered after sequence comparisons were performed on tyrosine kinases, and were noted to have both a catalytic and regulatory domain (60). These kinases are associated with members of the gp130 receptor family and upon ligand binding to the receptor, a conformational change in the intracellular region of the receptor allows phosphorylation of inactive JAK's causing it to become active (61). Once active, the JAK's use their kinase activity

to create binding sites which recruit STAT's (58). The JAK's are in the non-receptor tyrosine kinase (NRTK) family and are fairly conserved across species. Humans contain four members of this family, Jak1, Jak2, Jak3 and Tyrosine Kinase 2 (Tyk2) (62). While Jak1, Jak2 and Tyk2 are found throughout the human body, Jak3 is far more specific and found most commonly in blood cells (63).

Jak1 is an integral member of the signaling pathway involved in interleukin signaling and is associated with a family of cytokine receptors characterized by the presence of the common γ chain (γc) subunit. Jak1 is also used in signaling of the IL-6 receptor family which includes receptors such as IL-6 (the families namesake), IL-11, LIF and OSMR (62). These receptors are characterized by the presence of the gp130 subunit. In addition to these receptors, Jak1 is the mechanism of signaling for all type II cytokine receptors, and Jak1 knockout mice have been shown to have perinatal mortality, immune deficiencies and neurological deficits (64).

Jak2 has been shown to be essential for proper hematopoiesis, and is the main Jak involved in erythropoietin (EPO) signaling (65). Because of this, Jak2 knockout mice have embryonic lethality due to a failure to respond to erythropoietin (66). Jak2, along with being an integral component of EPO signaling, is also associated with other Interferon-γ hormone-like cytokines, such as Growth Hormone (GH) (67), thrombopoietin (TPO) (68) and prolactin (PRL)(69). IL-3 is also dependent on Jak2 for signal transduction (70). Jak2 overlaps with Jak1 in function as it is involved in gp130 subunit signaling as well (71).

An important player for immune system development and signaling is Jak3. This NRTK's only role is to bind to γc subunit containing receptors (72), and while this role is also carried out by Jak1, Jak3 is unique in that it is localized to hematopoietic cells (63). Interestingly. Jak3 loss or reduction was first observed in humans rather than in mice knockout studies and has

been linked to the development of Severe Combined Immune Deficiency (SCID) (73)(74). Subsequent knock-out studies have shown that mice will also develop SCID as a result of Jak3 loss, however few other symptoms are noted as a result of Jak3 loss (75)(76)(77).

While Tyk2 does not carry the same naming as the other Jak proteins, it is still considered to be in the same family as the other Janus kinases. Tyk2 was the first of the Jak proteins to be fully sequenced and cloned, and the protein carries the same name as the gene which codes for it (78). Of all the Jak proteins, Tyk2 was the first to be associated with interferon (IFN) signaling and signaling in the IL-6 class of receptors, however later this was proven to be untrue, and Tyk2 has now been shown to be associated only with IL-12 and LPS signaling (79)(80). Because of Tyk2's role in LPS signaling, Tyk2 knockout mice have been shown to be more susceptible to infection (62).

Jaks are activated after ligands bind to their associated receptor, which induces dimerization of the receptors (81). This binding brings two Jak proteins into close proximity to each other, allowing them to trans-phosphorylate each other into their active form. They are also able to phosphorylate tyrosine residues within the cytoplasmic domain of the receptor, which serve as binding sites for STAT proteins (82). Once a STAT protein binds to the C-terminus of the receptor, it too is phosphorylated by the Jak proteins, and becomes active. These active STAT proteins dimerize with each other and are shuttled into the nucleus where they act as transcription factors (81).

While the STATs are downstream of the JAKs, they were discovered prior to JAKs in 1988, although they had not yet received the name they bear today (83). The STAT family includes 7 proteins which act as transcription factors, regulating processes relating to cell proliferation and differentiation (84). The members of the STAT family are STAT1, STAT2,

STAT3, STAT4, STAT5a, STAT5b and STAT6, and each member shares a conserved structure (85). Each STAT protein plays a different role in transcription regulation of processes that are important in the normal function of cells, however when these processes become disrupted it can lead to disease. STATs, which are arguably oncogenes themselves, are also downstream of many oncogenic proteins and receptors which, when aberrantly active, can lead to cancer. This highly compounds the potential for STATs to lead to cancer, and two of the major players in cancer progression secondary to STAT activation are STAT3 and 5.

When functioning normally, STAT3 and 5 operate as regulators of pathways which control many growth factors including epidermal growth factor and platelet derived growth factor (86). While STAT3 knockout mice show embryonic lethality (87), using a tissue specific knock out system with Cre-Lox mechanisms has shown STAT3 to be involved in cell motility, wound healing, and apoptosis (88)(89). STAT5 plays an essential role in the development of immune cells (90), including Tregs, which serve to suppress and regulate the immune system (91). Given the roles of these STAT proteins, improper regulation of them can lead to increased cell proliferation, motility, failure to respond to apoptotic signals, and evasion of the immune system due to upregulation of Tregs. And, in fact, these transcription factors have been linked to a number of different cancers driven by these events, including hematopoietic cancers (92), lung cancer(93), colon cancer (94) and breast cancer (95).

While the JAK/STAT pathway is a well-known player in other malignancies, there is less known about the role of this pathway in synovial sarcoma. However, some research has shown that a subset of synovial sarcomas have increased levels and activity of STAT3 (96), and currently a clinical trial assessing the efficacy of the JAK1 inhibitor Itacitinib in many types of solid sarcomas is underway (97). While there is a small amount of research being done in this

area, there is unexplored potential for the targeting of this pathway in synovial sarcoma. In our studies, we have found an upregulation of the Oncostatin M Receptor, which is a member of the IL-6 family and known to use the JAK/STAT pathway for signaling, indicating that this pathway may play an important role in cancer progression.

1.5.2 The Members of the IL-6 Receptor Family

The Interleukin-6 (IL-6) family of receptors is a family of cytokine receptors which signal through the JAK/STAT pathway (98). This family is sometimes referred to as the gp130 family of cytokine receptors due to the presence of the gp130 subunit in nearly all of the receptors (99) (Figure 1.5). IL-6R was the first receptor in this family to be characterized and was cloned in 1988 by Yamasaki et al. (100). This family of receptors has been shown to play a role in the development and progression of cancer and are thus an important topic of research.

IL-6R is known to activate the STAT3 transcription factor (101) which leads to an inflammatory phenotype in cancer (102). IL-6 has been identified as a poor prognostic marker in breast cancer (103) and has been found to upregulate the expression of VEGF and NF-**κ**B, both of which are associated with a more aggressive and metastatic tumor (104). The cytokine receptor has also been implicated in colorectal cancer (105), pancreatic cancer (106) and renal cell carcinoma (107).

Because of its strong implications in cancer, many attempts to inhibit IL-6 and its receptor have been made. However, the ubiquitous role of IL-6 in many inflammatory processes have made the target less than ideal (108). The inhibition of IL-6 has long been a technique in treatment of multiple autoimmune diseases (109)(110)(111), resulting in multiple pharmaceuticals which could be tested in the treatment of cancer. However, there is only 1 FDA

approved IL-6 inhibitor which is approved for the treatment of cancer (112). The IL-11 and IL-27 receptors are similarly associated with cancer (113)(114)(115), however no current inhibitors for these receptors exist. LIFR has been shown to contribute to cancer progression (116)(117), and both LIFR and OSMR are important growth factors in Ewing sarcoma, a cancer similar to SS in that it is caused by a translocation mutation and arises in the mesenchymal tissue (118). There are currently two FDA approved drugs to inhibit LIFR, and pre-clinical studies of a drug currently termed EC359 have shown promise in this regard (119). The OSMR receptor has a strong connection to multiple types of cancer which is discussed further in chapter 1.6. Currently there is no research being performed on small molecule inhibitors of OSMR in cancer, however there are multiple studies utilizing antagonistic antibodies to inhibit OSMR (120) (121). IL-31 is known to play a role in cancer suppression (122)(123), and currently in clinical trials for the treatment of atopic dermatitis is the anti-IL-31 antibody Nemolizumab (124). However, there is no research investigating is receptor in the treatment of cancer. The last member of the IL-6 family, CNTFR, has had, perhaps, the least amount of research performed on its association with cancer, however one group has found that CNTFR inhibition can have a tumor suppressing effect in lung adenocarcinoma (125).

Despite the number of potential protein targets listed here, a combination of the rarity of SS leading to the disease being under researched, and the difficulties of treating a low mutational burden cancer result in there being little breakthroughs in the field of IL-6 receptor family inhibition.

1.6 Oncostatin M Receptor and its Implications in Cancer Development

Oncostatin M Receptor (OSMR) is a protein which has been implicated in many different cancer types (126)(127)(128). OSMR is a member of the IL-6 cytokine receptor family which is classified based on the presence of the gp130 sub-receptor. The IL-6 receptor family signals through the JAK/STAT pathway (129), activating JAK1, JAK2 or TYK2 (130), and regulates a number of biological functions including inflammation, hematopoiesis, and immune response (131)(Figure 1.6) . This transmembrane receptor receives the ligand oncostatin M (OSM) and is composed of the subunits gp130, which characterizes the IL-6 receptor family, and OSMRβ (132).

While the ligand was previously known, the receptor was first discovered in 1996 by Mosley et al. who were the first to characterize OSMR (133). This ligand-receptor pair earned its name when it was discovered to inhibit tumor growth in melanoma cells but to promote the growth of fibroblast cells (134). Since then, multiple reports of the dual nature of OSMR have been reported. OSMR has been found to suppress metastasis of lung adenocarcinoma through activation of the STAT1 pathway (135). Conversely, OSMR has also been linked to growth of malignancies. Research in gastric cancer found that OSMR was often overexpressed and was found to be an indicator of poor prognosis. It was determined that the OSMR receptor activates the STAT3 pathway leading to increased rates of proliferation and adhesion (127). Astroglioma has also been found to have increased proliferation rates and metastasis as a result of OSMR activation secondary to upregulation of adrenomedullin, another activator of the STAT3 pathway (136). There is also evidence of OSMR playing a role in the increase of Vascular Endothelial Growth Factor (VEGF) production in astroglioma, which leads to increased vascularity and growth promotion of tumors (137). OSMR expression in cervical cancer has been linked to a

poor prognosis, and was found to induce endothelial-mesenchymal transitions along with increased rates of metastasis (138) (139). Interestingly, research shows that OSMR activation can have both suppressing and promoting effects in breast cancer. Multiple groups have found that OSMR activation leads to growth suppression through activation of the STAT3 pathway and encourages cell differentiation which leads to better patient outcomes (140)(141)(142). However, other groups have found that OSMR activation can lead to increased metastasis in Estrogen Receptor (ER)+ cell lines through CD44 upregulation (143).

Due to the complex nature of the JAK/STAT pathway, it is evident that OSMR activation has multiple and widespread ramifications. Whether OSMR activation or inhibition is called for in the treatment of cancer must be evaluated on a case-by-case basis, as it could have both beneficial and detrimental effects. In order to help illuminate this controversy Chen et al. performed a pan-cancer analysis of the effects of OSM in various cancers utilizing data from The Cancer Genome Atlas (TCGA) and the Genotype-Tissue Expression (GTEx) databases (144). They show that OSM plays an integral role in inflammation as well as the tumor microenvironment, both of which are important factors in the progression of cancer. And while there is currently no published data on the role of OSM/OSMR in SS, this data suggests that this inflammation pathway can play an important role in the development of SS.

While the role of OSMR in SS remains unexplored, OSM has been identified as an integral growth factor in Kaposi's Sarcoma, a malignancy which almost always develops secondary to HIV infection (145). While it has been long known that OSM contributed to the progression of Kaposi's Sarcoma (146)(147), the mechanism by which this occurs was not explored until later, when it was found that OSM increased the presence of IL-6 and COX-2, both of which are associated with an inflammatory response (148).

The mounting evidence of the role of OSM/OSMR in cancer development highlights this receptor as an ideal target for therapy. However, due to the ligand/receptor binding mechanism, this approach has a high likelihood of failing due to off-target effects and refractory disease. OSM is known to interact directly with the gp130 subunit of the OSMR receptor with a low affinity. After this association occurs, the OSMRβ subunit enters and associates more strongly with the OSM-gp130 complex (133). Due to this mechanism, it is possible for OSM, or any OSM-like small molecule inhibitors, to bind with low affinity to any of the gp130 cytokine receptors and induce off-target effects resulting in toxicities. With the exception of the IL-31 receptor, all of the members of the IL-6 receptor family contain the gp130 subunit (Figure 1.5). Therefor the strategy of using an OSM mimicking small molecule inhibitor could potentially have off target effects on any member of the receptor family causing significant toxicities. Furthermore, as highlighted in section 1.3, inhibiting a single growth factor receptor in the JAK/STAT pathway has proven unsuccessful, and time after time has resulted in disease resistance due to the numerous other receptors which may activate this pathway. In order to overcome these challenges, a strategy must be developed which is able to target the OSMRβ subunit with high specificity and is also able to overcome disease resistance. We elected to develop a radioimmune therapy which targets OSMR to overcome these difficulties.

1.7 A Metastatic SS Mouse Model

The mouse model used in these experiments is one previously described by Barrott et al. (149). Prior to the development of this model, no mouse model had sufficiently exemplified the metastasis patterns seen in human SS, in which metastasis occurs frequently and most often to the lungs (150). This genetically modified mouse model provides a way to accurately model SS in an organism with a functioning immune system, unlike xenografted models of SS. Inserted

into the genome of these mice is the SS18-SSX2 translocation mutation which is responsible for driving SS (8)(11). Along with the translocation mutation fusion gene, a Green Fluorescence Protein (GFP) gene is inserted to allow for easy identification of tumor tissue from healthy tissue. This genetic mouse model serves as our non-metastatic model, as these mice form primary SS tumors but do not undergo metastasis. To model metastasis in these mice, an additional genetic modification has been made. By inducing a loss of PTEN, these tumors develop the characteristic metastasis of SS which is most often seen in the lungs (Figure 1.7).

This mouse model provides a number of benefits over other model types. Because these mice are genetically modified, they develop SS tumors *de novo* and in anatomically expected locations when compared to human SS. This can provide more accurate modeling of drug delivery than a xenografted model, which can only develop tumors in surgically accessible locations. Furthermore, these mice are not immunocompromised, allowing for investigation of impacts on the immune system and what role the immune system might play in both drug reactivity and tumor sensitization to immune response.

While this model carries many benefits, it also has its limitations. Because these mice are genetically modified to develop SS tumors, they do not provide data on human tumor protein expression. As will be discussed in Chapter 2, protein expression can vary from sample to sample, and could pose challenges in targeted therapy. This model cannot help us to investigate these expression variations in human tissues.

1.8 Radioimmune Therapeutic Strategies

1.8.1 Overview of RIT Clinical Trials and Outcomes

Radioimmune Therapy (RIT) is a type of systemic therapy which combines components of immune therapy with radiation therapy (151). This model of drug utilizes monoclonal

antibodies which serve as the targeting system for the drug and are highly specific for malignant tissue. Tethered to these cancer specific antibodies is a radioactive isotope which will deliver its radioactive payload to the cancerous cells once directed there by the antibody (Figure 1.8). As the field of oncology shifts to favor a more personalized treatment focus of therapy, RIT has become of higher interest as it can be tailored to the specific markers of a patients tumor (152).

While the idea of RIT might be gaining interest in the field of oncology, RIT has been an FDA approved treatment for cancer for 20 years. Ibritumomab tiuxetan (Zevalin) was the first RIT approved by the FDA in 2002 for the treatment of non-Hodgkin's lymphoma (153). This RIT utilizes an anti-CD20 monoclonal antibody to target cancerous cells, making it specific to B cells, the most common cells for lymphoma to arise from (154). Patients first receive this antibody tethered to the radioisotope indium-111 which releases gamma radiation and can be seen using imaging tools but does not have any tissue damaging properties. If this radioimmune therapy shows efficient localization to the target tissues, the patients then receive the antibody chelated to a yttrium-90 ion, which releases beta radiation and can damage the cancerous tissue (153).

Tositumomab (Bexxar) is a similar drug which was approved in 2003 for the treatment of relapsed or refractory non-Hodgkin's lymphoma (155), and was momentarily approved as a first-line treatment for the disease, although this approval has since been rescinded (156). Similar to Ibritumomab, Tositumomab is directed to diseased cells through us of an anti-CD20 monoclonal antibody. However this RIT chelates an Iodine-131 isotope to deliver its radioactive effects (155).

While non-Hodgkin's lymphoma is the only FDA approved indication for the use of RIT, there have been multiple clinical trials exploring the use of RIT in solid tumors in the past

decade. Currently, there is an ongoing Phase II trial exploring the use of 131I-omburtamab in the treatment of desmoplastic small round cell tumors as well as other cancers which can affect the peritoneum (157). This drug is composed of an anti-B7H3 antibody which is conjugated to an Iodine-131 radioisotope and is being administered in combination with external beam radiation therapy (158). While this trial is ongoing and therefor has no results as of yet, the phase I trial of this drug showed good tolerance by patients with little side effects and the antibody was shown to be highly selective for malignant tissues (159). While tumor growth suppression was not measured in the phase I trial, the phase II trial shows promise in this regard based on their prior results. This study also included patients with Ewing sarcoma, which is similar in many ways to SS. Currently there is also an ongoing clinical trial which is investigating the inhibition of this protein through an antagonistic antibody in multiple types of sarcoma including Ewing sarcoma, osteosarcoma, Rhabdomyosarcoma, highlighting the relevance to the field (160).

Another phase II trial utilizing I-131 in RIT is targeting medulloblastoma, a pediatric brain cancer, through the use of GD2 antibodies (161). While this study focuses on central nervous system cancers, patients with leptomeningeal cancers and high GD2 expressing cancers were also looked at in this study. Due to the locality of medulloblastoma, the trial saw slightly more severe side effects than are usually seen in RIT clinical trials, however these were not considered overly severe and the therapy seems beneficial as a salvage therapy for patients with GD2+ tumors (162). This research may also be translated into the treatment of SS as SS has also been shown to have an overexpression of GD2 (163).

A pilot study was performed looking at the use of the anti-HER2 antibody trastuzumab, which is FDA approved for the treatment of HER-2 positive breast cancer and goes by the name Herceptin (164), tethered to a Lutetium-177 isotope in the treatment of HER-2 positive breast

cancer (165). They found that the RIT was able to localize itself with high specificity to both primary and metastatic sites of disease, however despite these promising results no clinical trial has been initiated.

RIT is also being explored as an adjuvant therapy in the treatment of colorectal carcinoma, specifically that which has metastasized to the liver (166). A phase I study showed that an anti-CEA targeting RIT using I-131 was effective at suppressing relapse once patients were considered disease free. However, in the subsequent phase II study, while the treatment was successful in suppressing tumor growth, it resulted in hematotoxicity making it an unlikely treatment.

Perhaps one of the most aggressive and metastasis prone cancers is pancreatic cancer. This disease has proved extremely difficult to treat and has one of the lowest 5-year survival rates out of all cancers, at just 5-10% (167). In an attempt to increase the treatment options for these patients, an anti-Muc1 RIT using Yttrium-90 initiated clinical trials and proceeded into Phase III trials (168). While the therapy was well tolerated and saw tumor growth suppression in patients who were able to receive multiple doses of the RIT, in most cases, the disease progressed far too quickly for patients to be able to receive multiple doses and the drug never received FDA approval. This highlights the limits of RIT as a therapy which may take time to take effect, which is less than ideal for aggressive, fast-moving cancers. Because of this, RIT may have a role in combination or maintenance therapy rather than a first line treatment in some cancers.

While the number of clinical trials using RIT are numerous, only two therapies are FDA approved for the treatment of cancer. The field of RIT shows incredible promise to provide more treatment options for patients with few choices, however it is evident that more research is called

for in this field. SS lends itself as an ideal target for RIT therapy, as it does not progress at an accelerated rate like pancreatic cancer does, and patients are not likely to progress so quickly that they are unable to receive more than one dose. SS also has the benefit of typically being localized to places which can tolerate radiation therapy well, unlike metastatic colorectal carcinoma, which is most commonly found in the liver which is sensitive to radiation. Because of these advantages, we are confident that an RIT model of therapy will be well tolerated and have great benefit to SS patients.

1.8.2 Current Pre-Clinical Use of RIT in Cancer Treatment

In addition to the multiple ongoing clinical trials using RIT to treat various cancers, there are also a handful of pre-clinical studies attempting to develop new RIT's. One such study is using a Lead-212 isotope conjugated to an antibody which recognizes B7-H3 to treat ovarian cancer (169). This study has been able to efficiently synthesize this RIT and found that the drug was able to inhibit ovarian cell growth *in vitro*. They have also performed *in vivo* studies and found that the antibody sufficiently targeted the disease, and that mouse survival was extended with treatment. While further research is warranted to determine dosage and tolerability, this project shows promise as being a viable therapy after debulking surgery in ovarian cancer patients.

Ovarian cancer is not the only malignancy in which Lead-212 is being used in RIT. By using a different antibody which targets CD38, a transmembrane receptor which is often overexpressed in multiple myeloma cells, an RIT is being developed which can target multiple myeloma and deliver radiotherapy via the attached Lead-212 isotope (170). This drug has shown the ability to suppress tumor growth in both *in vitro* and *in vivo* studies and showed good distribution to sites of disease. These results paired with the fact that the only current FDA

approved RITs are for the treatment of hematological malignancies suggest that this RIT will find success in the treatment of multiple myeloma.

Isotopes besides Lead are being investigated for their potential use in RIT as well. Recent research has shown that an RIT model using Copper^{67} attached to an anti-HER2 antibody can be used as a theranostic agent in breast cancer (171). Not only did this research show that this RIT was able to treat mice xenografted with breast cancer, but it was also shown to be an efficient imaging tool, highlighting the potential of RITs to have multiple uses in the clinic. This is also an example of an RIT effectively treating a solid tumor, something which has been a challenge in the field previously.

While there is an abundance of research on the chemistry and components of RIT, there is very little research exploring the use of RIT drugs in the treatment of solid tumors. The field of RIT in oncology is rich with foundational research and in need of translational, pre-clinical studies to further this drug model into the clinic.

1.8.3 The Components and Versatility of RIT

RIT is emerging as an effective way to treat solid tumors with both clinical and pre-clinical studies underway. Typically, there are three major components to RIT's: the antibody, which serves as a targeting system, a chelator which can be conjugated to the antibody and which can hold a radioisotope, and finally the radioisotope itself, which serves to deliver radiation to the cancer cells once brought into proximity to them by the antibody. The relative simplicity and interchangeability of RITs is a great boon to the drug model, as each component can be exchanged for something similar until success is found.

Perhaps the most easily exchanged component is that of the antibody due to the constant region being similar between antibodies but the variable region having vastly different targets

based on what antibody is used. This results in the easy exchange of antibodies if one protein target does not result in sufficient cancer specificity. Because of the need for high specificity, monoclonal antibodies are typically selected rather than polyclonal antibodies (172). This helps to eliminate off-target effects and binding. While whole antibodies are frequently used, it is also possible to use antibody fragments in RIT (173). One reason to consider the use of antibody fragments rather than full length antibodies is that the decreased size can result in improved pharmacokinetics and tumor permeability of the RIT (174). The selection of which targeting antibody or antibody fragment is a critical one in the realm of RIT, as it can greatly determine the specificity of the treatment, as well as the retention time and possibility for off target effects.

In order to attach radiometals to these antibodies or antibody fragments, the use of a bifunctional chelator is needed. These are molecules which have both the ability to chelate a metal, as well as a functional group which allows them to be conjugated to other molecules such as proteins (175). While there are numerous bifunctional chelators which could be selected for use in RIT (Table 1.2**)**, they typically fall into two categories: linear or macrocyclic (176). Both categories are good options each with their own benefits and pitfalls. Linear bifunctional chelators tend to have faster and more efficient radiolabeling of metals, however macrocyclic bifunctional chelators are more stable (177).

Table 1.2 Examples of Various Bifunctional Chelators and Their Structures

DTPA	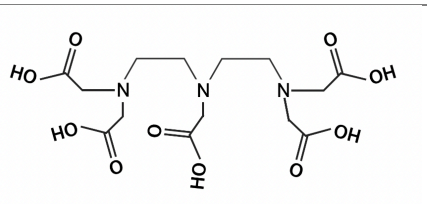
DOTA	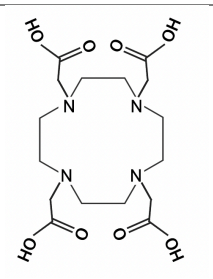
TCMC	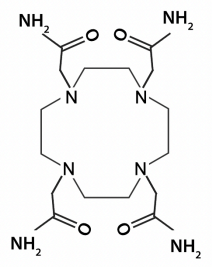
NOTA	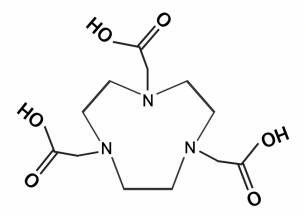
NETA	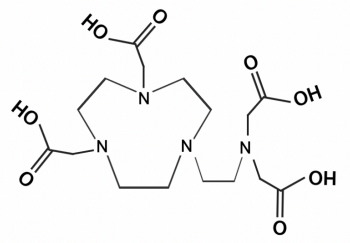

While bifunctional chelators can be attached directly to the antibody with a stable covalent interaction, there are some situations in which a linker is preferred. The use of PEG linkers of different lengths has been investigated and found to alter the tumor uptake and metabolism of RIT's (178), which would allow researchers to further fine-tune RIT pharmacokinetics according to their needs. Other linkers such as arylsulfate are cleavable once administered, and release the attached moiety from the antibody (179). While most applications being explored pertain to antibody-drug conjugates (ADC's), they could also be applied to RIT's.

The selection of which radioisotope to use is an extremely important decision which can affect the behavior of the RIT. Many parameters must be considered including the chelation stability, the half-life, the metabolism, potential toxicities, the cost, and the availability of the isotope (180). Another key consideration when selecting an isotope is what type of radioactive decay is called for. The three most commonly used emissions used in RIT are gamma rays, beta particles and alpha particles (181)(182), and each has its own unique properties.

Gamma rays have been very popular in the rising field of theranostics, in which a drug has both therapeutic and diagnostic potential. Gamma emitting particles can be detected using Single Photon Emission Computed Tomography (SPECT) and used as an imaging tool. By selecting a gamma emitter as the radioisotope, the RIT is repurposed from a treatment to an imaging tool, and once administered can be used to detect and monitor sites of disease (183). Another type of radiation which can be used for monitoring and diagnostics is positron emission.

Positrons emitted by radioisotopes can be detected using Positron Emission Tomography (PET) to monitor and image a disease (184).

While gamma ray and positron emitting isotopes do little damage to tissues while acting as imaging tools, beta and alpha particle emitters are able to deliver tissue damaging radiation which is useful in the treatment of cancer. Beta particle emissions are short range and only travel short distances in tissues. Compared to alpha particles, beta particles do much less tissue damage which makes them ideal for RIT, where the cell death is intended to be extremely precise and not extending into potentially healthy tissues (185). Alpha particle emitters can also be used in RIT and have the advantage of having a longer range and affecting more tissue at a time, which can be advantageous in certain circumstances (186).

Even after the desired type of radiation has been selected, there are still many parameters to consider. An important factor which can greatly impact how an RIT behaves in the human body is that of the isotope half-life. This will determine how long the radioactive isotope remains in the body and could determine whether the therapy is effective, as well as how toxic it is. The half-lives of the radiometals currently being researched in RIT vary greatly based on the needs of the therapy (180)(Table 1.3), however in general, it is ideal to have a half-life of no more than a few days while still having an acceptable amount of time to produce the drug and administer it.

Table 1.3 Commonly Used Radioisotopes

Isotope	Radiation Type	Half-Life (Hrs)
Ga^{67}	Gamma	78.3
Tc^{99}	Gamma	6.01
In^{111m}	Gamma	67.4
Sc^{44}	Positron	3.9
Mn^{52g}	Positron	132
Cu^{64}	Positron	12.7
Ga^{68}	Positron	1.13
Y^{86}	Positron	14.7
Zr^{89}	Positron	79.2
Y^{90}	Beta, Gamma	64.8
Cu^{67}	Beta, Gamma	62.4
I^{131}	Beta, Gamma	192.5
Pb^{212}	Beta	10.6
At^{211}	Alpha	7.2

The RIT model of therapy offers many benefits over other treatment options in oncology. Because it is a systemic radiation therapy the drug can treat sites of disease directly without irradiating healthy tissues which often happens with direct beam radiation therapy. Furthermore, its systemic nature means that all sites of disease can be treated at once, regardless of whether the sites of disease have been identified or not (187). RIT also has the potential to overcome the development of refractory disease due to inducing cell death through a non-specific mechanism

of proximity to radiation rather than inhibiting a specific metabolic pathway (181). It is well known that most tumors have a heterogenous microenvironment, and therefore, even a tumor with high expression of the RIT's protein target is likely to have a few malignant cells which do not express the protein (188). These cells are still susceptible to death through RIT, as they only need to be in proximity to the therapy, rather than directly bound to it. In this way, the risk of refractory disease development as a result of treatment is expected to be decreased when compared to conventional therapies.

Another potential benefit of RIT is its potential to increase the antigenicity of tumor cells. The effects of radiation on peripheral cells which survive the radiation but experience enough exposure to induce mutational effects could lead to increased antigenicity of the cells, causing an immune response against them and further aiding in the treatment of the disease. RIT also promotes itself over other therapies by being a theranostic therapy. Using a gamma ray or positron emitting isotope can transform RIT from a therapy to a diagnostic compound and used to diagnose and monitor a patient. Finally, a benefit to using an RIT model of therapy is that it is not specific for a type of disease but can be used to treat any disease which overexpresses the protein target. Because the antibody component of RIT only binds to a cell surface protein and is not designed to interfere with any pathways that protein might be involved in, it has a broader scope of what diseases it could treat. For instance, while OSMR has a dual nature in cancer discussed in section 1.6, sometimes promoting cell growth and sometimes suppressing growth, it is still a viable target as the effects of receptor activation are inconsequential in this therapy; it must only be expressed on the cancer cells. Due to the conserved basic structure of all antibodies, it is also a potential strategy to alter the target of the monoclonal antibody with which the RIT is

composed of. This would require little alteration to the methods and should not cause any large changes to the results of treatment.

While RIT offers a new approach in which many of the challenges of cytotoxic therapy are circumvented, it too has its downfalls. One difficulty of RIT, as with all targeted therapies, is ensuring that the target is specific enough for effective reduction in malignancy without off-target effects. Because protein expression varies from tumor to tumor and patient to patient, there is always the chance that a targeted therapy performs poorly in a subset of the population (189). The use of gamma ray or positron emitting isotopes in RIT provides a safeguard against the treatment of this subset and should prevent excessive toxicities (190). By being able to visualize how the drug is distributed in a patient prior to the administration of tissue damaging isotopes, the administration of RIT to patients who will respond poorly can be avoided.

Another challenge to RIT is the short half-life as a result of the radioactive isotopes along with the protein structure. The time available between production and administration is limited making the logistics of production challenging. However, a few FDA radioactive drug compounds, such as Xofigo (Radium^{223} dichloride)(191), Bexxar (Tositumomab with Iodine^{131})(192), and Zevalin (Ibritumomab tiuxetan Yttrium^{90})(193) have made their way into clinics, showing that this challenge can be overcome.

The production of biologic drugs presents its own set of challenges, from which RIT is not exempt. Not only is the compound less stable than a small molecule inhibitor would be, but it has the potential to induce an allergic reaction in the patient as well (194). While these factors present challenges which need to be taken into consideration, there are numerous biologic drugs in the market highlighting that that these obstacles are not insurmountable.

1.9 Copper Isotopes and Oxidative States

Copper is a naturally occurring metal with an atomic number of 29. Not only is it useful in many industrial pursuits, but it is also an essential metal for living organisms (195). There are 29 isotopes of copper, Cu^{63} and Cu^{65} which are stable, and 27 other isotopes which are radioactive and less stable (196). While both stable isotopes of copper are found in nature, Cu^{63} is more abundant, accounting for approximately 69% of naturally occurring copper (197). Of all 27 radioisotopes of copper, ^{67}Cu is the most stable having the longest half-life of approximately 2½ days (61.8 hours) (198). This radioisotope was first discovered in 1948 by Goeckermann et al. who identified a number of new isotopes as a product of bismuth fusion (199). ^{67}Cu gives off short-range beta emissions which are capable of causing tissue damage, making it an ideal radioisotope for use in the field of medicine.

Elemental copper can form different oxidation states which can affect its properties. The most commonly found oxidation states of copper are Cu(I) and Cu(II) (200). Cu(I) is most often found in the form of cuprous oxide (Cu_2O) and the copper has an oxidation state of +1 (201). Other Cu(I) compounds exist as well, such as cuprous chloride (Cu_2Cl_2) and cuprous sulfide (Cu_2S) but cuprous oxide is the most common form found naturally (202). Cu(I) is more stable in a solid state than an aqueous state and in its pure form is insoluble in water (202)(200). Cu(II) has an oxidation state of +2 and is most commonly found as cupric oxide (Cu_2O), although, as with Cu(I), other forms exist. Cu(II) is more stable in aqueous solutions and is the favored oxidation state of this metal (200).

The oxidation state of copper can greatly affect the way in which it will interact with other compounds. For instance, in the case of copper capture in the NOTA chelator Cu(II) is selected as it is preferred by the chelator and more stable in an aqueous solution making capture

easier. The pentadentate structure of ^{67}Cu (II) in the NOTA chelator provides a stable complex which is unlikely to release the isotope (Figure 1.9). NOTA also prefers copper to other metals it may encounter in the body, making it unlikely to be replaced (203). The stability of this chelator-metal complex is necessary as free Cu(II) can result in DNA damage (204). Furthermore, the release of a radioactive isotope into the body could be detrimental. The ^{67}Cu provided by the Idaho Accelerator Center is Cu(II) in HCl.

1.10 Hypothesis and Research Objectives

Given the foundation laid by the afore mentioned research, I developed the hypothesis that: Oncostatin M Receptor is a viable therapeutic target for radioimmune therapy in the treatment of synovial sarcoma. The data presented here shows my investigation into this hypothesis and may be broken down into three goals and specific aims. Firstly, we will determine the expression patterns of OSMR in our models both at the RNA and protein levels. We also confirm that OSMR expression is largely limited to SS tissue. Secondly, we aimed to design and synthesize a novel anti-OSMR RIT which was able to bind to OSMR both *in vitro* and *in vivo*, as well as able to capture radioactive isotopes. Finally, we aimed to evaluate the pharmacokinetics of this novel RIT and investigate its residency time within the metabolic organs as well as how well it is targeted to sites of disease. We concur that these preliminary findings support our hypothesis, and that further research is indicated for this project.

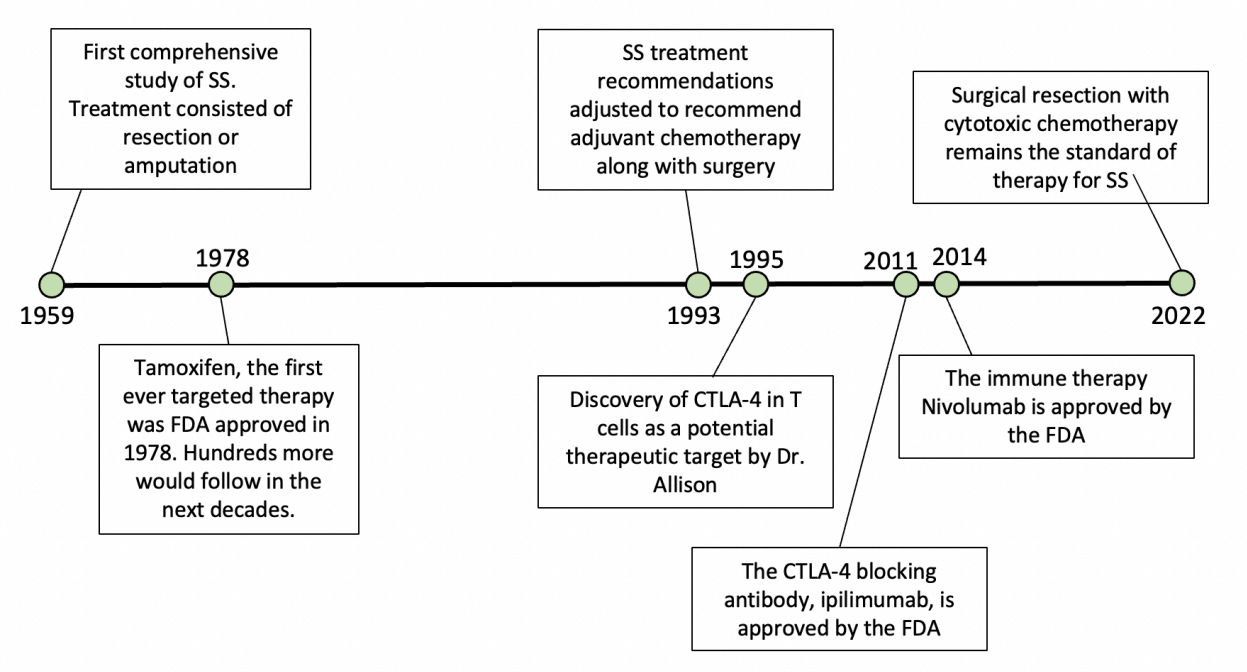

Figure 1.1 Timeline of Major Oncology Discoveries (Bottom) Alongside the Progression of SS Treatment (Top). Despite the major discoveries which occurred since 1959 in the field of oncology, including targeted therapy, whole genome sequencing (2003) and the advent of immunotherapy, no advancements have been made in the treatment of SS.

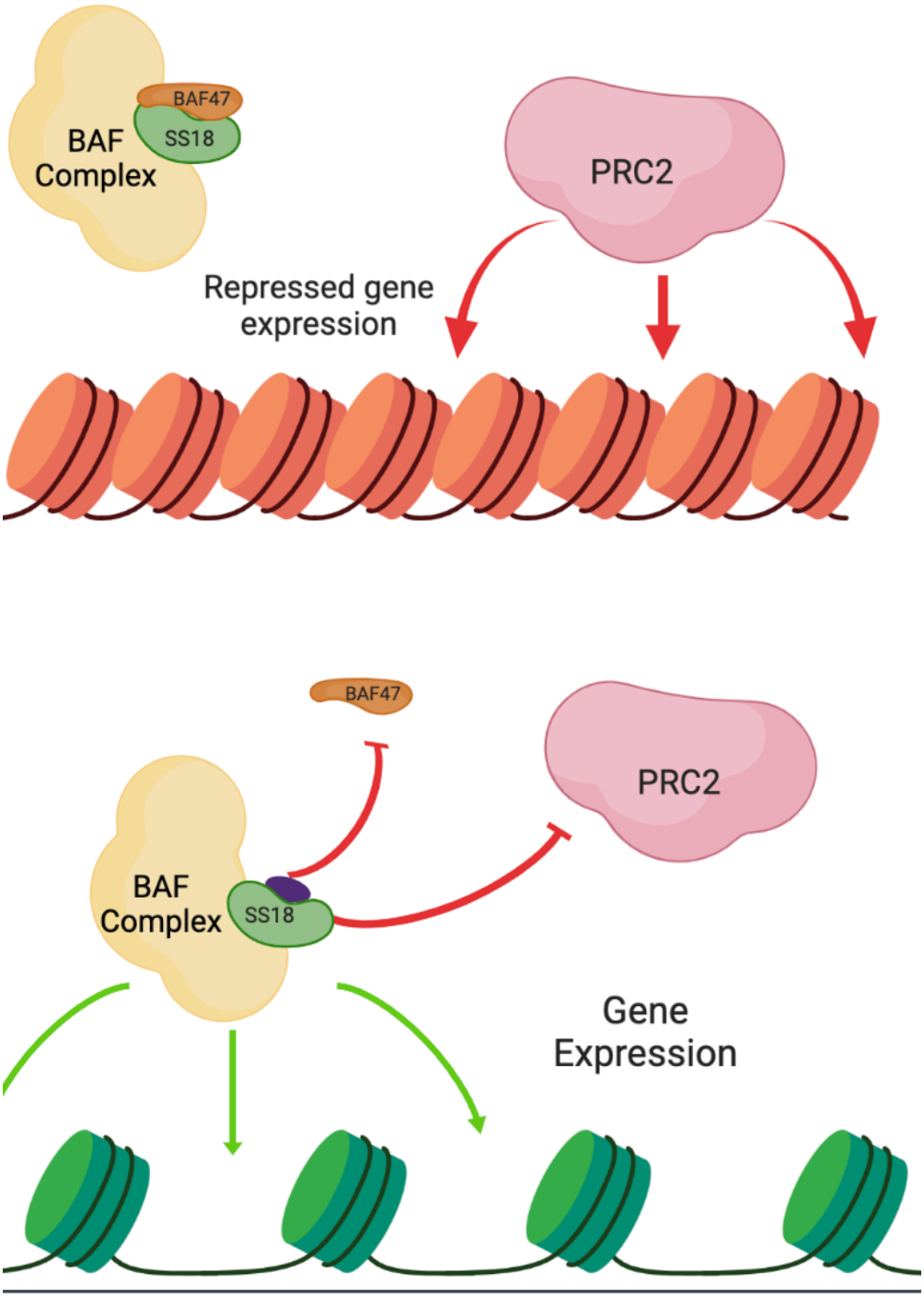

Figure 1.2 The Role of SS18 in the BAF Complex. Wild type SS18 associates with BAF47 and the BAF complex does not interfere with PRC2, allowing it to suppress gene expression. When the SS18-SSX fusion protein is present, it displaces BAF47 and retargets the BAF complex to disrupt PRC2 gene suppression, resulting in activated gene expression.

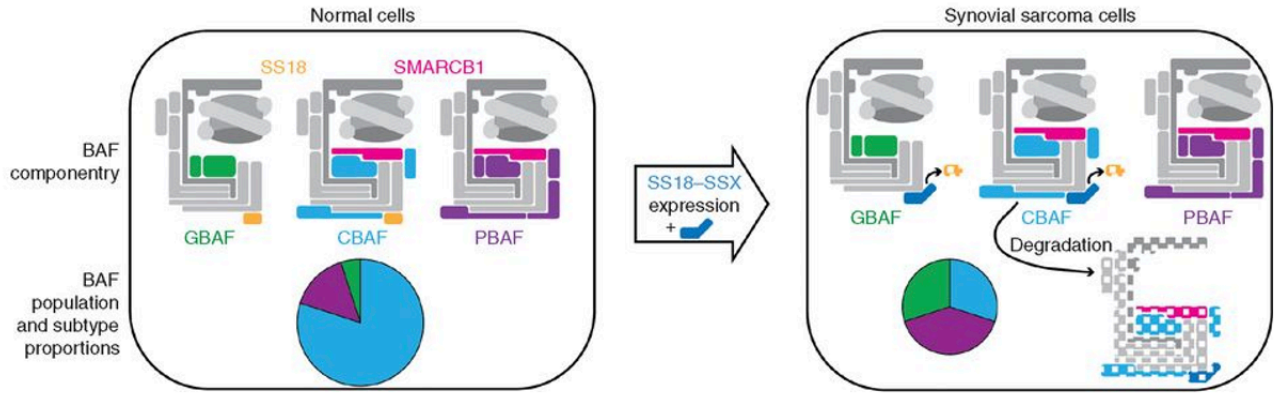

Figure 1.3 Mechanism of SS18-SSX Fusion Proposed by Li et al. Inclusion of the SS18-SSX fusion protein results in degradation of the cBAF complex. This results in altered ratios of BAF complexes resulting in altered epigenetic regulation. Jinxiu Li, Timothy S. Mulvihill, Li Li, Jared J. Barrott, Mary L. Nelson, Lena Wagner, Ian C. Lock, Amir Pozner, Sydney Lynn Lambert, Benjamin B. Ozenberger, Michael B. Ward, Allie H. Grossmann, Ting Liu, Ana Banito, Bradley R. Cairns, Kevin B. Jones; A Role for SMARCB1 in Synovial Sarcomagenesis Reveals That SS18–SSX Induces Canonical BAF Destruction. Cancer Discov 1 October 2021; 11 (10): 2620–2637. https://doi.org/10.1158/2159-8290.CD-20-1219

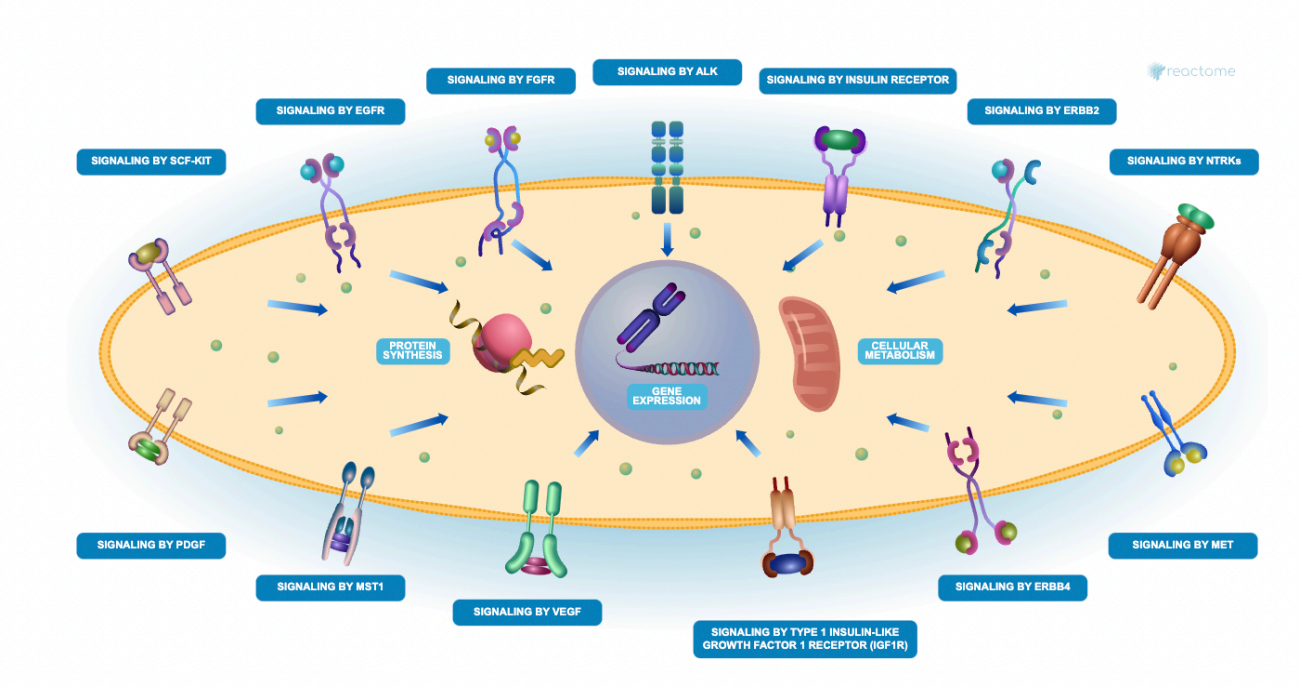

Figure 1.4 Diagram of Members of the RTK Family and the Results of Signaling.

Reactome | Signaling by Receptor Tyrosine Kinases [Internet]. [cited 2022 Feb 22]. Available from: https://reactome.org/content/detail/R-HSA-9006934

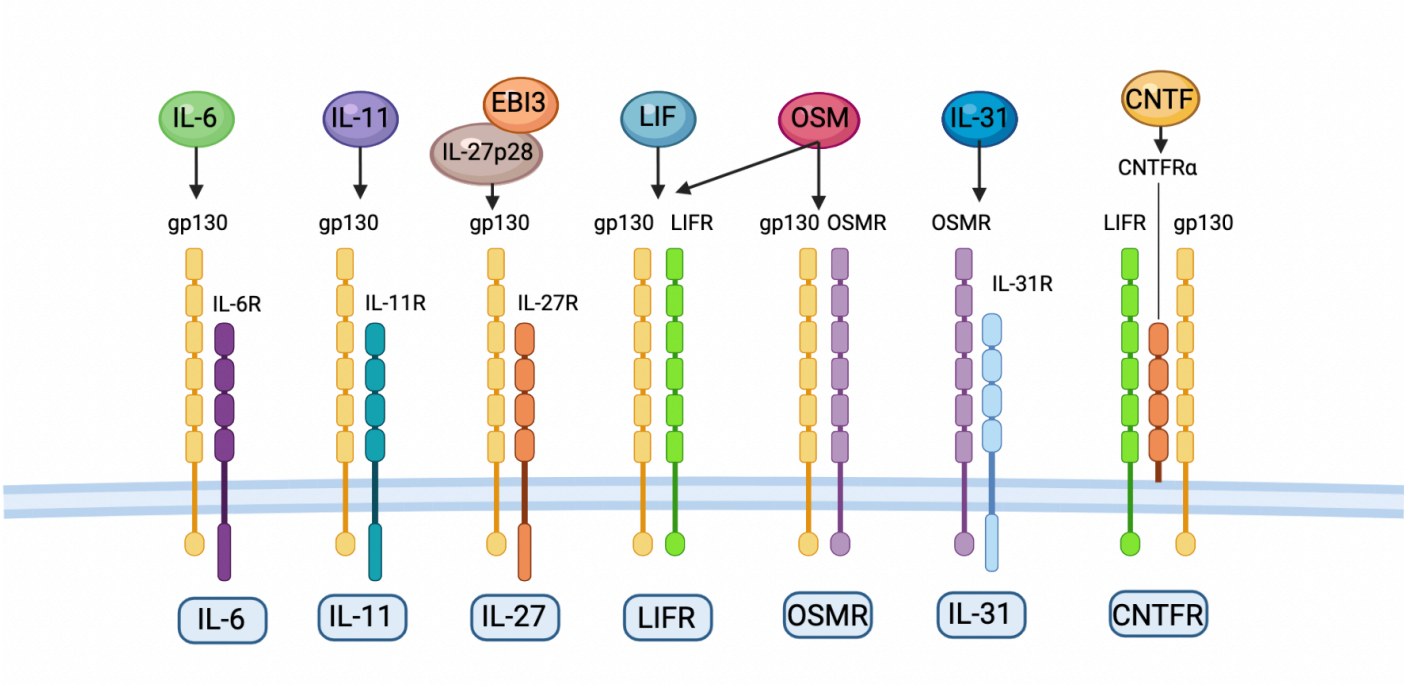

Figure 1.5 The IL-6 Receptor Family and Their Ligands. With the exception of IL-31, all of the receptor family members contain the gp130 subunit. Both OSMR and IL-31 contain the OSMRβ subunit. Image created with Biorender.

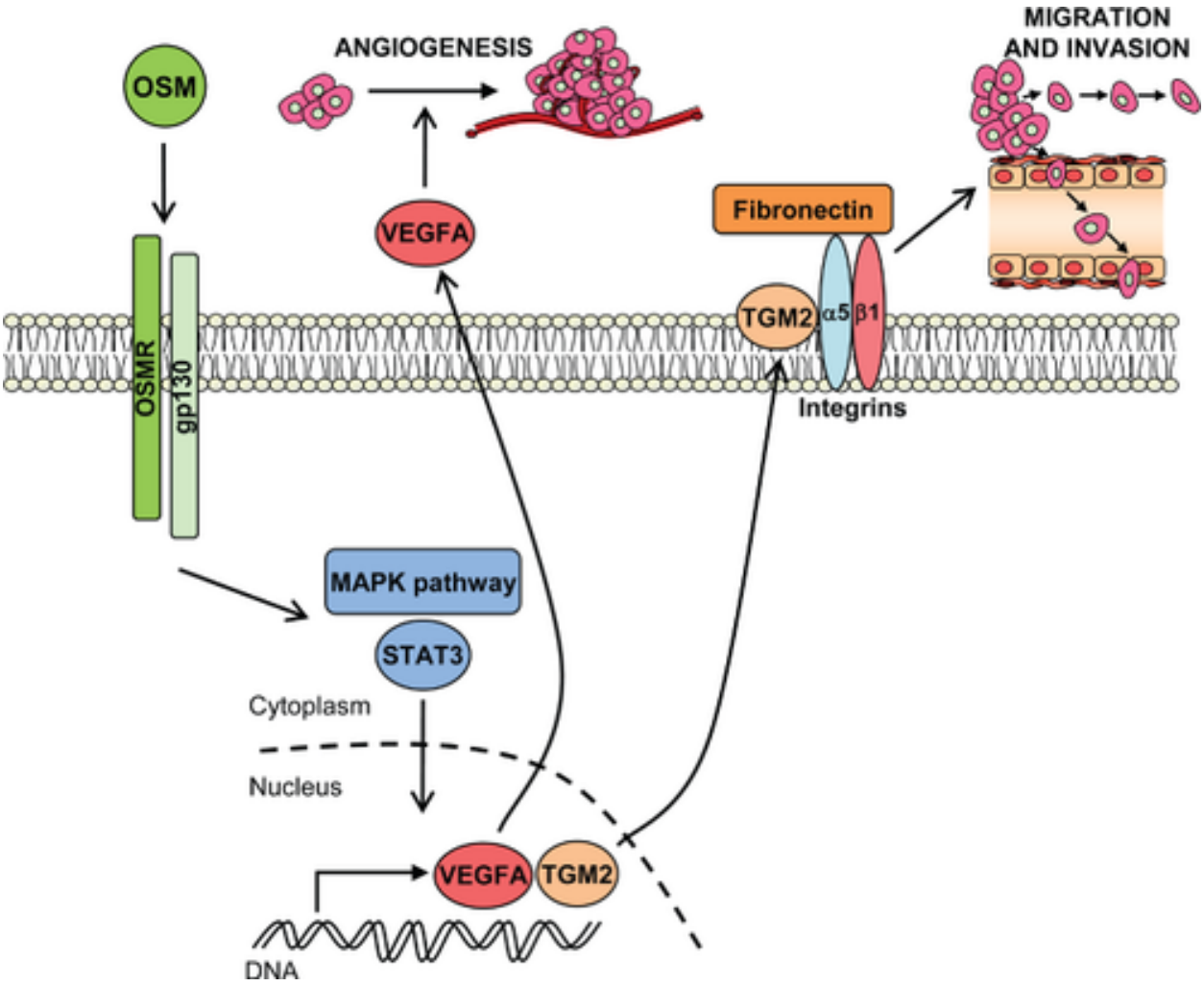

Figure 1.6 The OSMR Pathway Leading to Angiogenesis, Migration and Invasion. **Caffarel MM, Coleman N. Oncostatin M receptor is a novel therapeutic target in cervical squamous cell carcinoma. The Journal of Pathology. 2014;232(4):386–90.**

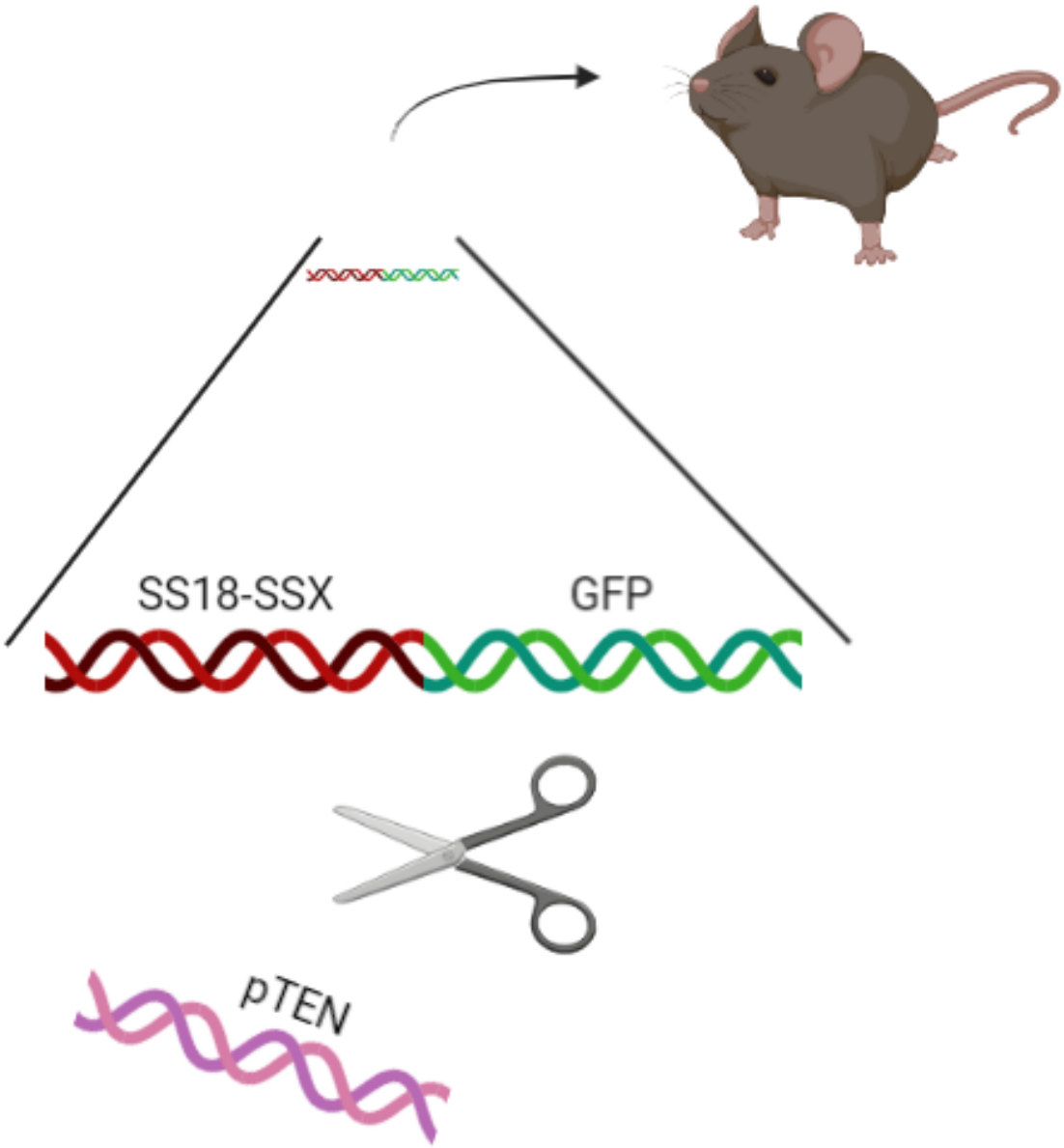

Figure 1.7 A Metestatic Mouse Model for Synovial Sarcoma. The SS18-SSX fusion gene is inserted into the genome, along with a GFP gene. pTEN is removed from the genome. Image created with Biorender.

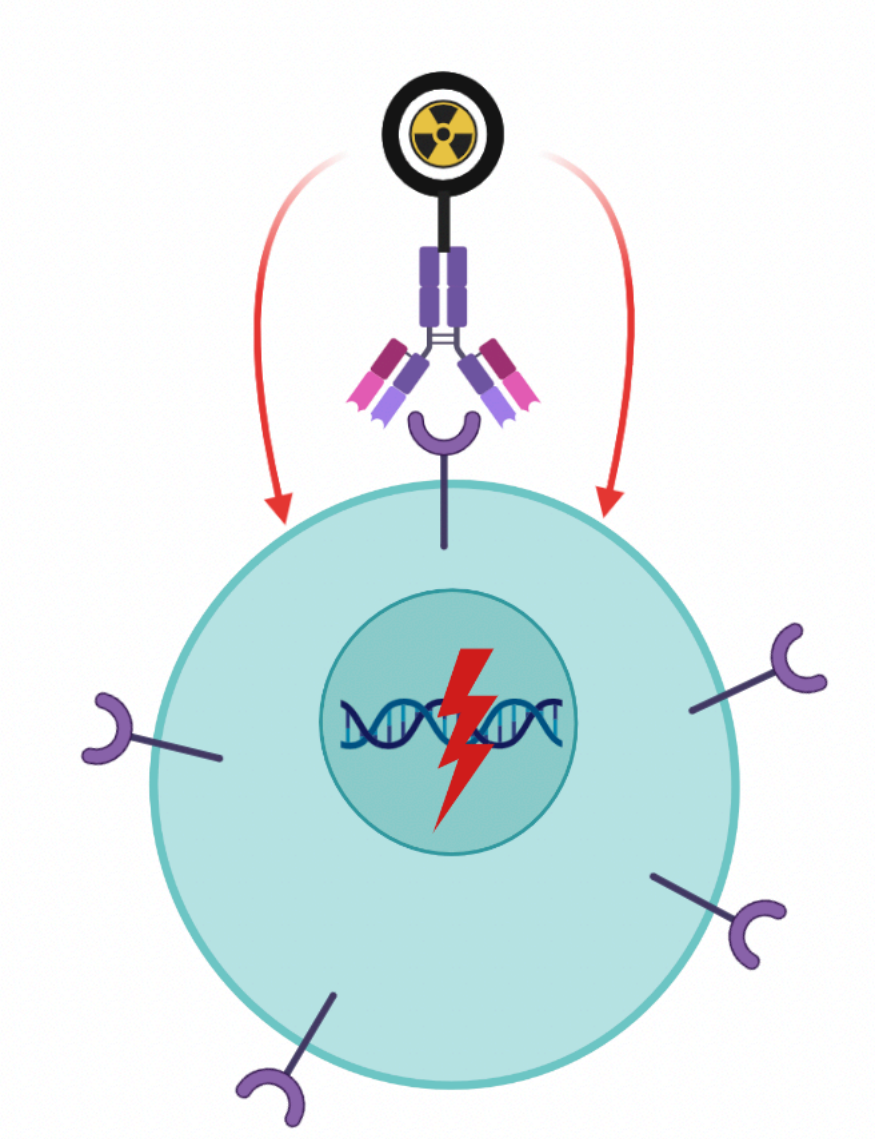

Figure 1.8 Illustration of Radioimmune Therapy Mechanism. The antibody targets proteins specific to cancer cells. Once bound, the attached radioligand can deliver its radioactive payload to the cell, causing DNA damage and inducing cell death. Image created with Biorender.

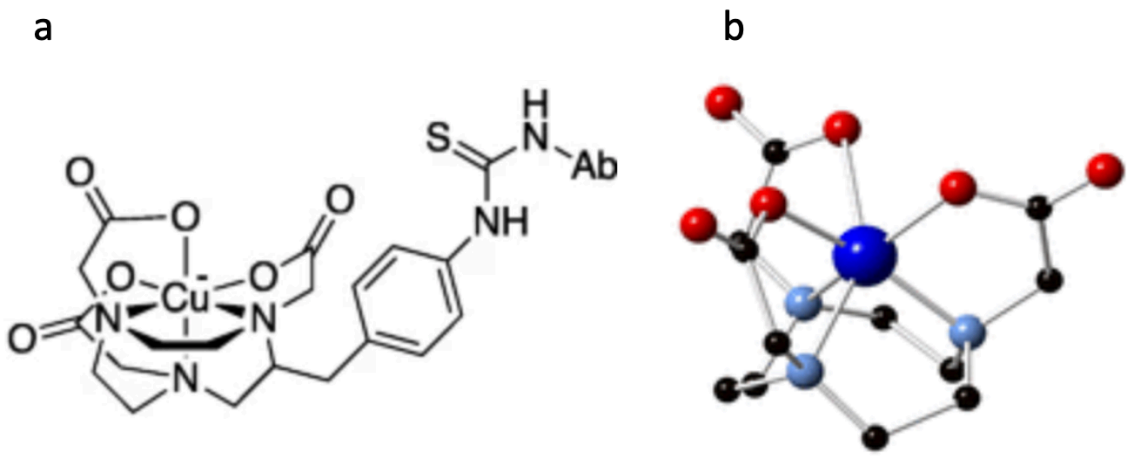

Figure 1.9 The Pentadentate Structure of ^{67}Cu(II) in the NOTA Chelator. (a) 2D chemical structure of Cu(II) bound to the NOTA chelator. Ab represents the antibody. (b) A 3D rendering of Cu(II) chelated by NOTA. Only the chelating structure of the bifunctional chelator is depicted. Copper is depicted as dark blue, Nitrogen is light blue, Oxygen is red and Carbon is black. Carbon-bound hydrogens have been omitted for clarity. Source: (a) Witney TH, Blower PJ. The chemical tool-kit for molecular imaging with radionuclides in the age of targeted and immune therapy. Cancer Imaging. 2021 Jan 30;21(1):18. (b) Kubíček V, Böhmová Z, Ševčíková R, Vaněk J, Lubal P, Poláková Z, et al. NOTA Complexes with Copper(II) and Divalent Metal Ions: Kinetic and Thermodynamic Studies. Inorg Chem. 2018 Mar 19;57(6):3061–72.

2. Oncostatin M Receptor as a Viable Target for Therapy in Synovial Sarcoma

2.1 Introduction

Synovial sarcoma has remained an extremely difficult disease to treat with limited therapy options. One factor which has contributed to this difficulty is the low tumor mutational burden of SS with a median TMB of 1.7 mutations/Mb (205). This low rate of genetic mutations leads to a lack of aberrant protein expression within the cell or on the cell surface. Because of this, there is little to differentiate between malignant and healthy host cells causing the development of targeted therapy to be difficult. Inflammatory pathways have been identified as being upregulated in some SS's. In order to identify potential protein targets for therapy in SS tissue, RNAseq analysis was performed on the SS tissues from the mouse model previously discussed in Chapter 1.7. Particular attention was paid to the data of inflammatory pathways and OSMR was identified as a potential target for therapy.

2.2 Methods

2.2.1 RNAseq Analysis

Data was acquired using accession number GSE81476. Methods used are previously described in Barrott el al., PMID: 27956588 (149). Statistical analysis was performed using a one-way ANOVA test followed by a 2-tailed T-test.

2.2.2 Experimental Animals

All procedures were approved by the Idaho State University Institutional Animal Care and Use Committee protocol 775. The mouse models used in these experiments were the Rosa26-LSL-SSM2/SSM2 (Previously described Halder el al., PMID: 17418413 (206), which

contains the SS18-SSX2 fusion oncogene and is termed non-metastatic, and the Rosa26-LSL-SS18-SSX2/SS18-SSX2;Ptenlox5/lox5 (Previously described Barrott el al., PMID: 27956588 (149)), which contains the SS18-SSX2 fusion oncogene as well as a TATcre mediated Pten removal mechanism and is termed the metastatic model. Mice were bred and weaned at 3 weeks of age. At one month, mice received a subcutaneous 10 uL injection of 50 uM TATcre protein (Excellgen Cat.# EG-1001) into the left hind limb to initiate sarcomagensis. The site of injection was sterilized topically with 70% ethanol prior to injection to reduce the risk of infection. Mice were monitored for tumor development and typically developed tumors between 3-4 months. Mice were monitored for signs of distress, ulceration or difficulty ambulating secondary to tumor growth and euthanasia was employed in these cases. Both male and female mice were used in all studies.

2.2.3 RTqPCR

Reverse transcriptase quantitative Polymerase Chain Reaction (RTqPCR) was performed on samples obtained from both metastatic and non-metastatic models. RNA was extracted from samples using a Quick-RNATM MiniPrep Plus kit (Zymo Research Cat.# R1058) and cDNA was made using Qscript cDNA Supermix (Quantabio Cat.# 95048). cDNA was amplified and measured using the Eppendorf Mastercycler Realplex2. Data was normalized using a delta CT calculation and analyzed using a one-way ANOVA followed by a 2-tailed t-test.

2.2.4 IHC

Immunohistochemistry (IHC) was performed using the metastatic mouse model (described above) Tissue was stained using a rabbit anti-mouse polyclonal antibody targeting

Oncostatin M Receptor (OSMR) (ABclonal Cat.# A6681). All other reagents were obtained from the Pierce Peroxidase Detection Kit (Thermofisher Cat.# 36000) and manufacturers protocol was followed. Briefly, a goat anti-rabbit secondary antibody was applied to the tissues, followed by an anti-goat strep-HRP tertiary antibody. Samples were counterstained with hematoxylin, dehydrated and mounted. Slides were analyzed through a Leica DM6B widefield microscope and imaged with the attached Leica DFC450-C digital camera.

2.2.5 Western Blotting

Western blotting was performed using both the metastatic and non-metastatic mouse models (described above). Roughly 50 mg of tumor tissue was obtained from each mouse. Samples were digested enzymatically with RIPA buffer (0.15 M NaCl, 0.05 M tris-cl, 1 M NP-40, 0.5 M Sodium Deoxycholate, 0.1 M SDS) and homogenized mechanically. Protein concentration of each sample was measured using the Qubit 3 Fluorometer (Thermofisher Invitrogen Cat.# Q3321) and samples were prepared by loading 430 ug of protein per sample. This high protein concentration was used due to the low concentration of OSMR per sample and 430 ug was selected based on the sample with the lowest concentration. Samples were run on a Novex 4-12% Tris-glycine gel (Thermofisher Cat.# XP04120BOX) at 160 volts until proper separation of bands had been achieved. Next, the samples were transferred from the gel to an Immun-Blot® LF PVDF membrane (Bio-Rad Cat.# 162-0263) and processed for imaging using an anti-OSMR rabbit polyclonal antibody (ABclonal Cat.# A6681) as a primary antibody and fluorescently labelled using an anti-rabbit IgG-CFL 680 (Santa Cruz Biotechnology Cat.# sc-516252) as a secondary antibody. Imaging was performed on an Azure c600 system and the OSMR fluorescent label was excited at 790 nM and was visible at 800 nM appearing red in the

image. The GAPDH fluorescent label was excited at 680 nM and was visible at 700 nM appearing green in the image.

2.3 Results

Because of previous evidence that SS exhibits an inflammatory profile (149), inflammatory pathways were examined for upregulated targets through RNAseq analysis. OSMR was identified as being overexpressed and was considered an ideal target due to it being a membrane bound, extracellular protein as well as its specificity to malignant tissue. It was observed that OSMR was expressed at high levels in metastatic SS tissue whereas there was no expression in the normal muscle tissue (Figure 2.1 a). Furthermore, the metastatic SS mouse model expressed OSMR at a 22.4-fold increase over the non-metastatic model with a P-value of 0.005, suggesting that an OSMR targeted treatment might be more effective against aggressive tumor phenotypes.

In order to confirm the aberrant expression of OSMR in tumor tissue, we first performed RTqPCR. Using both a metastatic and a non-metastatic mouse model, 3 mice from each group were selected at random and the RNA expression levels were measured. A sample of non-malignant muscle tissue was used as a control. Interestingly, it was found that the expression of OSMR varied greatly between samples seemingly independent of metastatic status (Figure 2.1 b). Further repetition of this experiment with other mice showed the same pattern of great variation in OSMR expression independent of metastatic status. We found no statistically significant difference in OSMR expression between the metastatic and non-metastatic groups. These data cause us to conclude that in our mouse model, OSMR expression is independent of metastatic status. Both male and female mice were used in these studies.

To evaluate the potential for off-target toxicities of an anti-OSMR treatment, we also measured the OSMR expression of various organs. While the brain, liver and kidneys had minimal OSMR expression, it was noted that there are low levels of OSMR expression in the heart (Figure 2.1 b). However, this expression is much lower than that of the OSMR-high tumors and, while the risks of cardiotoxicity induced by an anti-OSMR drug should be investigated, we believe that the risk is minimal to patients with a high OSMR expression tumor profile.

To further explore these expression patterns, western blotting was performed to measure the presence of OSMR protein in these same samples (Figure 2.2 a). Three bands of the OSMR subunit were detected which correlate to the OSMR receptor at 135 kda which is composed of the OSMRβ subunit and a gp130 subunit, the IL-31 receptor at 100 kda which is composed of the OSMRβ subunit and the IL-31 RA subunit, and the OSMRβ subunit alone at 75 kDa. As with the RTqPCR data, the OSMR expression appeared to be independent of metastatic status as both sample groups had great variation in OSMR expression. Furthermore, the protein expression levels coincided with the RNA expression levels, further confirming the hypothesis that the RNAseq data on randomly selected mice which showed a correlation between OSMR expression and metastatic status. However, while the tumor samples had varying degrees of OSMR expression, the normal muscle tissue showed no expression indicating that OSMR is a viable target for therapy regardless of metastatic status. This data also highlights the difficulty in predicting which patients will respond well to an anti-OSMR therapy, as aggressive tumor type is not an indication of OSMR expression.

Immunohistochemistry staining for OSMR protein was also performed in both primary tumor samples and lung metastatic samples (Figure 2.2 b). We found that OSMR is expressed in both primary and metastatic sites of disease and is found distributed throughout the malignancy. This

indicates that an anti-OSMR therapy would be effective at controlling tumor growth at both primary and metastatic sites.

2.4 Discussion

Synovial sarcoma remains a disease with few treatment options and even fewer aberrant proteins which a therapy could be developed to target. Previous research has shown that SS exhibits an inflammatory profile (149). Because inflammation is a hallmark of cancer (207) and has been associated with sarcomagensis (208), these pathways were investigated through RNAseq analysis. Of interest in this analysis was the overexpression of OSMR, a receptor of the IL-6 family which is associated with inflammation and cell growth (127). This RNAseq data showed a statistically significant correlation between OSMR expression and metastasis in SS (Figure 2.1 a), where metastatic samples showed high OSMR expression while non-metastatic samples and muscle tissue showed no OSMR expression. Interestingly, when OSMR expression was measured by RTqPCR, this relationship was not seen and no statistical significance was observed, and OSMR expression was found to be independent of metastatic status while still being unexpressed in the muscle tissue (Figure 2.1 b). We hypothesize that this discrepancy is caused by a slight variation in the mouse models used. While the RNAseq analysis was performed on a mouse model which was heterozygous for the SS18-SSX2 mutation, the mouse model used in the RTqPCR data was homozygous for this mutation. It is possible that this difference causes an increase in the inflammatory profile of the cancer and results in OSMR overexpression in less aggressive tumors as well as the more aggressive tumors which metastasize. While the heterozygous model only exhibits OSMR expression in the most aggressive of tumors. Alternatively, we hypothesize that this is due to a sampling bias in which

mice with high OSMR expression were selected from the metastatic group and mice with low OSMR expression were selected from the non-metastatic group.

To evaluate what off-target effects might be expected from targeting OSMR and which organs might be affected, we performed RTqPCR on the major organs of the mice (Figure 2.1 b). We found that the brain, liver, kidney, and spleen showed no OSMR expression suggesting that they would have good tolerance to an anti-OSMR treatment. While the heart showed low levels of OSMR expression (Figure 2.1 b), we feel that these levels are minimal compared to the levels seen expressed in the tumor. While the potential for cardiotoxicities should be explored further, we expect to find that an anti-OSMR therapy will have minimal effect on the heart. Furthermore, the current standard of care for synovial sarcoma is treatment with doxorubicin (209), which causes significant cardiotoxicities and the amount a patient can receive over their life time must be limited due to these toxicities (210). Because of this, a novel therapy which has the potential for cardiotoxicities may still be an advancement in this field.

To confirm the presence of OSMR protein in tumor samples we employed the use of Western blotting. OSMR was found to be present in SS while absent in muscle tissue, further confirming that OSMR is an ideal target for therapy. OSMR was detected in 3 distinct bands by Western blot which correlated to 75 kda, 100 kda and 135 kda. The smallest band at 75 kda corresponds to the OSMRβ subunit alone, while the 100 kda and 135 kda bands correspond to the OSMRβ subunit as part of the IL-31 and OSMR receptors respectively. The presence of OSMRβ in IL-31 has the potential to lead to off-target effects as an anti-OSMR therapy could bind to IL-31 as well as OSMR. However, research has shown that OSMRβ knock-out mice, while having abnormal blood count values, are viable and without significant abnormalities (87).

Because of this we expect that, while an anti-OSMR therapy may affect the IL-31 receptor, the toxicities will be minimal and acceptable.

Immunohistochemistry was performed on both primary and metastatic sites of disease and it was found that OSMR is expressed throughout the malignancy in both primary and secondary sites of disease. This combined with the overexpression of OSMR in tumor tissue compared to muscle tissue, and the low expression of OSMR in other major organs lead us to believe that OSMR is an ideal target for therapy. We also conclude that metastatic status is not an indicator of OSMR expression, as this receptor can be expressed in both metastatic and non-metastatic SS.

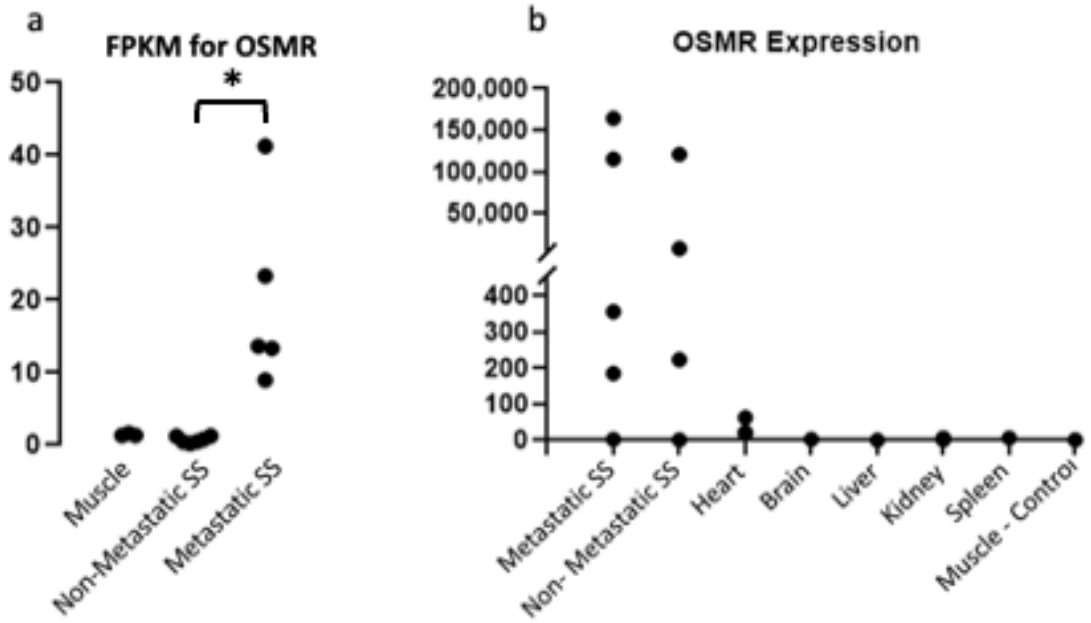

Figure 2.1 OSMR Expression is Independent of Metastatic Status. (a) RNAseq data of metastatic and non-metastatic tumors as well as normal muscle tissue shows a correlation between metastatic status and OSMR expression. * P-value < 0.05. (b) RTqPCR shows no such correlation and that both states can have high or low OSMR expression with no statistical significance found when comparing the two. Low expression of OSMR was also noted in the heart. McCollum S, Kalivas A, Kirkham M, Kunz K, Okojie J, Pavek A, et al. Oncostatin M Receptor as a Therapeutic Target for Radioimmune Therapy in Synovial Sarcoma. Pharmaceuticals. 2022 Jun;15(6):650.

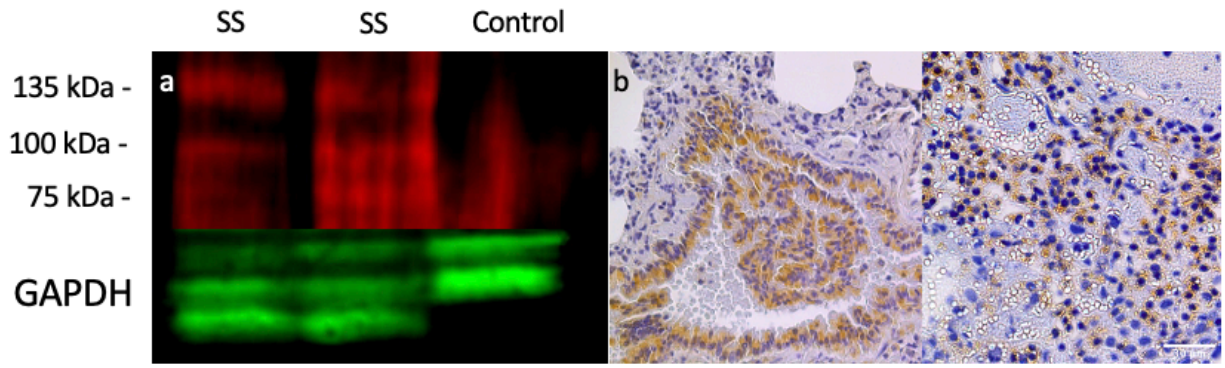

Figure 2.2 Protein expression of OSMR. (a) Western blot using immunofluorescent tags. OSMR is in red and control GAPDH is in green. Three bands were detected corresponding to the OSMR receptor (135 kda), IL-31 receptor (100 kda), and the OSMR subunit alone (75 kda). Samples 1 and 2 are metastatic tumor samples, sample 3 is normal muscle tissue. (b) Immunohistochemistry staining of lung metastasis (left) and primary tumor (right). OSMR expression stains brown in tissue samples. McCollum S, Kalivas A, Kirkham M, Kunz K, Okojie J, Pavek A, et al. Oncostatin M Receptor as a Therapeutic Target for Radioimmune Therapy in Synovial Sarcoma. Pharmaceuticals. 2022 Jun;15(6):650.

3. Synthesis of a Novel Radioimmune Therapy Targeting Oncostatin M Receptor

3.1 Introduction

Oncostatin M Receptor (OSMR) has been identified as being overexpressed in some synovial sarcomas. This overexpression is unique as SS has very few cell surface proteins which differentiate it from normal tissue due to its low mutational burden (13). Having identified a unique protein target which could be targeted through therapy, we began the synthesis of a novel radioimmune therapy (RIT). This model of therapy was chosen due the reduced potential for refractory disease, as well as the drug models' ability to act as a theranostic drug, having both therapeutic and diagnostic capabilities. The efficacy, stability, and binding ability of this novel drug were evaluated, along with the ability of this RIT to capture radioactive copper isotopes. Our results show that this drug model has potential to be an effective and novel theranostic pharmaceutical for use in OSMR expressing SS.

3.2 Methods

3.2.1 Antibody-Drug Conjugate and Antibody-Fluorescence Conjugate Synthesis

3.2.1.1 Antibody Purification

The ADC was made using a monoclonal anti-OSMR antibody (Sino Biological Cat.# 11226-R002). First, the antibodies were purified to eliminate the presence of any ions or contaminants. This was done using a Slide-A-LyzerTM dialysis cassette (ThermoFisher Cat.# 66373). Briefly, EDTA was added to the antibody sample and placed in the cassette. The cassette was then incubated in Sodium Citrate buffer 0.1 M with a pH of 6.5. The sample was removed

and concentrated using a Vivaspin 500 protein concentrator (Sartorius Cat.# VS0191) and centrifuged at 10,000 g and 4°C for 1 hour. Once protein was concentrated the concentration was measured using the Qubit 3 Fluorometer (Thermofisher 380 Cat.# Q33216).

3.2.1.2 Chelator Conjugation

After the anti-OSMR monoclonal antibody had been purified, it was incubated at room temperature in the presence of a 40 molar excess of NOTA chelator (Macrocyclics Cat.# B-605) and the reaction allowed to proceed for 2 hours. Then the reaction was moved to 4° C and allowed to incubate overnight. Once the conjugation was complete, the excess chelator was removed using a Vivaspin 500 protein concentrator (Sartorius Cat.# VS0191).

3.2.1.3 AFC Preparation

The antibody was purified as described above. Antibody-Fluorescent Conjugate (AFC) was prepared using a Zip Alexa Fluor Rapid Antibody Labelling Kit (Invitrogen Cat. Z11235) and manufacturers protocol was followed. Briefly, a 1mg/mL solution of an anti-OSMR monoclonal antibody (Sino Biological Cat.# 11226-R002) was added to a 1 M solution of Sodium Bicarbonate containing the fluorescent dye and incubated at room temperature for 15 minutes.

3.2.2 Sandwich ELISA Binding Assay

A sandwich ELISA was performed using a Human OSMR beta ELISA kit (Novus Biologics Cat.# NBP2-68083). Plate was first treated with human OSMR beta protein by adding 100 uL of 10ng/mL. Plate was incubated at 37° Celsius for 90 minutes. Liquid was aspirated

from plate and treated with AFC 0.15 µg /uL, pure OSMR antibody 0.15 µg /uL, or PBS as a control. Plate was incubated for 1 hour and liquid aspirated. Biotinylated antibody was applied to wells according to manufacturer's protocol and incubated at 37° Celsius for 1 hour. Liquid was removed and plates were washed with wash buffer according to manufacturer's protocol. HRP solution was applied to each well and incubated for 30 minutes at 37° Celsius. Plates were washed and substrate reagent was applied and incubated for 15 minutes at 37° Celsius and protected from light. Stop solution was added to each well prior to measurement on a Varioskan LUX multimode microplate reader (Thermofisher Cat.# VL0000D0). Statistical analysis was performed using a one-way ANOVA test.

3.2.3 Thermal Shift Stability Assay

Unconjugated monoclonal antibody and the conjugated ADC were prepared in sodium citrate buffer at 25mM, 50mM, 75mM and 100mM. Each concentration of sodium citrate was brought to a pH of either 6.5, 7.0, 7.5 or 8.0. Each sample condition was run in triplicate in a 96 well plate and included SYPRO Orange dye (Sigma-Aldrich Cat.# S5692) at a concentration of 5x. Plate was analyzed using an Eppendorf Mastercycler Realplex2 where the temperature was steadily increased from 30°C to 95°C over the course of 20 minutes. Results were analyzed using a one-way ANOVA test.

3.2.4 Copper^{67} Isotope Capture

^{67}Cu was provided by the Idaho Accelerator Center in HCl. The isotope was added to the immunoconjugate in sodium citrate buffer and incubated at room temperature for 20 minutes to allow for capture.

3.2.5 Thin Layer Chromatography

Thin layer chromatography was performed using instant thin layer chromatography plates (iTLC) to separate the compounds (Agilent Cat.# SGI0001) Briefly, the sample was placed at the origin and allowed to dry for roughly 5 minutes. Then the plate was placed in buffer and allowed to develop. Once finished, the plate was cut into sections and each section measured for radioactivity using a Ludlum 3030 sample counter. For definition experiments, the plate was cut into three pieces (top, middle and bottom) and the activity found on the middle section measured to determine the level of definition. For copper capture experiments, the plate was cut into two pieces and the ratio of activity on the bottom vs the top was compared. Background radiation measurements were performed approximately every 10 minutes.

3.3 Results

In order to achieve high specificity for the treatment target and eliminate side effects caused by off-target effects, an anti-OSMR monoclonal antibody was selected as the main structure of this RIT therapy (Figure 3.1). Next, the literature regarding multiple chelators was analyzed to identify which would have the best stability, binding ability and copper capture rate. Based on research comparing bifunctional chelators performed by Cooper et al (177), we considered multiple chelators including p-SCN-Bn-DOTA, p-SCN-Bn-NOTA and sar-CO2H. However, we ultimately decided to move forward with the p-SCN-Bn-NOTA chelator, referred to hereafter as NOTA, due to its high serum stability, efficient radio-labeling and ideal metabolism (Figure 3.2 a). Due to the added challenge of performing pre-clinical studies with a radioactive agent, we also developed an Antibody-Fluorescent Conjugate (AFC), in which the

chelator was replaced with the fluorescent molecule, Alexa Fluor 647, which could be detected and used as a measurement of the presence of the conjugate in a safer manner (Figure 3.2 b). This fluorophore binds to the same residues as NOTA and should mimic the properties of the conjugate without being radioactive and is measurable through fluorescent excitation.

A sandwich ELISA binding assay was performed to assess the ability of the conjugate to bind to its target OSMR receptor post conjugation, and to ensure that the addition of a moiety to the lysine residues of the antibody did not interfere with binding. To do this, the AFC was applied to a sandwich ELISA containing OSMR protein and binding was measured through fluorescent excitation. We found that the AFC was capable of binding to the protein showing that the attachment of groups to the lysine residues of this antibody does not interfere with the binding capabilities of the drug (Figure 3.3).

Next the stability of the ADC was tested through a thermal-shift assay. This assay was performed in the absence of radioactive materials due to the ^{67}Cu limited effects on the stability of the antibody. Samples of the ADC were placed in sodium citrate buffer at varying concentrations and pH's to determine which conditions provide the most stable environment. The rate of denaturation of the proteins was measured through detection of Sypro Orange fluorescent dye. It was found that the ADC was most stable in sodium citrate at a concentration of 100 mM and a pH of 6.5; (Figure 3.4 a), however it was also found to be stable at a variety of different conditions. Results were analyzed using a one-way ANOVA test and no statistically significant difference was observed between the ADC and the mAb. We determined that the conjugation of the NOTA chelator did not greatly affect the stability of the antibody, with only a minimal decrease in the stability compared to that of the native antibody (Figure 3.4 b).

To confirm the ability of the ADC to efficiently capture Copper^{67} ions, thin layer chromatography was utilized. After allowing the ADC to associate and capture copper isotopes, samples were placed on iTLC plates, a glass microfiber paper with silica gel. After elution of the samples, the plates were cut in half and the radioactivity of the free copper at the top of the plate was compared with the activity of the captured copper at the bottom of the plate (Figure 3.5 a). Because the literature is variable in which buffers would be best for such an experiment, multiple buffers were tested, and the definition achieved on the plate under different conditions was measured. We found that a Sodium Citrate buffer provided the best results (Figure 3.5 b).We found that the ADC was able to capture ^{67}Cu somewhat efficiently, and that the capture rate was concentration dependent requiring an excess of ^{67}Cu (Figure 3.6).

3.4 Discussion

As described in section 2, the cell surface receptor protein OSMR has been identified as being overexpressed in some SS cases and has been shown to be an ideal target for therapy. We elected to target this protein with an RIT model of therapy. An emerging field in biological pharmaceuticals, RIT uses antibodies to direct radiation directly to the site of disease (211)(176). After systemic injection of an RIT, the drug then circulates throughout the body finding all sites where the antibody can bind. This means that the drug will not only have high specificity for its target but will also be able to find all sites of metastasis (187). Once bound to the malignant cells, the radiation can kill the bound cell as well as the surrounding cells, regardless of their epitope expression (212). Theoretically this will result in lower rates of drug resistance and refractory disease. Furthermore, the effects of radiation on peripheral cells which survive the

radiation but experience enough exposure to induce mutational effects could lead to increased antigenicity of the cells, causing an immune response against them (213).

We have developed an RIT model therapy which targets OSMR using an anti-OSMR monoclonal antibody conjugated to the bifunctional chelator NOTA. This chelator was selected after extensive review of the literature, and was ultimately selected for its stability, ease of conjugation, and high isotope capture efficiency (177). NOTA has one of the highest serum stabilities of all the bifunctional chelators, and its radiolabeling efficiency has been found to be approximately 99%, which is typical of bifunctional chelators (177). NOTA conjugates to lysine residues on antibodies through a thiourea linkage, and no catalyst is needed to drive this reaction. Instead, only a molar excess of chelator to antibody is required, making this reaction simple and cost effective.

Within the drug model, this chelator is used to capture the radioisotope $Copper^{67}$, which is a beta radiation emitting isotope capable of damaging tissues which are in close proximity. $Copper^{67}$ was chosen for many reasons; a beta emitter was desired for its short-range radiation effects, as the therapy should only affect the tissues it is in direct proximity to in order to avoid off-target effects. It also has an ideal half-life of approximately two and a half days. This allows sufficient time for the isotope to be manufactured, incorporated into the RIT drug model and administered to the patient, while still being short enough to not have to strong of an effect as to cause toxicities. $Copper^{67}$, while being an ideal isotope for RIT, is not commonly produced or easily obtained. We have the unique opportunity and advantage of collaborating the Idaho Accelerator Center which is the only facility in the world to currently produce $Copper^{67}$ isotopes. This collaboration provides us with advantageous access to resources many do not have, and we chose to take advantage of this opportunity to develop a novel therapy.

In addition to the RIT, we also elected to develop and antibody-fluorescence conjugate (AFC). This AFC uses a fluorescence moiety which also binds to the lysine residues of the antibody, and so has the same binding sites as the NOTA chelator. Thus, the AFC has similar properties to the RIT, however, does not contain any radioactive components. This improves the safety when studying this novel drug model where the radioactive components are not necessary. It also aids in the visualization of drug distribution as the fluorescence moiety is visible with nIR.

Because additional moieties had been conjugated to the anti-OSMR monoclonal antibody, the binding ability of the ADC was tested through a sandwich ELISA binding assay to ensure that the additional groups were not interfering with the antibodies' ability to bind to OSMR. Through use of the AFC, we were able to show that this drug is able to bind to OSMR with the additional moieties (Figure 3.3). A one-way ANOVA test was performed and a p-value of < 0.05 was observed. This suggests that the drug will be able to bind efficiently to its target *in vivo* and reduce the potential for off-target effects.

The stability of the ADC was also evaluated and compared to the antibody through the use of a thermal shift assay. The drug was tested under multiple conditions, and it was determined that is was most stable in Sodium citrate buffer at a concentration of 100 mM at a pH of 6.5 (Figure 3.4 a). When compared to the stability of the naked antibody, no statistically significant difference was observed and the antibody-chelator conjugate was stable up to a temperature of 75° Celsius which is sufficient for therapeutic use (Figure 3.4 b). This data indicates that the RIT will be stable *in vivo* and that the chelator will not disassociate from the antibody after administration.

Finally, we evaluated the ability of this novel RIT to capture isotopes efficiently. Through collaboration with the Idaho Accelerator Center, we first worked to develop an assay

which could test this quickly and cost-effectively. Thin layer chromatography (TLC) was selected as the RIT could be easily separated from the free, uncaptured Copper^{67} isotopes (Figure 3.5 a). Because the RIT structure is so large, when placed at the origin on the TLC plate, it is unable to travel up the plate with the solvent front. Therefore, any radioactivity observed at the origin of the plate can be attributed to isotopes which are captured by the conjugated NOTA chelator, while the free and uncaptured copper isotopes are small enough to move with the solvent front and would be detected at the top of the plate.

Because there is currently no literature which describe methods similar to these which we could reference, we tested multiple buffer types using this method (Figure 3.5 b). We aimed to determine which buffer would provide the best definition on the plate with little radioactive material being seen in the middle of the plate, between the origin and the solvent front. Of the buffers tested, we found that sodium citrate yielded the best plate definition and used this buffer moving forward.

Using these methods, the percentage of Copper^{67} isotopes captured by the RIT was measured (Figure 3.6). Our data shows that the RIT did not have efficient copper capture until an excess of 15 times more copper as antibody. This data is not in line with what is seen in the literature with others reporting much higher rates of capture (177)(214). We plan to revisit this and hope to improve our capture rate in the future.

One hypothesis for why our capture rate is decreased is that the RIT used in those experiments had degraded. Having a biologic protein component in the anti-OSMR antibody results in the possibility for the drug to degrade if not stored at optimal temperatures. Further supporting this hypothesis is LC-MS data of the RIT run by the University of Arizona, which indicated that the antibody had denatured into smaller fragments (data not shown). To combat

this in the future, thermal shift assays will be performed on each batch of new RIT synthesized to ensure that the drug is intact.

These results suggest that an anti-OSMR RIT can not only be successfully synthesized, being both stable and capable of $Copper^{67}$ capture, but will be able to treat SS as a systemic therapy. We feel that this model of therapy is beneficial for those with few treatment options and is ideal for treating tumors with heterogenous mutations as RIT can induce cell death in cells through a mechanism of proximity rather than altering a metabolic pathway. Further research is required to optimize the synthesis of this therapy; however, the promise of these results indicate the need to continue this research.

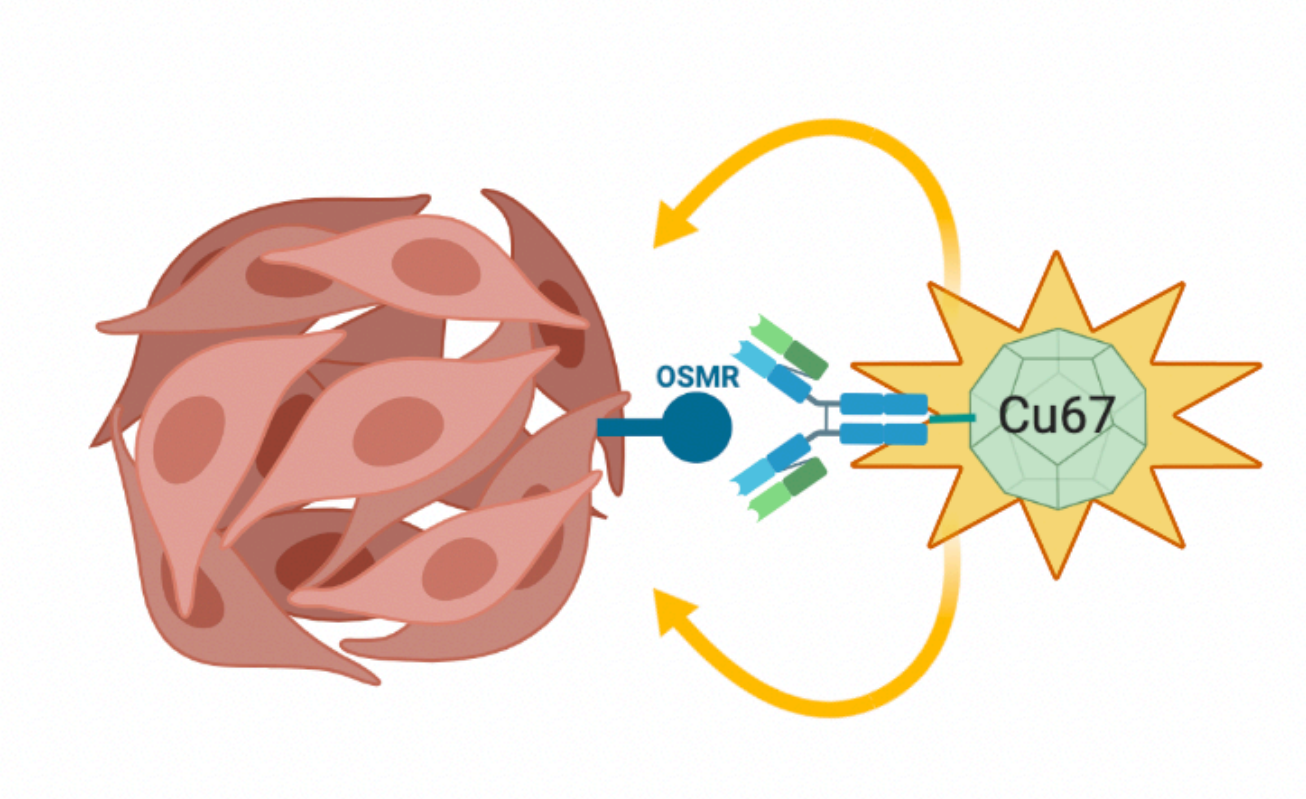

Figure 3.1 Illustration of Radioimmune Therapy Drug Model. An anti-OSMR monoclonal antibody conjugated to Copper^{67} captured by the NOTA chelator is shown bound to the OSMR protein allowing radiation from Copper^{67} to kill the sarcoma cells. Image created with Biorender

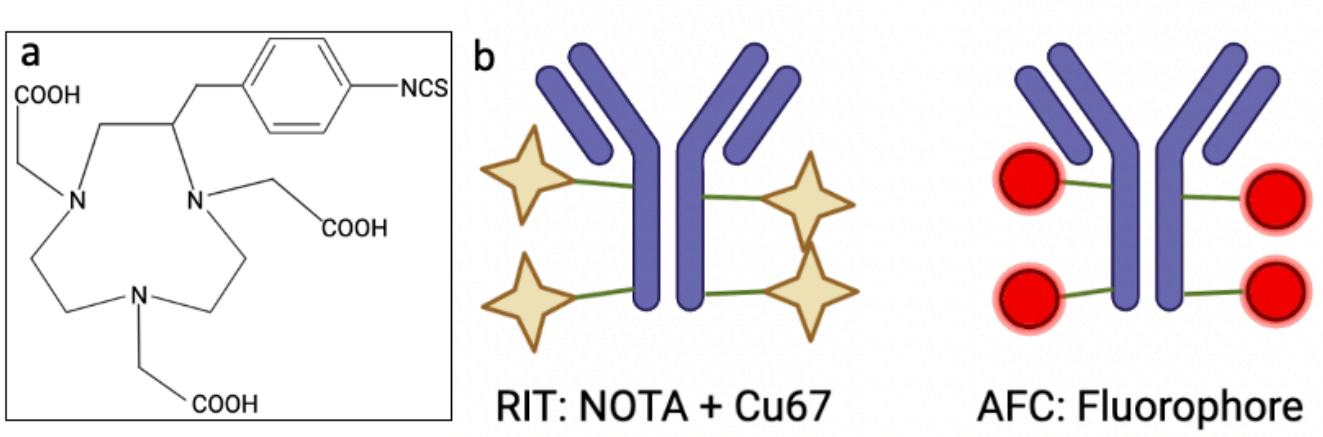

Figure 3.2 Schematic of Radioimmune Therapy. (a) Chemical structure of p-SCN-Bn-NOTA. (b) Illustration of the Radioimmune Therapy (RIT) and Antibody-Fluorescent Conjugate (AFC). Images created with Biorender.

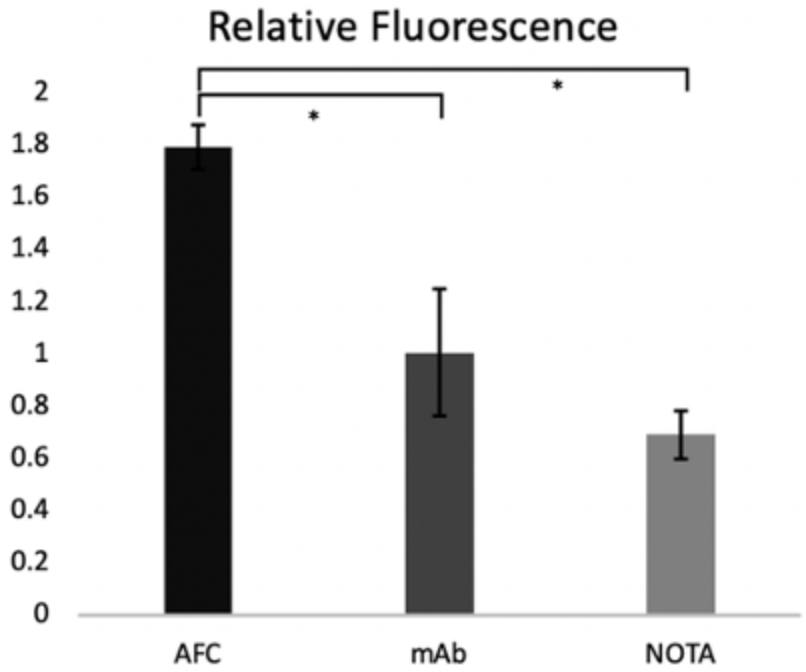

Figure 3.3 Sandwich ELISA Binding Assay. Relative fluorescence of the AFC, monoclonal antibody and chelator measured by sandwich ELISA. * P-Value < 0.05. McCollum S, Kalivas A, Kirkham M, Kunz K, Okojie J, Pavek A, et al. Oncostatin M Receptor as a Therapeutic Target for Radioimmune Therapy in Synovial Sarcoma. Pharmaceuticals. 2022 Jun;15(6):650.

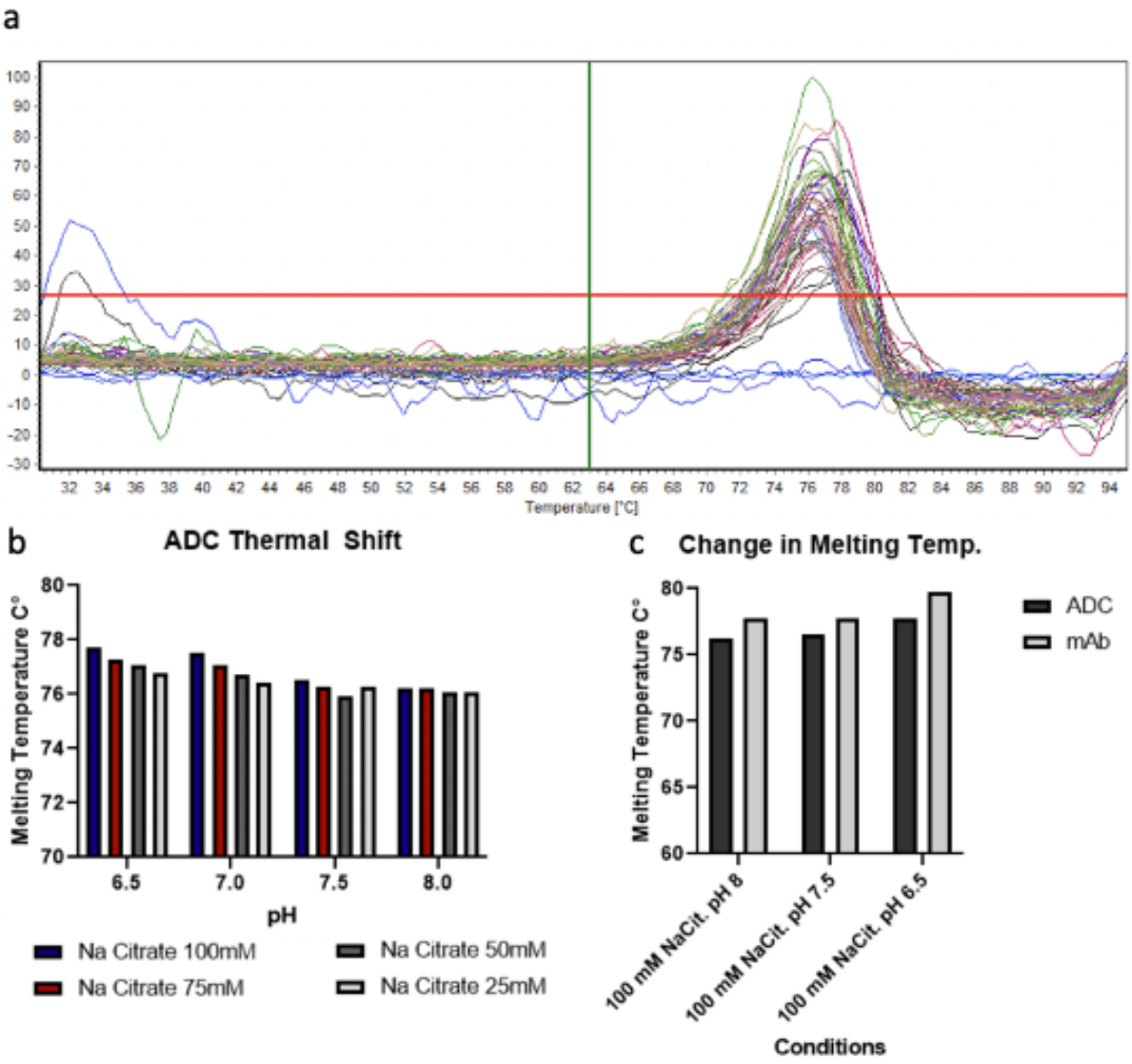

Figure 3.4 Stability of ADC Under Different Conditions. (a) Raw data from thermal shift assay graphing the denaturation of the antibodies as temperature increases. (b) Melting temperature of the RIT in various conditions, the conjugate was found to be stable under various conditions with no statistical significance noted between buffer concentrations or pH. (c) Change in melting temperature of the RIT as compared to the unconjugated monoclonal antibody no statistical significance was observed when comparing the unconjugated antibody to the ADC.

McCollum S, Kalivas A, Kirkham M, Kunz K, Okojie J, Pavek A, et al. Oncostatin M Receptor as a Therapeutic Target for Radioimmune Therapy in Synovial Sarcoma. Pharmaceuticals. 2022 Jun;15(6):650.

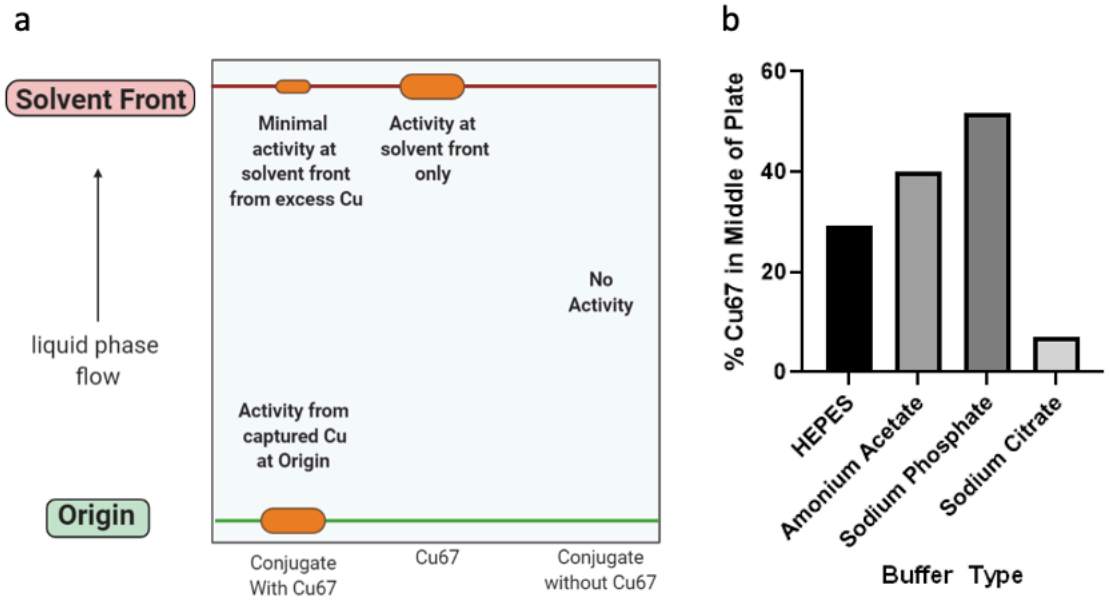

Figure 3.5 Copper Capture Measurement Experimental Design Using Thin Layer Chromatography. (a) Illustration of how TLC tests were performed. (b) Results of testing multiple buffer types for best definition achieved on TLC plate. Best definition was measured as the conditions with the least amount of radioactivity in the middle of the TLC plate. McCollum S, Kalivas A, Kirkham M, Kunz K, Okojie J, Pavek A, et al. Oncostatin M Receptor as a Therapeutic Target for Radioimmune Therapy in Synovial Sarcoma. Pharmaceuticals. 2022 Jun;15(6):650.

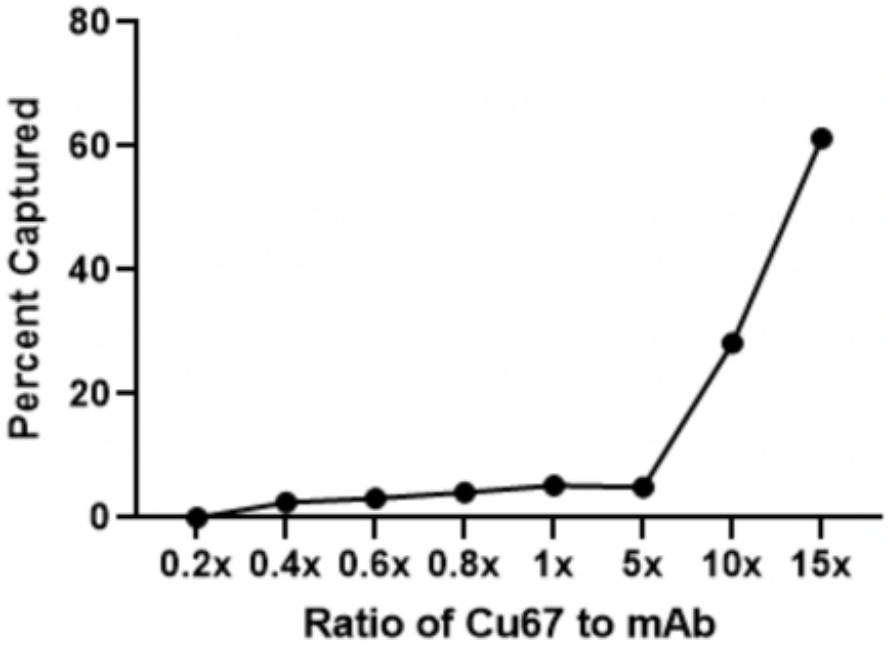

Figure 3.6 Copper Capture Results. Graph showing percentage of total copper captured as ratio of Copper^{67} to monoclonal antibody increases. McCollum S, Kalivas A, Kirkham M, Kunz K, Okojie J, Pavek A, et al. Oncostatin M Receptor as a Therapeutic Target for Radioimmune Therapy in Synovial Sarcoma. Pharmaceuticals. 2022 Jun;15(6):650.

4. Evaluation of the Pharmacokinetics and Pharmacodynamics of the Novel RIT

4.1 Introduction

Radioimmune therapy is a form of systemic radiation therapy which has been gaining interest in recent years. In the previous chapter, we established that an anti-OSMR RIT can be synthesized effectively and is stable and capable of isotope capture. Having successfully constructed this therapy, we evaluated the ability of this drug to bind to OSMR *in vitro* as well as the pharmacokinetics of this RIT *in vivo* using SS mouse models. To reduce the risk of radiation exposure, some experiments were carried out with the AFC described in section 3. We found that this drug is well targeted to sites of disease, even being observed in previously unknown sites of metastasis. We believe that this form of therapy has great potential for treating SS and may provide another option of therapy for patients with recurrent disease.

4.2 Methods

4.2.1 Cell Cultures

Cell cultures were maintained using an ThermoFisher Forma™Series II Water-Jacketed CO2 Incubator (ThermoFisher Cat.# 3130). Cultures were monitored daily and passaged when cells reached 80% confluency. Passaging was performed using a Labconco Purifer Class II Safety Cabinet (Labconco Cat.# 36209-04) and 1-2 million cells were transferred to a new culture dish to maintain the cell line. DMEM media with 10% Fetal Bovine Serum and 1% Penecillin-Streptomycin was used.

4.2.2 *In Vitro* AFC Assay

Cells were plated in a 96-well plate at a concentration of 10,000 cells per well and allowed to incubate at 37° C for 24 hours. The cell line used was Yamato synovial sarcoma. After the 24 hour incubation, the AFC was applied to the cells and incubated at 37° C for 30 minutes at a concentration of 1ug/uL in media. The media containing AFC was then removed and replaced with fresh media. The plates were placed in an ImageXpress® Pico (Molecular Devices Cat.# 1XPICO) at 37° C and monitored with photos taken every 30 minutes for a 24-hour period. Images were analyzed using ImageJ.

4.2.3 Mouse Models

Using the metastatic synovial sarcoma mouse model; Rosa26-LSL-SS18-SSX2/SS18-311 SSX2;Ptenlox5/lox5 (149), mice were selected at 4 weeks of age and injected subcutaneously with TATCre protein (Excellgen Cat.# EG-1001) in their left hind limb. Both male and female mice were used. Mice were monitored for signs of tumor development. All protocols were approved by the Idaho State University's institutional animal care and use committee protocol 775.

4.2.4 Murine 48 Hour Tumor AFC Accumulation Study

Mice from the metastatic model previously described were selected 10-14 weeks after receiving a TAT-Cre injection to their left hind limb. Mice were treated via a tail vein injection of AFC at 0.4 mg/kg or received a saline control. Mice were harvested 48 hours later and tissues imaged for AFC retention using the Azure C600 imager with nIR imaging properties. The AFC was excited at 650 nm and emission was detected at 665 nm. GFP was excited at 450 nm and

emission was detected at 510 nm. Fluorescence levels were quantified using ImageJ software and normalized to the control values.

4.2.5 Murine 6 Hour Pharmacokinetics and Blood AFC Level Study

4.2.5.1 Mouse Treatment and Sample Collection

Mice from the models previously described were selected which either had not received a TATcre injection or had not developed tumors after injection. Mice were treated via a tail vein injection of AFC at 0.4 mg/kg or received a saline control. Mice were monitored and euthanized at various time points. 7 mice were treated, 6 of which received AFC and 1 received saline control. Euthanization times were at 10 minutes, 30 minutes, 1 hour, 2 hours, 4 hours and 6 hours. One mouse was sacrificed at each time point, with the saline control mouse also being euthanized at 10 minutes. Blood draws were performed immediately through the vena cava and further dissection followed.

4.2.5.2 Whole Organ Imaging

Mice were dissected immediately after euthanization. Whole organs and tissues were imaged for AFC retention using the Azure C600 imager with nIR imaging properties. The AFC was excited at 650 nm and emission was detected at 665 nm.

4.2.5.3 Quantification of Organ AFC Retention

After imaging, 50 mg of each organ were digested with mild cell lysis buffer and homogenized mechanically. Samples were centrifuged and100 uL of the supernatant was placed in a black 96-well plate. Samples were read with a Varioskan Lux Multimode Microplate Reader

(ThermoFisher Cat.# VL0000D0). The AFC was excited at 648 nm and emission was detected at 666 nm.

4.2.5.4 AFC Blood Concentration Levels

Blood was drawn from the vena cava and placed into Greiner Bio-One MiniCollect Capillary Blood Collection System Tubes (Fisher Scientific Cat.# 22-030-402). The blood was centrifuged, and the supernatant removed and placed in a black 96-well plate and samples were read with a Varioskan Lux Multimode Microplate Reader (ThermoFisher Cat.# VL0000D0). The AFC was excited at 648 nm and emission was detected at 666 nm.

4.3 Results

To assess the ability of this novel RIT to bind to OSMR *in vitro*, the AFC was applied to SS cell cultures and monitored using an automated cell imaging system with confocal microscopy. The AFC was applied to the cells for 30 minutes and the cells washed to remove any unbound drug. The cultures were then imaged over a period of 24 hours. The AFC was observed to bind to the cells at a low concentration of 6.7 pM (1ug/uL). While cell binding was observed, it was only observed bound to a few cells per well. This is likely due to the low concentration at which these cells were dosed, and future studies at higher concentrations are planned. It is also possible that the low number of cells observed bound to the AFC is due to heterogeneity within the cell culture resulting in only some of the cells expressing OSMR. Further studies will be required to determine the proper dosing for this AFC in cell cultures. The

drug was able to be observed bound to the cells immediately after the 30-minute incubation and wash and was observed up to 22 hours.

Next, the pharmacokinetics of the RIT were assessed using a metastatic mouse model for SS. Four mice were selected which had received a previous TATCre injection and had developed tumors of sufficient size. The AFC was injected intravenously through the tail vein and mice harvested 48 hours later. The mice were dissected and the tumors along with kidneys, liver, spleen, lungs and heart were harvested and imaged through nIR fluorescence. Because the mouse model has a genetic modification which induces the expression of Green Fluorescence Protein (GFP) in SS cells, the malignancies could be easily observed, and some areas of metastasis were noted in the spleen of the AFC-3 mouse (Figure 4.2 a). Next, imaging of the AFC was performed, and it was noted that there was exceptional targeting of the drug to sites of disease, with no drug seen accumulating in significant quantities in any other areas. It was also noted that the drug not only localized to the primary tumor site but was also present in the sites of metastasis. Outside of the sites of disease, no accumulation of the AFC was seen in any other organs (Figure 4.2 a). The fluorescence of the organs was quantified using image J software and the value for each organ was normalized to its corresponding control tissue (Figure 4.2 b). It was confirmed that little AFC was seen accumulating outside of tumor tissue. These results indicate that an anti-OSMR antibody is an effective targeting strategy for therapy in SS. This study used both male (n=3) and female (n=1) mice and no differences were observed between the two. The control mouse was male.

Having seen AFC accumulation in the spleen of one mouse, we next confirmed that these nodules were in fact SS metastasis. Using immunohistochemistry, we stained the tissue for the presence of GFP, an indicator of the presence of the t(X:18) translocation mutation which causes

SS. We found that GFP was present (Figure 4.3 a) indicating that these nodules were sites of SS disease, and that the AFC was efficiently being directed to both the primary and metastatic sites of disease.

Because varying levels of AFC uptake were noted in the murine pharmacokinetic study, we next evaluated the correlation between OSMR expression and AFC uptake. Using Reverse Transcriptase Quantitative Polymerase Chain Reaction (RTqPCR), the RNA levels of OSMR expression were measured of each of the four tumors. We found that the OSMR expression correlated to the uptake of AFC noted in the pharmacokinetic study, indicating that the AFC was directed to sites of disease via the anti-OSMR antibody rather than another mechanism (Figure 4.3 b). It was also noted that despite some of the tumors having low levels of OSMR expression, the AFC was still capable of targeting the disease with high specificity suggesting that even tumors with low levels of OSMR expression would be a candidate for this therapy.

Finally, the blood and tissue concentration of the AFC was measured in mice over time. The AFC was injected, and mice harvested at time points ranging from 10 minutes to 6 hours. Both male and female mice were used and no differences were observed between the two. Through fluorescent imaging of whole organs, it was observed that the AFC began accumulating in the kidneys after 10 minutes, and was cleared from the kidneys after approximately 4 hours (Figure 4.4). We also saw that the AFC began to accumulate in the liver at 1 hour and was fully cleared by hour 6 (Figure 4.4). To quantify these results, the organ tissue was homogenized and the fluorescence measured with a Varioskan Lux plate reader. This data confirmed that the highest AFC concentration was found in the kidney at approximately 1 hour, and that this accumulation dissipated by hour 4. Similarly, the accumulation in the liver peaked at hour 4 but dissipated by hour 6 (Figure 4.5 a). The AFC concentration of the blood was also measured, with

a high concentration seen early on at time points 10 and 30 minutes, however this decreased greatly by 1 hour and continued to decrease being nearly undetectable by hour 6 (Figure 4.5 b). This, paired with our data which shows that the AFC showed a high accumulation in sites of disease even 48 hours after administration, shows that this drug is metabolized well by the body and quickly directed to the tumor where it remains for a sufficient amount of time.

4.4 Discussion

SS is a deadly disease which currently has few FDA approved therapeutic options. Here we show that our novel RIT which targets OSMR has potential as a therapy for SS. Through *in vitro* studies, we have shown that the AFC is capable of binding to cells for up to 22 hours at extremely low concentrations (Figure 4.1). This indicates that's the RIT will be able to bind to SS cells for a sufficient time to deliver its radioactive payload and induce cell death.

Through *in vivo* studies using a murine model, the AFC was visualized through NIR imaging. It was found that the AFC had excellent targeting to sites of disease, being found in both the primary tumor as well as metastasis which was found in the spleen (Figure 4.2 a). Furthermore, no accumulation was seen in other organs suggesting that the RIT will have sufficient targeting to sites of disease and will limit off-target effects which could induce toxicities (Figure 4.2 b). Varying degrees of AFC accumulation were noted in the tumor samples of this study. To further explore this accumulation, the OSMR expression levels of the tumors were evaluated, and it was found that the tumors with a higher OSMR expression level had a higher amount of AFC accumulation (Figure 4.3 b). This data suggests that the anti-OSMR monoclonal antibody is an effective targeting system for this therapy, and will direct the

radioisotopes to only sites of disease. Because of this, this therapy is unlikely to have off-target effects which may result in toxicities.

Finally, the tissue and blood accumulation of the AFC was evaluated. By measuring the AFC concentration in various organs and the blood at different time points after treatment, we were able to show that the AFC passes through both the kidneys and liver in under 6 hours. We also found that the blood concentration of the AFC steadily decreases after injection reaching a nearly undetectable level by hour 6. Because of this, we believe that the RIT will be adequately metabolized and directed to sites of disease quickly, limiting the time for the radioisotope to affect non-diseased tissues.

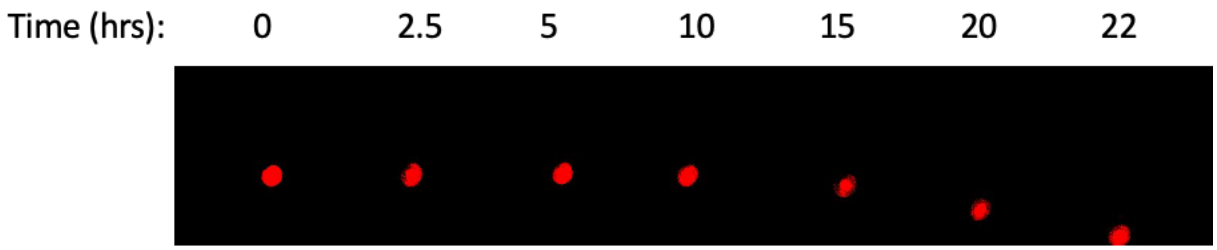

Figure 4.1 *In Vitro* AFC Binding Assay. The AFC was applied, and cells imaged every 30 minutes. The AFC appears red and is bound to the outer membrane of the cell.

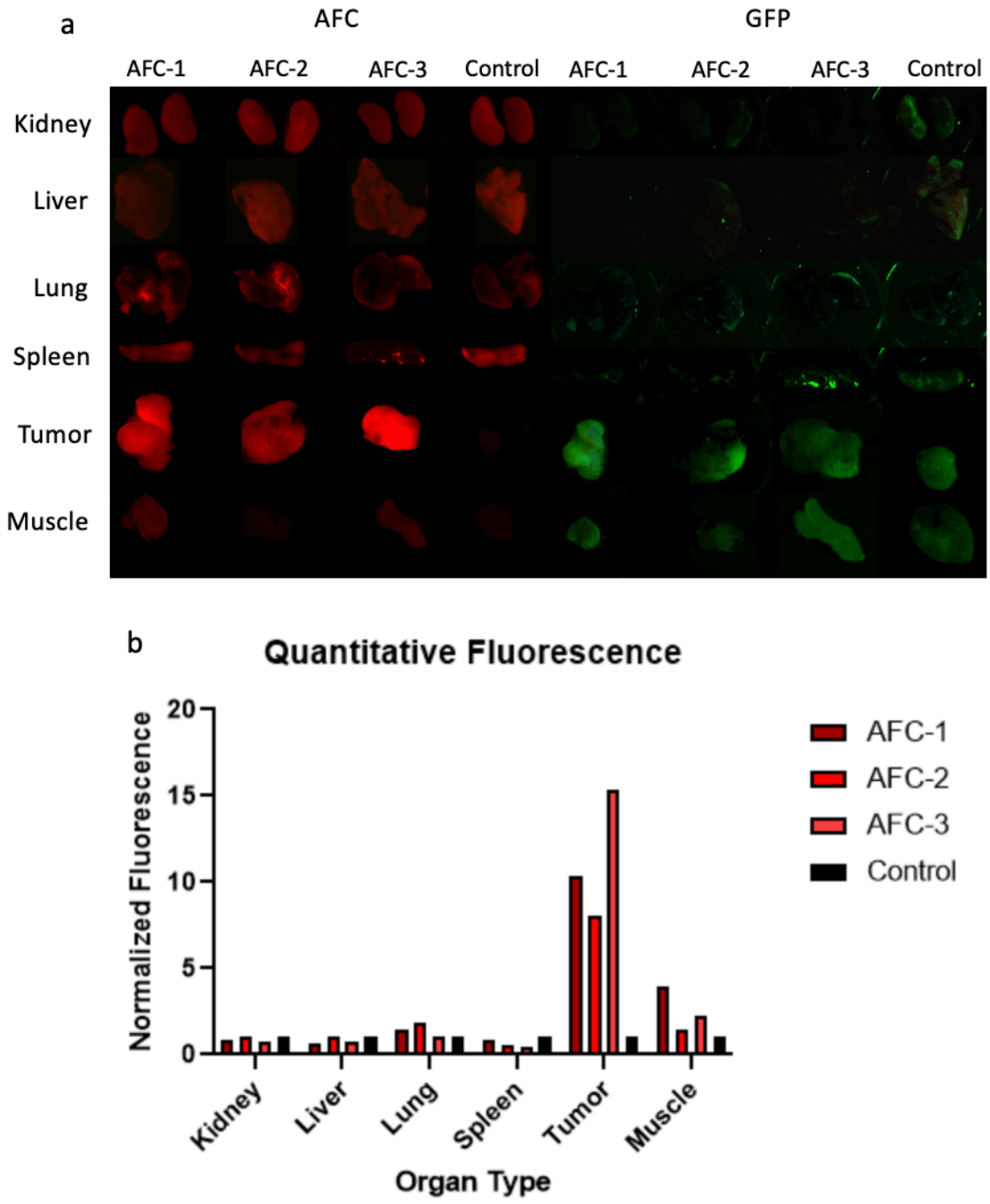

Figure 4.2 Visualization of Pharmacokinetics of the AFC in Mice. (a) Fluorescent imaging of mouse organs after treatment with either AFC or control. Samples 1-3 received AFC treatment and sample 4 received saline control. AFC appears red (Left) and SS tissue appears green due to GFP (Right). McCollum S, Kalivas A, Kirkham M, Kunz K, Okojie J, Pavek A, et al. Oncostatin M Receptor as a Therapeutic Target for Radioimmune Therapy in Synovial Sarcoma. Pharmaceuticals. 2022 Jun;15(6):650. (b) Quantification of fluorescence from figure 4.2 a. Each tissue type is normalized to the corresponding control.

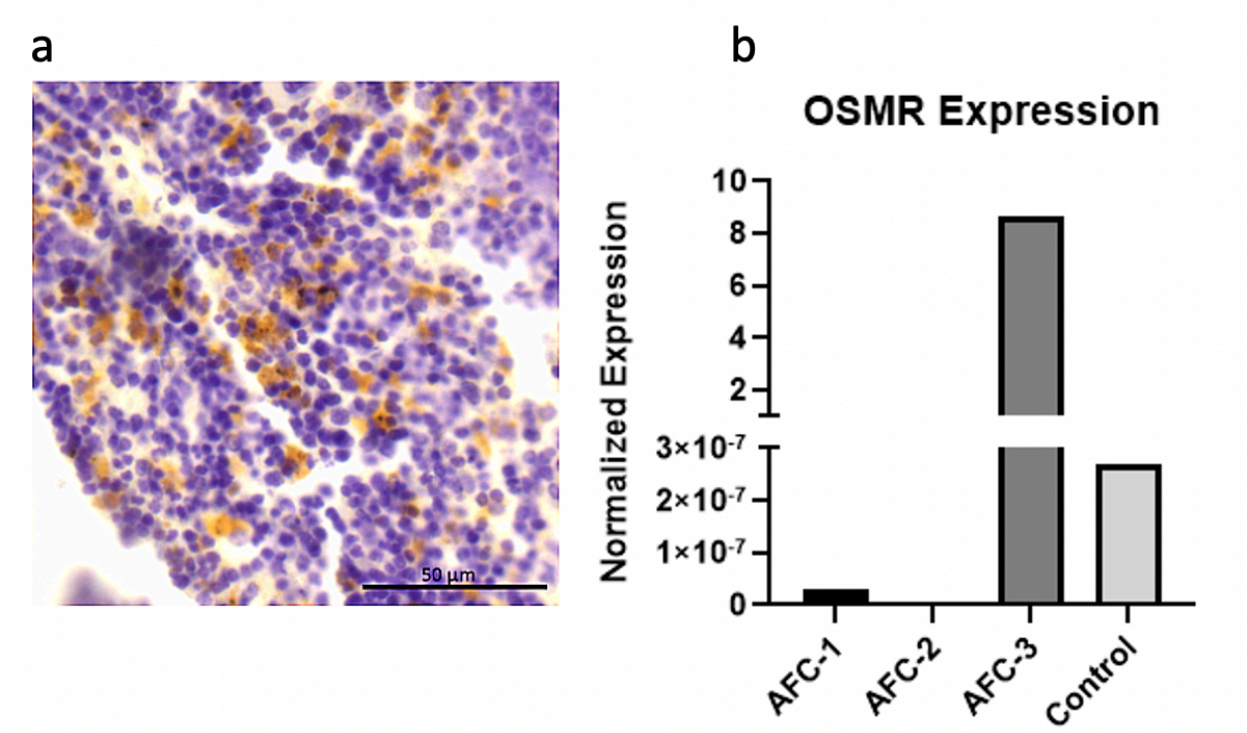

Figure 4.3 Evaluation of OSMR Expression as Compared to AFC Accumulation. (a) Immunohistochemistry of spleen metastasis for GFP from AFC- 3 sample. GFP presence indicates sites of disease and appears brown. (b) RTqPCR data showing expression levels of OSMR. AFC and Control samples correlate to Figure 4.2. McCollum S, Kalivas A, Kirkham M, Kunz K, Okojie J, Pavek A, et al. Oncostatin M Receptor as a Therapeutic Target for Radioimmune Therapy in Synovial Sarcoma. Pharmaceuticals. 2022 Jun;15(6):650.

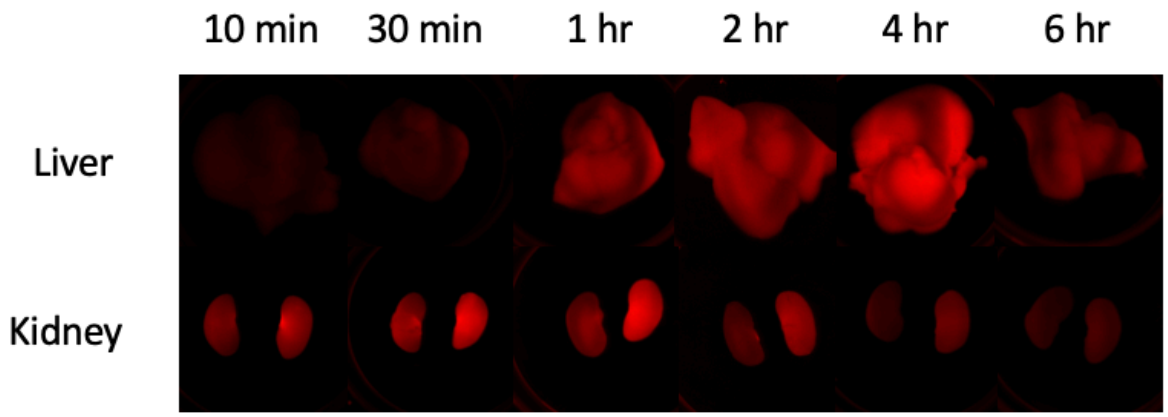

Figure 4.4 Visualization of Renal and Hepatic AFC Accumulation Over Time. Fluorescent imaging of mouse organs after treatment with AFC. Mice were euthanized and organs harvested at various timepoints and imaged. AFC appears as red fluorescence.

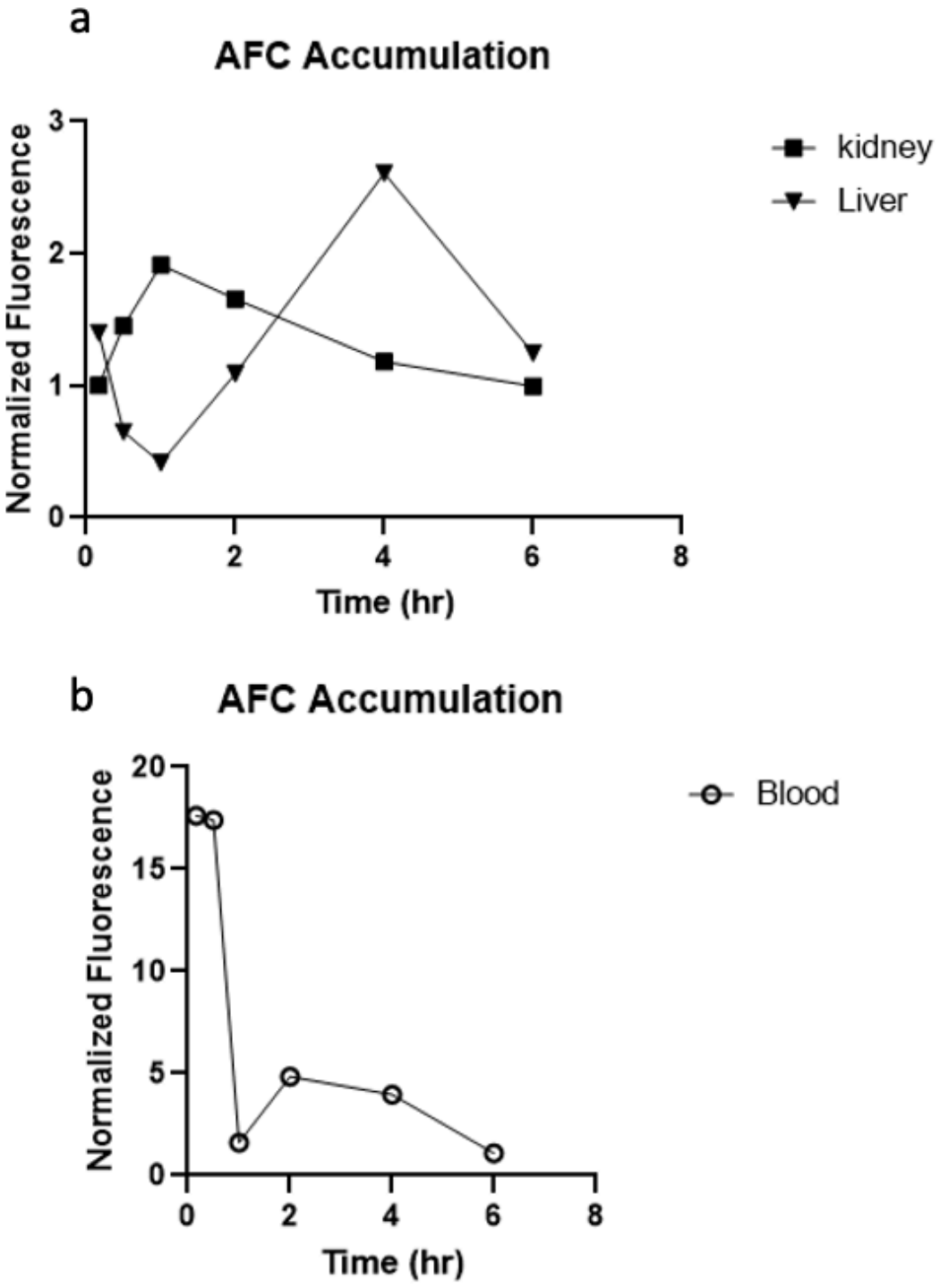

Figure 4.5 Quantification of AFC Accumulation in the Tissues and Blood. (a) AFC accumulation seen in the kidney and liver over time. (b) AFC accumulation seen in the blood over time.

5. Conclusions

5.1 The Present State of Synovial Sarcoma Treatment

Synovial sarcoma is a rare pediatric cancer which has affected many adolescents and young adults. While the current standard of care for this disease, doxorubicin in combination with an ifosphamide based therapy, gives patients a 5-year survival rate of 60%, this statistic drops dramatically if the disease metastasizes (215). While this therapy regime has found success in the treatment of SS, there are many complications which can occur with treatment. As the only option for systemic treatment for SS, if a patient does not respond or develops refractory disease, they are left with no other options for systemic treatment, highlighting the need for advancement in this field. Furthermore, doxorubicin has a lifetime cumulative dose limit due to cardiotoxicities, which limits the amount of treatment a patient can receive (216). These complications could be circumvented by the addition of another systemic treatment option to the field of synovial sarcoma.

One challenge in developing novel therapies for SS treatment is the low mutational burden of SS. With a median TMB of 1.7 mutations per Mb, there are very few aberrantly expressed proteins unique to the diseases tissue which could be targeted (205). This is one contributing factor for why only generally cytotoxic agents are currently used to treat SS. However, if a novel protein target could be identified which is specific to SS tissue, it could be targeted with therapy. This would not only provide patients with another treatment option, but would likely have fewer side effects due to its specificity, increasing the likelihood that a patient would be able to continue the therapy for longer.

SS is a unique cancer in that it is driven by a single translocation mutation t(X:18) which does not result in any targetable mutated proteins (217). Affecting only the SS18 protein in the SWI/SNF complex, this mutation causes redirection of the complex resulting in far reaching and convoluted epigenetic changes(8)(11). These changes are not easily reversed making the most common driving mutation of SS unavailable for targeting.

Despite the challenges in developing novel therapies for SS, there are many ongoing clinical and pre-clinical trials investigating new strategies to treat SS. As discussed in chapter 1.3, there are multiple pre-clinical studies investigating the use of RTK inhibitors in the treatment of SS. While these studies show promise, preliminary results have shown that many of these drugs may have difficulty with refractory disease development, as there are multiple RTK pathways which a malignancy can use to proliferate. Some drugs, such as anlotinib, try to combat this by actin across multiple RTK receptors to prevent refractory disease and have found more success (33). Perhaps with more data, these types of therapies will make their way into the clinic.

Another approach currently being undertaken to treat SS is that of the SPEARHEAD-1 phase II trial which is investigating the use of CAR-T therapy in the treatment of synovial sarcoma (43). This trial is using T cells which are genetically altered to target the testis antigen MAGE-A4 which has been found to be upregulated in some SS's. CAR-T therapy has been an very promising strategy in the field of oncology, and has the potential to change the way we treat solid tumors. While these strategies show great promise for improving the chances of survival for synovial sarcoma patients, the lack of protein targets which can be targeted by therapy continues to be a problem in this field. However, in my research, I have identified the cell surface receptor OSMR as being overexpressed in SS making it a viable target for therapy.

5.2 The Identification of OSMR as a Viable Target for Therapy

Oncostatin M Receptor is a member of the IL-6 family of receptors and is known to activate the JAK/STAT pathway (98) (129), which has been identified as a driving pathway for cancer (56)(57)(58). OSMR was identified as being overexpressed in SS through RNAseq analysis focusing on inflammatory pathways to identify new protein targets which might be targeted by therapy (149). Interestingly, while the RNAseq data suggested that OSMR was only expressed in metastatic tumors, further investigation into this expression pattern through RTqPCR and western blot indicated that both metastatic and non-metastatic tumors can express high levels of OSMR, however this expression can vary widely between samples. (Figure 2.1 and 2.2) While the metastatic status of the SS may not indicate OSMR expression, our data suggests that there is sufficient evidence that OSMR is highly expressed in a subset of SS and is a viable target for therapy.

While small molecule inhibitors have been a great benefit to the field of targeted therapy in oncology, the binding mechanism of OSM to its receptor suggests that this may not be an ideal model of therapy for this receptor. OSM first interacts with the gp130 subunit of the receptor, a subunit which is characteristic of all IL-6 receptors (133)(99). Because of this, an OSM-like small molecule inhibitor could potentially interfere with the action of any IL-6 receptor, causing excessive toxicities. Due to this binding mechanism we elected to target this receptor through RIT.

5.3 Development of a Novel RIT Targeting SS

RIT is an up-and-coming therapy model in the field of oncology. While not a new idea, it has long laid dormant as the only FDA approved RIT's are for hematological cancers (153)(155). However, recently it has seen more attention as many pre-clinical studies are investigating its use

in various cancers, including solid tumors (see Chapter 1.7.2). The versatility of this drug model certainly accounts for some of this increased interest, as many of the components may be altered or switched out to suit the needs of researchers and patients.

We elected to use this model of therapy to target OSMR in SS due to the specificity of the main structural antibody for its target, which will likely reduce toxicities. Using a monoclonal anti-OSMR antibody as the main structure of this drug, we then conjugated the chelator NOTA, selected for its stability, capture efficiency and conjugation rates (177), to this antibody in order to be able to capture radioisotopes. Given our access to the Idaho Accelerator Center and our collaboration with them providing us unique access to ^{67}Cu isotopes, we chose to incorporate this isotope into our RIT. ^{67}Cu is an ideal isotope for use in RIT given its half-life and beta emitting qualities.

We have synthesized and evaluated this novel RIT and have shown that it is capable of binding to OSMR (Figure 3.3). We have also shown that this drug is stable under various conditions (Figure 3.4) and is capable of ^{67}Cu isotope capture (Figure 3.5 a). Because of variable literature on the subject, we have tested multiple methodologies in TLC to determine the best way to measure the isotope capture (Figure 3.5 b), however more research is needed in order to determine how to improve the capture rates and increase the rates to what is seen in the literature (Figure 3.6). Despite this setback, we feel that this data indicates that an anti-OSMR RIT is capable of being synthesized, and is a viable therapy for the treatment of SS.

5.4 Preclinical Studies of a Novel Anti-OSMR RIT

Having determined that OSMR is overexpressed in some synovial sarcomas, and that an RIT model of therapy can be synthesized without the antibody losing its binding ability or stability, we began evaluating the pharmacokinetics of this drug in both *in vitro* and *in vivo* studies. We have shown that the AFC is capable of binding to SS cells within 30 minutes of exposure and stays bound to the cell for 22 hours (Figure 4.1). We have also shown that the AFC is well targeted to sites of disease within our SS mouse models, binding to both the primary tumor and sites of metastasis, and being observed there 48 hours after administration. Furthermore, we did not see any drug accumulation outside of the tumors, indicating that the anti-OSMR antibody is a sufficient targeting system for this drug model (Figure 4.2). We were able to show that the AFC accumulation and binding to sites of disease is OSMR-expression level dependent, with higher OSMR expressing tumors binding more of the AFC (Figure 4.3). Finally, we have shown that the AFC does not have a prolonged accumulation in the kidneys or liver of our mouse models, with levels being nearly undetectable by hour 6. This indicates that the RIT can be sufficiently metabolized and will not linger in the kidneys or liver, reducing the possibility for toxicities in these organs. We also show that the blood concentration of the AFC is greatly reduced 6 hours after treatment, suggesting that the RIT will be quickly directed to sites of disease. Given this data, we feel confident that this RIT is a viable therapeutic option for the treatment of SS, and that future research is indicated.

5.5 Challenges and Criticisms

This dissertation presents research investigating the use of an anti-OSMR RIT in the treatment of SS. While this model of therapy shows much potential, there are many challenges and potential pitfalls of this new therapy. One of the biggest challenges for an OSMR targeted therapy is the variability in OSMR expression between samples. Figure 2.1 b exemplifies the variation seen within our own model, with some mice from both metastatic and non-metastatic groups showing high levels of OSMR expression, while others from both groups show little to no OSMR expression. It is likely that this pattern will be observed in humans as well, with some SS patients having high levels of OSMR expression and others having low expression. This suggests that this RIT therapy will not be approved for treatment of all SS tumors, but rather would be indicated only for patients with tumors exhibiting a high level of OSMR expression. It is also possible that only the smallest subset of human SS patients will show OSMR expression, and that OSMR ultimately is not an ideal target for therapy in humans. In this case, it would become necessary to select another protein target which is more abundant in human samples. RIT models of therapy possess the benefit of containing interchangeable components, and a different monoclonal antibody can become the backbone of the therapy with minor adjustments. An example of an alternate protein target is that of NY-ESO 1, which is commonly overexpressed in human synovial sarcoma patients (218). However, mice do not carry the gene for this protein (219), making it difficult to study in animal models.

During our investigation into the elimination of this RIT through the kidneys and liver, we find that the RIT has a residency time of approximately 4 hours in the kidneys and 3 hours in the liver (Figures 4.4 and 4.5). While this residency time is not exceptionally long, it is possible that the RIT begins to exert its tissue damaging effects in these organs, resulting in kidney and

liver toxicities. Further studies are indicated to evaluate the effect that the RIT will have on these organs in which the RIT is given to mice over a longer period of time, and they are evaluated for liver and kidney toxicities. An effective way to evaluate the mice for drug induced liver and kidney damages would be the methods proposed by Vasquez and Peterson, in which they use NIR fluorescent probes which bind to various markers for cell death and damage (220). While this research group accessed IVIS SpectrumCT imaging for visualization of the anesthetized mice prior to euthanization and imaging of whole organs, these protocols could be effectively adapted to the equipment currently available in the Barrott lab. After an intraperitoneal injection of the NIR probes, mice may be euthanized, and their liver and kidneys removed for NIR imaging in the Azure c600 system. Should toxicities be seen, adjustments may be required to the components of the RIT to remedy this. If these adjustments do not rectify the toxicities, another model of therapy may be called for.

The RTqPCR data presented in figure 2.1 suggests the heart as another possible organ to experience toxicities. Low levels of OSMR expression in the heart could results in this RIT binding to heart tissue as well as tumor tissue, resulting in irradiation of the heart. This type of toxicity would be concerning, especially to patients who have received a doxorubicin-based treatment in the past, as doxorubicin is also known to cause cardiotoxicities (221). Further research is indicated to evaluate the potential for cardiotoxicities with this novel RIT. One way to test this would be through the use of PET scanning with the ^{64}Cu variant of RIT, and visualizing how much, if any, RIT accumulates in the cardiac tissues. Should significant RIT accumulation in the heart be observed, it will likely be necessary to select an alternate protein target.

While there are currently FDA approved radiopharmaceuticals with similar or shorter half-lives of this proposed RIT (222)(223)(224) it is possible that the limiting half-life of

approximately 62 hours will prove a logistical challenge for the location and accessible recourses of ISU. While it is evident that these challenges are not insurmountable and have been overcome by others, should this prove challenging, another isotope with a longer half-life could be selected.

Currently the methods for conjugating this RIT rely on non-specific, stochastic, binding of the chelator to available lysine residues. This provides the benefit of easy and simple binding methods; however, the conjugation is far from regulated resulting in variation in the drug-antibody ratio (DAR) from antibody to antibody. While this variation is present in many other antibody-drug conjugates and can be accounted for, there would be benefits in altering the conjugation methods to a site-specific binding method. This can be done in a number of ways, and while these methods would be more time consuming and less cost effective, they would provide us with precisely bound chelator and known and predictable locations. One such way to initiate site-specific conjugation is with unnatural amino acids. By genetically modifying antibody-producing organisms to produce the desired antibody with the inclusion of unnatural amino acids, a conjugation method selective for these unnatural amino acids can be used (225). In this way, the location of conjugation of the chelator could be highly controlled, and the DAR regulated. This could help to overcome potential challenges with dosing, as well as variability in RIT development.

During our evaluation of this RIT, Liquid Chromatography-Mass Spectrometry (LC-MS) data provided to us by the University of Arizona indicated that our antibody-chelator conjugate had undergone degradation (data not shown). After receiving this data, we have begun to monitor our conjugate for degradation through thermal shift assays and have found that only approximately 1 in 4 conjugation reactions result in degradation. This is likely why our capture

efficiency results are decreased when compared to what is seen in the literature, and it is anticipated that once this degradation is eliminated, our capture efficiency will improve. A thorough investigation of our methods is indicated to determine which step is causing this degradation. It is possible that contamination with proteases is occurring which is resulting in enzymatic degradation. This could be avoided with the use of protease inhibitors in the conjugation reaction, and should these be found to not interfere with the conjugation, should perhaps be added moving forward. Another possibility is that the centrifugation-filtration step is too vigorous for these proteins to withstand. As of yet, degradation has not been observed in conjugation reactions which do not undergo this step, although further investigation is required to sufficiently identify this step as the culprit. Finally, as the conjugation reaction occurs at room temperature (approximately 27 °C), performing this reaction at cooler temperatures such as 4 °C may help.

5.6 Summary

Here we detail the study and development of a novel RIT. The data presented here indicates the promise of this project and the necessity for future research. In order for this project to continue, data such as the effect of the RIT on mouse tumor size and toxicity studies would need to be obtained. There is also the exciting avenue of research regarding the use of ^{64}Cu, which can be used in PET imaging.

While this RIT shows promise as a targeted therapy for SS, there will be challenges in the development and clinical translation of this drug model, which currently is not seen outside of hematological malignancies. One potential challenge is that of predicting which patients will have sufficient OSMR expression for the therapy to direct itself to sites of disease. One solution

to this would be to test the expression levels from biopsy samples, however these are not always available. This therapy model offers an elegant solution to this problem in that it is a theranostic agent. By replacing the Beta emitting ^{67}Cu with the positron emitting form of the isotope, ^{64}Cu, the RIT becomes a diagnostic agent capable of being seen on PET scans without causing tissue damage (171). By using this scanning method prior to the administration of the tissue damaging ^{67}Cu variant, patients who will experience poor targeting of the drug to their disease can be identified prior to the drug being administered. This will greatly reduce the number of patients who experience toxicities and little benefit from the drug, due to being a poor candidate for the therapy.

Another possible challenge for this therapy is the relatively short half-life of ^{67}Cu. With approximately 2.5 days to not only synthesize the drug, but also administer it into a patient with sufficient time for it to act, the logistics and development of the therapy will have to be fine-tuned for this drug to translate into the clinic. While this will be challenging, the current use and FDA approval of other RIT's and radioactive drugs shows that this challenge can be overcome (see Chapter 1.7.1).

Despite these challenges, this model of therapy has great potential in the field of oncology. Furthermore, our data show that an anti-OSMR RIT can be synthesized effectively, and that this drug shows adequate pharmacokinetics to be well tolerated and specific to SS which overexpresses OSMR. We conclude that OSMR is a viable target for radioimmune therapy in the treatment of synovial sarcoma.

Citations

1. Synovial Sarcoma: Background, Pathophysiology, Etiology [Internet]. [cited 2021 Nov 2]. Available from: https://emedicine.medscape.com/article/1257131-overview

2. Cancer of soft tissue including heart - Cancer Stat Facts [Internet]. SEER. [cited 2021 Aug 25]. Available from: https://seer.cancer.gov/statfacts/html/soft.html

3. Synovial Sarcoma - National Cancer Institute [Internet]. 2019 [cited 2021 Aug 25]. Available from: https://www.cancer.gov/pediatric-adult-rare-tumor/rare-tumors/rare-soft-tissue-tumors/synovial-sarcoma

4. Crocker DW, Stout AP. Synovial sarcoma in children. Cancer. 1959 Dec;12:1123–33.

5. Ladenstein R, Treuner J, Koscielniak E, d'Oleire F, Keim M, Gadner H, et al. Synovial sarcoma of childhood and adolescence. Report of the German CWS-81 study. Cancer. 1993 Jun 1;71(11):3647–55.

6. SS18F - Overview: Synovial Sarcoma (SS), 18q11.2 (SS18 or SYT) Rearrangement, FISH, Tissue [Internet]. [cited 2022 Jan 4]. Available from: https://www.mayocliniclabs.com/test-catalog/overview/35303#Clinical-and-Interpretive

7. Clark J, Rocques PJ, Crew AJ, Gill S, Shipley J, Chan AM, et al. Identification of novel genes, SYT and SSX, involved in the t(X;18)(p11.2;q11.2) translocation found in human synovial sarcoma. Nat Genet. 1994 Aug;7(4):502–8.

8. Kadoch C, Crabtree GR. Reversible Disruption of mSWI/SNF (BAF) Complexes by the SS18-SSX Oncogenic Fusion in Synovial Sarcoma. Cell. 2013 Mar 28;153(1):71–85.

9. Middeljans E, Wan X, Jansen PW, Sharma V, Stunnenberg HG, Logie C. SS18 Together with Animal-Specific Factors Defines Human BAF-Type SWI/SNF Complexes. PLOS ONE. 2012 Mar 19;7(3):e33834.

10. Peterson CL, Herskowitz I. Characterization of the yeast SWI1, SWI2, and SWI3 genes, which encode a global activator of transcription. Cell. 1992 Feb 7;68(3):573–83.

11. Li J, Mulvihill TS, Li L, Barrott JJ, Nelson ML, Wagner L, et al. A Role for SMARCB1 in Synovial Sarcomagenesis Reveals That SS18–SSX Induces Canonical BAF Destruction. Cancer Discov. 2021 Oct 1;11(10):2620–37.

12. McBride MJ, Pulice JL, Beird HC, Ingram DR, D'Avino AR, Shern JF, et al. The SS18-SSX Fusion Oncoprotein Hijacks BAF Complex Targeting and Function to Drive Synovial Sarcoma. Cancer Cell. 2018 Jun 11;33(6):1128-1141.e7.

13. Chalmers ZR, Connelly CF, Fabrizio D, Gay L, Ali SM, Ennis R, et al. Analysis of 100,000 human cancer genomes reveals the landscape of tumor mutational burden. Genome Med. 2017 Apr 19;9(1):34.

14. Marabelle A, Fakih M, Lopez J, Shah M, Shapira-Frommer R, Nakagawa K, et al. Association of tumour mutational burden with outcomes in patients with advanced solid tumours treated with pembrolizumab: prospective biomarker analysis of the multicohort, open-label, phase 2 KEYNOTE-158 study. Lancet Oncol. 2020 Oct 1;21(10):1353–65.

15. Trautmann M, Sievers E, Aretz S, Kindler D, Michels S, Friedrichs N, et al. SS18-SSX fusion protein-induced Wnt/β-catenin signaling is a therapeutic target in synovial sarcoma. Oncogene. 2014 Oct;33(42):5006–16.

16. Brien GL, Remillard D, Shi J, Hemming ML, Chabon J, Wynne K, et al. Targeted degradation of BRD9 reverses oncogenic gene expression in synovial sarcoma. van Lohuizen M, Sawyers CL, editors. eLife. 2018 Nov 15;7:e41305.

17. Isfort I, Cyra M, Elges S, Kailayangiri S, Altvater B, Rossig C, et al. SS18-SSX–Dependent YAP/TAZ Signaling in Synovial Sarcoma. Clin Cancer Res. 2019 Jun 15;25(12):3718–31.

18. Wu SP, Cooper BT, Bu F, Bowman CJ, Killian JK, Serrano J, et al. DNA Methylation–Based Classifier for Accurate Molecular Diagnosis of Bone Sarcomas. JCO Precis Oncol. 2017 Nov 1;(1):1–11.

19. Regulation and Role of EZH2 in Cancer [Internet]. [cited 2022 Jan 7]. Available from: https://www.e-crt.org/journal/view.php?doi=10.4143/crt.2014.46.3.209

20. Changchien YC, Tátrai P, Papp G, Sápi J, Fónyad L, Szendrői M, et al. Poorly differentiated synovial sarcoma is associated with high expression of enhancer of zeste homologue 2 (EZH2). J Transl Med. 2012 Oct 30;10(1):216.

21. Jiang T, Wang Y, Zhou F, Gao G, Ren S, Zhou C. Prognostic value of high EZH2 expression in patients with different types of cancer: a systematic review with meta-analysis. Oncotarget. 2015 Dec 14;7(4):4584–97.

22. Research C for DE and. FDA approves tazemetostat for advanced epithelioid sarcoma. FDA [Internet]. 2020 Jan 24 [cited 2022 Jan 7]; Available from: https://www.fda.gov/drugs/resources-information-approved-drugs/fda-approves-tazemetostat-advanced-epithelioid-sarcoma

23. Kawano S, Grassian AR, Tsuda M, Knutson SK, Warholic NM, Kuznetsov G, et al. Preclinical Evidence of Anti-Tumor Activity Induced by EZH2 Inhibition in Human Models of Synovial Sarcoma. PLOS ONE. 2016 Jul 8;11(7):e0158888.

24. Shen JK, Cote GM, Gao Y, Choy E, Mankin HJ, Hornicek FJ, et al. Targeting EZH2-mediated methylation of H3K27 inhibits proliferation and migration of Synovial Sarcoma in vitro. Sci Rep. 2016 Apr 29;6(1):25239.

25. Ito T, Ouchida M, Morimoto Y, Yoshida A, Jitsumori Y, Ozaki T, et al. Significant growth suppression of synovial sarcomas by the histone deacetylase inhibitor FK228 in vitro and in vivo. Cancer Lett. 2005 Jun 28;224(2):311–9.

26. National Cancer Institute (NCI). A Phase II Study of Single Agent Depsipeptide (FK228) in Metastatic or Unresectable Soft Tissue Sarcomas [Internet]. clinicaltrials.gov; 2017 May [cited 2022 Jan 5]. Report No.: study/NCT00112463. Available from: https://clinicaltrials.gov/ct2/show/study/NCT00112463

27. Laporte AN, Poulin NM, Barrott JJ, Wang XQ, Lorzadeh A, Werff RV, et al. Death by HDAC Inhibition in Synovial Sarcoma Cells. Mol Cancer Ther. 2017 Dec 1;16(12):2656–67.

28. Banito A, Li X, Laporte AN, Roe JS, Sanchez-Vega F, Huang CH, et al. The SS18-SSX Oncoprotein Hijacks KDM2B-PRC1.1 to Drive Synovial Sarcoma. Cancer Cell. 2018 Mar 12;33(3):527-541.e8.

29. Advenchen Laboratories, LLC. A Phase III Study of AL3818 (Anlotinib, Catequentinib) Hydrochloride Monotherapy in Subjects With Metastatic or Advanced Alveolar Soft Part Sarcoma, Leiomyosarcoma and Synovial Sarcoma [Internet]. clinicaltrials.gov; 2021 Nov [cited 2022 Jan 13]. Report No.: NCT03016819. Available from: https://clinicaltrials.gov/ct2/show/NCT03016819

30. Shen G, Zheng F, Ren D, Du F, Dong Q, Wang Z, et al. Anlotinib: a novel multi-targeting tyrosine kinase inhibitor in clinical development. J Hematol OncolJ Hematol Oncol. 2018 Sep 19;11(1):120.

31. Chugh R, Wathen JK, Maki RG, Benjamin RS, Patel SR, Meyers PA, et al. Phase II multicenter trial of imatinib in 10 histologic subtypes of sarcoma using a bayesian hierarchical statistical model. J Clin Oncol Off J Am Soc Clin Oncol. 2009 Jul 1;27(19):3148–53.

32. Ho AL, Schwartz GK. Targeting of Insulin-Like Growth Factor Type 1 Receptor in Ewing Sarcoma: Unfulfilled Promise or a Promising Beginning? J Clin Oncol. 2011 Dec 1;29(34):4581–3.

33. Van Tine BA, Chawla SP, Trent JC, Wilky BA, Chugh R, Chmielowski B, et al. A phase III study (APROMISS) of AL3818 (Catequentinib, Anlotinib) hydrochloride monotherapy in subjects with metastatic or advanced synovial sarcoma. J Clin Oncol. 2021 May 20;39(15_suppl):11505–11505.

34. Patwardhan PP, Musi E, Schwartz GK. Preclinical Evaluation of Nintedanib, a Triple Angiokinase Inhibitor, in Soft-tissue Sarcoma: Potential Therapeutic Implication for Synovial Sarcoma. Mol Cancer Ther. 2018 Nov 1;17(11):2329–40.

35. Commissioner O of the. FDA Approves First Treatment for Group of Progressive Interstitial Lung Diseases [Internet]. FDA. FDA; 2020 [cited 2022 Jan 12]. Available from: https://www.fda.gov/news-events/press-announcements/fda-approves-first-treatment-group-progressive-interstitial-lung-diseases

36. Popat S, Mellemgaard A, Fahrbach K, Martin A, Rizzo M, Kaiser R, et al. Nintedanib plus docetaxel as second-line therapy in patients with non-small-cell lung cancer: a network meta-analysis. Future Oncol Lond Engl. 2015;11(3):409–20.

37. Eli Lilly and Company. A Randomized, Open-Label Phase 1/2 Study Evaluating Ramucirumab in Pediatric Patients and Young Adults With Relapsed, Recurrent, or Refractory Synovial Sarcoma [Internet]. clinicaltrials.gov; 2022 Jan [cited 2022 Jan 11]. Report No.: NCT04145700. Available from: https://clinicaltrials.gov/ct2/show/NCT04145700

38. Lowery CD, Blosser W, Dowless M, Renschler M, Perez LV, Stephens J, et al. Anti-VEGFR2 therapy delays growth of preclinical pediatric tumor models and enhances anti-tumor activity of chemotherapy. Oncotarget. 2019 Sep 17;10(53):5523–33.

39. Costa MI, Boldrini JL, Bassanezi RC. Optimal chemical control of populations developing drug resistance. IMA J Math Appl Med Biol. 1992;9(3):215–26.

40. Ferrari A, Gronchi A, Casanova M, Meazza C, Gandola L, Collini P, et al. Synovial sarcoma: A retrospective analysis of 271 patients of all ages treated at a single institution. Cancer. 2004;101(3):627–34.

41. Adaptimmune. A Phase 2 Single Arm Open-Label Clinical Trial of ADP-A2M4 SPEAR™ T Cells in Subjects With Advanced Synovial Sarcoma or Myxoid/Round Cell Liposarcoma [Internet]. clinicaltrials.gov; 2021 Nov [cited 2022 Jan 13]. Report No.: NCT04044768. Available from: https://clinicaltrials.gov/ct2/show/NCT04044768

42. Iura K, Maekawa A, Kohashi K, Ishii T, Bekki H, Otsuka H, et al. Cancer-testis antigen expression in synovial sarcoma: NY-ESO-1, PRAME, MAGEA4, and MAGEA1. Hum Pathol. 2017 Mar;61:130–9.

43. D'Angelo SP, Van Tine BA, Attia S, Blay JY, Strauss SJ, Valverde Morales CM, et al. SPEARHEAD-1: A phase 2 trial of afamitresgene autoleucel (Formerly ADP-A2M4) in patients with advanced synovial sarcoma or myxoid/round cell liposarcoma. J Clin Oncol. 2021 May 20;39(15_suppl):11504–11504.

44. FHD-609 in Subjects With Advanced Synovial Sarcoma [Internet]. 2016 [cited 2022 Jan 14]. Available from: https://www.cancer.gov/about-cancer/treatment/clinical-trials/search/v?id=NCI-2021-08516

45. Treatment With FHD-609 Begins in Phase 1 Synovial Sarcoma Study [Internet]. Targeted Oncology. [cited 2022 Jan 18]. Available from: https://www.targetedonc.com/view/treatment-with-fhd-609-begins-in-phase-1-synovial-sarcoma-study

46. Jancewicz I, Siedlecki JA, Sarnowski TJ, Sarnowska E. BRM: the core ATPase subunit of SWI/SNF chromatin-remodelling complex—a tumour suppressor or tumour-promoting factor? Epigenetics Chromatin. 2019 Nov 13;12(1):68.

47. Manning G, Whyte DB, Martinez R, Hunter T, Sudarsanam S. The protein kinase complement of the human genome. Science. 2002 Dec 6;298(5600):1912–34.

48. Ghosh S, Marrocco I, Yarden Y. Chapter One - Roles for receptor tyrosine kinases in tumor progression and implications for cancer treatment. In: Kumar R, Fisher PB, editors. Advances in Cancer Research [Internet]. Academic Press; 2020 [cited 2022 Feb 3]. p. 1–57. (Receptor Tyrosine Kinases; vol. 147). Available from: https://www.sciencedirect.com/science/article/pii/S0065230X20300348

49. Feng Q, Guo P, Wang J, Zhang X, Yang HC, Feng JG. High expression of SDF-1 and VEGF is associated with poor prognosis in patients with synovial sarcomas. Exp Ther Med. 2018 Mar;15(3):2597–603.

50. Brahmi M, Lesluyes T, Dufresne A, Toulmonde M, Italiano A, Mir O, et al. Expression and prognostic significance of PDGF ligands and receptors across soft tissue sarcomas. ESMO Open. 2021 Jan 29;6(1):100037.

51. Zhou WY, Zheng H, Du XL, Yang JL. Characterization of FGFR signaling pathway as therapeutic targets for sarcoma patients. Cancer Biol Med. 2016 Jun;13(2):260–8.

52. Ferrara N, Gerber HP, LeCouter J. The biology of VEGF and its receptors. Nat Med. 2003 Jun;9(6):669–76.

53. Carmeliet P. VEGF as a key mediator of angiogenesis in cancer. Oncology. 2005;69 Suppl 3:4–10.

54. Andrae J, Gallini R, Betsholtz C. Role of platelet-derived growth factors in physiology and medicine. Genes Dev. 2008 May 15;22(10):1276–312.

55. Ornitz DM, Itoh N. The Fibroblast Growth Factor signaling pathway. Wiley Interdiscip Rev Dev Biol. 2015 Jun;4(3):215–66.

56. Gutiérrez-Hoya A, Soto-Cruz I. Role of the JAK/STAT Pathway in Cervical Cancer: Its Relationship with HPV E6/E7 Oncoproteins. Cells. 2020 Oct 15;9(10):2297.

57. Vainchenker W, Constantinescu SN. JAK/STAT signaling in hematological malignancies. Oncogene. 2013 May;32(21):2601–13.

58. Thomas SJ, Snowden JA, Zeidler MP, Danson SJ. The role of JAK/STAT signalling in the pathogenesis, prognosis and treatment of solid tumours. Br J Cancer. 2015 Jul;113(3):365–71.

59. Ghoreschi K, Laurence A, O'Shea JJ. Janus kinases in immune cell signaling. Immunol Rev. 2009 Mar;228(1):273–87.

60. Harrison DA. The JAK/STAT Pathway. Cold Spring Harb Perspect Biol. 2012 Mar;4(3):a011205.

61. Brooks AJ, Dai W, O'Mara ML, Abankwa D, Chhabra Y, Pelekanos RA, et al. Mechanism of activation of protein kinase JAK2 by the growth hormone receptor. Science. 2014 May 16;344(6185):1249783.

62. Yamaoka K, Saharinen P, Pesu M, Holt VE, Silvennoinen O, O'Shea JJ. The Janus kinases (Jaks). Genome Biol. 2004;5(12):253.

63. Kawamura M, McVicar DW, Johnston JA, Blake TB, Chen YQ, Lal BK, et al. Molecular cloning of L-JAK, a Janus family protein-tyrosine kinase expressed in natural killer cells and activated leukocytes. Proc Natl Acad Sci U S A. 1994 Jul 5;91(14):6374–8.

64. Rodig SJ, Meraz MA, White JM, Lampe PA, Riley JK, Arthur CD, et al. Disruption of the Jak1 gene demonstrates obligatory and nonredundant roles of the Jaks in cytokine-induced biologic responses. Cell. 1998 May 1;93(3):373–83.

65. Witthuhn BA, Quelle FW, Silvennoinen O, Yi T, Tang B, Miura O, et al. JAK2 associates with the erythropoietin receptor and is tyrosine phosphorylated and activated following stimulation with erythropoietin. Cell. 1993 Jul 30;74(2):227–36.

66. Parganas E, Wang D, Stravopodis D, Topham DJ, Marine JC, Teglund S, et al. Jak2 is essential for signaling through a variety of cytokine receptors. Cell. 1998 May 1;93(3):385–95.

67. Argetsinger LS, Campbell GS, Yang X, Witthuhn BA, Silvennoinen O, Ihle JN, et al. Identification of JAK2 as a growth hormone receptor-associated tyrosine kinase. Cell. 1993 Jul 30;74(2):237–44.

68. Drachman JG, Griffin JD, Kaushansky K. The c-Mpl ligand (thrombopoietin) stimulates tyrosine phosphorylation of Jak2, Shc, and c-Mpl. J Biol Chem. 1995 Mar 10;270(10):4979–82.

69. Campbell GS, Argetsinger LS, Ihle JN, Kelly PA, Rillema JA, Carter-Su C. Activation of JAK2 tyrosine kinase by prolactin receptors in Nb2 cells and mouse mammary gland explants. Proc Natl Acad Sci U S A. 1994 Jun 7;91(12):5232–6.

70. Silvennoinen O, Witthuhn BA, Quelle FW, Cleveland JL, Yi T, Ihle JN. Structure of the murine Jak2 protein-tyrosine kinase and its role in interleukin 3 signal transduction. Proc Natl Acad Sci U S A. 1993 Sep 15;90(18):8429–33.

71. Heinrich PC, Behrmann I, Müller-Newen G, Schaper F, Graeve L. Interleukin-6-type cytokine signalling through the gp130/Jak/STAT pathway. Biochem J. 1998 Sep 1;334(Pt 2):297–314.

72. Russell SM, Johnston JA, Noguchi M, Kawamura M, Bacon CM, Friedmann M, et al. Interaction of IL-2Rβ and γc chains with Jak1 and Jak3: Implications for XSCID and XCID. Science. 1994;266(5187):1042–5.

73. Macchi P, Villa A, Giliani S, Sacco MG, Frattini A, Porta F, et al. Mutations of Jak-3 gene in patients with autosomal severe combined immune deficiency (SCID). Nature. 1995 Sep 7;377(6544):65–8.

74. Russell SM, Tayebi N, Nakajima H, Riedy MC, Roberts JL, Aman MJ, et al. Mutation of Jak3 in a patient with SCID: essential role of Jak3 in lymphoid development. Science. 1995 Nov 3;270(5237):797–800.

75. Nosaka T, van Deursen JM, Tripp RA, Thierfelder WE, Witthuhn BA, McMickle AP, et al. Defective lymphoid development in mice lacking Jak3. Science. 1995 Nov 3;270(5237):800–2.

76. Park SY, Saijo K, Takahashi T, Osawa M, Arase H, Hirayama N, et al. Developmental defects of lymphoid cells in Jak3 kinase-deficient mice. Immunity. 1995 Dec;3(6):771–82.

77. Thomis DC, Gurniak CB, Tivol E, Sharpe AH, Berg LJ. Defects in B lymphocyte maturation and T lymphocyte activation in mice lacking Jak3. Science. 1995 Nov 3;270(5237):794–7.

78. Firmbach-Kraft I, Byers M, Shows T, Dalla-Favera R, Krolewski JJ. tyk2, prototype of a novel class of non-receptor tyrosine kinase genes. Oncogene. 1990 Sep;5(9):1329–36.

79. Stahl N, Boulton TG, Farruggella T, Ip NY, Davis S, Witthuhn BA, et al. Association and activation of Jak-Tyk kinases by CNTF-LIF-OSM-IL-6 beta receptor components. Science. 1994 Jan 7;263(5143):92–5.

80. Karaghiosoff M, Steinborn R, Kovarik P, Kriegshäuser G, Baccarini M, Donabauer B, et al. Central role for type I interferons and Tyk2 in lipopolysaccharide-induced endotoxin shock. Nat Immunol. 2003 May;4(5):471–7.

81. Rawlings JS, Rosler KM, Harrison DA. The JAK/STAT signaling pathway. J Cell Sci. 2004 Mar 15;117(Pt 8):1281–3.

82. O'Shea JJ, Murray PJ. Cytokine signaling modules in inflammatory responses. Immunity. 2008 Apr;28(4):477–87.

83. Levy DE, Kessler DS, Pine R, Reich N, Darnell JE. Interferon-induced nuclear factors that bind a shared promoter element correlate with positive and negative transcriptional control. Genes Dev. 1988 Apr;2(4):383–93.

84. Clevenger CV. Roles and Regulation of Stat Family Transcription Factors in Human Breast Cancer. Am J Pathol. 2004 Nov;165(5):1449–60.

85. Loh CY, Arya A, Naema AF, Wong WF, Sethi G, Looi CY. Signal Transducer and Activator of Transcription (STATs) Proteins in Cancer and Inflammation: Functions and Therapeutic Implication. Front Oncol [Internet]. 2019 [cited 2022 Jan 26];9. Available from: https://www.frontiersin.org/article/10.3389/fonc.2019.00048

86. Sadowski HB, Shuai K, Darnell JE, Gilman MZ. A common nuclear signal transduction pathway activated by growth factor and cytokine receptors. Science. 1993 Sep 24;261(5129):1739–44.

87. Takeda K, Noguchi K, Shi W, Tanaka T, Matsumoto M, Yoshida N, et al. Targeted disruption of the mouse Stat3 gene leads to early embryonic lethality. Proc Natl Acad Sci U S A. 1997 Apr 15;94(8):3801–4.

88. Sano S, Itami S, Takeda K, Tarutani M, Yamaguchi Y, Miura H, et al. Keratinocyte-specific ablation of Stat3 exhibits impaired skin remodeling, but does not affect skin morphogenesis. EMBO J. 1999 Sep 1;18(17):4657–68.

89. Takeda K, Kaisho T, Yoshida N, Takeda J, Kishimoto T, Akira S. Stat3 activation is responsible for IL-6-dependent T cell proliferation through preventing apoptosis: generation and characterization of T cell-specific Stat3-deficient mice. J Immunol Baltim Md 1950. 1998 Nov 1;161(9):4652–60.

90. Hoelbl A, Kovacic B, Kerenyi MA, Simma O, Warsch W, Cui Y, et al. Clarifying the role of Stat5 in lymphoid development and Abelson-induced transformation. Blood. 2006 Jun 15;107(12):4898–906.

91. Burchill MA, Yang J, Vogtenhuber C, Blazar BR, Farrar MA. IL-2 receptor beta-dependent STAT5 activation is required for the development of Foxp3+ regulatory T cells. J Immunol Baltim Md 1950. 2007 Jan 1;178(1):280–90.

92. Wingelhofer B, Neubauer HA, Valent P, Han X, Constantinescu SN, Gunning PT, et al. Implications of STAT3 and STAT5 signaling on gene regulation and chromatin remodeling in hematopoietic cancer. Leukemia. 2018 Aug;32(8):1713–26.

93. Xu YH, Lu S. A meta-analysis of STAT3 and phospho-STAT3 expression and survival of patients with non-small-cell lung cancer. Eur J Surg Oncol J Eur Soc Surg Oncol Br Assoc Surg Oncol. 2014 Mar;40(3):311–7.

94. Du W, Wang YC, Hong J, Su WY, Lin YW, Lu R, et al. STAT5 isoforms regulate colorectal cancer cell apoptosis via reduction of mitochondrial membrane potential and generation of reactive oxygen species. J Cell Physiol. 2012 Jun;227(6):2421–9.

95. Sonnenblick A, Salgado R, Brohée S, Zahavi T, Peretz T, Van den Eynden G, et al. p-STAT3 in luminal breast cancer: Integrated RNA-protein pooled analysis and results from the BIG 2-98 phase III trial. Int J Oncol. 2018 Feb;52(2):424–32.

96. Chen CL, Loy A, Cen L, Chan C, Hsieh FC, Cheng G, et al. Signal transducer and activator of transcription 3 is involved in cell growth and survival of human rhabdomyosarcoma and osteosarcoma cells. BMC Cancer. 2007 Jun 28;7:111.

97. Fred Hutchinson Cancer Research Center. A Pilot Study Examining the Impact of the Jak1 Inhibitor Itacitinib on the Sarcoma Tumor Immune Microenvironment [Internet]. clinicaltrials.gov; 2021 Dec [cited 2022 Jan 31]. Report No.: NCT03670069. Available from: https://clinicaltrials.gov/ct2/show/NCT03670069

98. Morris R, Kershaw NJ, Babon JJ. The molecular details of cytokine signaling via the JAK/STAT pathway. Protein Sci. 2018;27(12):1984–2009.

99. White UA, Stephens JM. The gp130 Receptor Cytokine Family: Regulators of Adipocyte Development and Function. Curr Pharm Des. 2011;17(4):340–6.

100. Yamasaki K, Taga T, Hirata Y, Yawata H, Kawanishi Y, Seed B, et al. Cloning and Expression of the Human Interleukin-6 (BSF-2/IFNβ 2) Receptor. Science. 1988 Aug 12;241(4867):825–8.

101. Niwa Y, Kanda H, Shikauchi Y, Saiura A, Matsubara K, Kitagawa T, et al. Methylation silencing of SOCS-3 promotes cell growth and migration by enhancing JAK/STAT and FAK signalings in human hepatocellular carcinoma. Oncogene. 2005 Sep;24(42):6406–17.

102. Catlett-Falcone R, Landowski TH, Oshiro MM, Turkson J, Levitzki A, Savino R, et al. Constitutive activation of Stat3 signaling confers resistance to apoptosis in human U266 myeloma cells. Immunity. 1999 Jan;10(1):105–15.

103. Tripsianis G, Papadopoulou E, Anagnostopoulos K, Botaitis S, Katotomichelakis M, Romanidis K, et al. Coexpression of IL-6 and TNF-α: prognostic significance on breast cancer outcome. Neoplasma. 2014;61(2):205–12.

104. Wakabayashi H, Hamaguchi T, Nagao N, Kato S, Iino T, Nakamura T, et al. Interleukin-6 receptor inhibitor suppresses bone metastases in a breast cancer cell line. Breast Cancer Tokyo Jpn. 2018 Sep;25(5):566–74.

105. Komoda H, Tanaka Y, Honda M, Matsuo Y, Hazama K, Takao T. Interleukin-6 levels in colorectal cancer tissues. World J Surg. 1998 Aug;22(8):895–8.

106. Holmer R, Goumas FA, Waetzig GH, Rose-John S, Kalthoff H. Interleukin-6: a villain in the drama of pancreatic cancer development and progression. Hepatobiliary Pancreat Dis Int HBPD INT. 2014 Aug;13(4):371–80.

107. Ishibashi K, Koguchi T, Matsuoka K, Onagi A, Tanji R, Takinami-Honda R, et al. Interleukin-6 induces drug resistance in renal cell carcinoma. Fukushima J Med Sci. 2018;64(3):103–10.

108. Siltuximab (Sylvant) Gains FDA Approval ... But Not For Multiple Myeloma [Internet]. The Myeloma Beacon. [cited 2022 Mar 2]. Available from: https://myelomabeacon.org/news/2014/04/28/siltuximab-sylvant-fda-approval/

109. Danese S, Vermeire S, Hellstern P, Panaccione R, Rogler G, Fraser G, et al. Randomised trial and open-label extension study of an anti-interleukin-6 antibody in Crohn's disease (ANDANTE I and II). Gut. 2019 Jan 1;68(1):40–8.

110. Wallace DJ, Strand V, Merrill JT, Popa S, Spindler AJ, Eimon A, et al. Efficacy and safety of an interleukin 6 monoclonal antibody for the treatment of systemic lupus erythematosus: a phase II dose-ranging randomised controlled trial. Ann Rheum Dis. 2017 Mar 1;76(3):534–42.

111. Kevzara (Sarilumab): A Novel IL-6 Receptor Antagonist for Rheumatoid Arthritis. 2017 Aug 10 [cited 2022 Mar 2]; Available from: https://www.ahdbonline.com/supplements/2438-kevzara-sarilumab-a-novel-il-6-receptor-antagonist-for-rheumatoid-arthritis

112. Wu X, Xiao H, Li C, Lin J. Abstract 186: FDA approved drug Bazedoxifene as a novel inhibitor of IL 6 and IL 11/GP130 signaling for osteosarcoma therapy. Cancer Res. 2017 Jul 1;77(13_Supplement):186.

113. Johnstone CN, Chand A, Putoczki TL, Ernst M. Emerging roles for IL-11 signaling in cancer development and progression: Focus on breast cancer. Cytokine Growth Factor Rev. 2015 Oct 1;26(5):489–98.

114. Nishina T, Deguchi Y, Ohshima D, Takeda W, Ohtsuka M, Shichino S, et al. Interleukin-11-expressing fibroblasts have a unique gene signature correlated with poor prognosis of colorectal cancer. Nat Commun. 2021 Apr 16;12(1):2281.

115. Upregulation of IL-11, an IL-6 Family Cytokine, Promotes Tumor Progression and Correlates with Poor Prognosis in Non-Small Cell Lung Cancer - FullText - Cellular Physiology and Biochemistry 2018, Vol. 45, No. 6 - Karger Publishers [Internet]. [cited 2022 Mar 2]. Available from: https://www.karger.com/Article/FullText/488166

116. Tang W, Ramasamy K, Pillai SMA, Santhamma B, Konda S, Pitta Venkata P, et al. LIF/LIFR oncogenic signaling is a novel therapeutic target in endometrial cancer. Cell Death Discov. 2021 Aug 16;7(1):1–10.

117. Guo H, Cheng Y, Martinka M, McElwee K. High LIFr expression stimulates melanoma cell migration and is associated with unfavorable prognosis in melanoma. Oncotarget. 2015 Sep 22;6(28):25484–98.

118. David E, Tirode F, Baud'huin M, Guihard P, Laud K, Delattre O, et al. Oncostatin M is a growth factor for Ewing sarcoma. Am J Pathol. 2012 Nov;181(5):1782–95.

119. Viswanadhapalli S, Luo Y, Sareddy GR, Santhamma B, Zhou M, Li M, et al. EC359: A First-in-Class Small-Molecule Inhibitor for Targeting Oncogenic LIFR Signaling in Triple-Negative Breast Cancer. Mol Cancer Ther. 2019 Aug;18(8):1341–54.

120. Kucia-Tran JA, Tulkki V, Scarpini CG, Smith S, Wallberg M, Paez-Ribes M, et al. Anti-oncostatin M antibody inhibits the pro-malignant effects of oncostatin M receptor overexpression in squamous cell carcinoma. J Pathol. 2018 Mar;244(3):283–95.

121. Geethadevi A, Nair A, Parashar D, Ku Z, Xiong W, Deng H, et al. Oncostatin M Receptor-Targeted Antibodies Suppress STAT3 Signaling and Inhibit Ovarian Cancer Growth. Cancer Res. 2021 Oct 15;81(20):5336–52.

122. He Y, Zhang X, Pan W, Tai F, Liang L, Shi J. Interleukin-31 Receptor α Is Required for Basal-Like Breast Cancer Progression. Front Oncol [Internet]. 2020 [cited 2022 Mar 8];10. Available from: https://www.frontiersin.org/article/10.3389/fonc.2020.00816

123. Di Salvo E, Allegra A, Casciaro M, Gangemi S. IL-31, itch and hematological malignancies. Clin Mol Allergy. 2021 Jun 12;19(1):8.

124. Kabashima K, Matsumura T, Komazaki H, Kawashima M. Trial of Nemolizumab and Topical Agents for Atopic Dermatitis with Pruritus. N Engl J Med. 2020 Jul 9;383(2):141–50.

125. Kim JW, Marquez CP, Kostyrko K, Koehne AL, Marini K, Simpson DR, et al. Antitumor activity of an engineered decoy receptor targeting CLCF1–CNTFR signaling in lung adenocarcinoma. Nat Med. 2019 Nov;25(11):1783–95.

126. Junk DJ, Bryson BL, Smigiel JM, Parameswaran N, Bartel CA, Jackson MW. Oncostatin M promotes cancer cell plasticity through cooperative STAT3-SMAD3 signaling. Oncogene. 2017 Jul;36(28):4001–13.

127. Yu Z, Li Z, Wang C, Pan T, Chang X, Wang X, et al. Oncostatin M receptor, positively regulated by SP1, promotes gastric cancer growth and metastasis upon treatment with Oncostatin M. Gastric Cancer. 2019 Sep 1;22(5):955–66.

128. Zhu M, Che Q, Liao Y, Wang H, Wang J, Chen Z, et al. Oncostatin M activates STAT3 to promote endometrial cancer invasion and angiogenesis. Oncol Rep. 2015 Jul 1;34(1):129–38.

129. Hermanns HM. Oncostatin M and interleukin-31: Cytokines, receptors, signal transduction and physiology. Cytokine Growth Factor Rev. 2015 Oct;26(5):545–58.

130. Stahl N, Farruggella TJ, Boulton TG, Zhong Z, Darnell JE, Yancopoulos GD. Choice of STATs and other substrates specified by modular tyrosine-based motifs in cytokine receptors. Science. 1995 Mar 3;267(5202):1349–53.

131. Heinrich PC, Behrmann I, Haan S, Hermanns HM, Müller-Newen G, Schaper F. Principles of interleukin (IL)-6-type cytokine signalling and its regulation. Biochem J. 2003 Aug 15;374(Pt 1):1–20.

132. Richards CD. The enigmatic cytokine oncostatin m and roles in disease. ISRN Inflamm. 2013 Dec 8;2013:512103.

133. Mosley B, De Imus C, Friend D, Boiani N, Thoma B, Park LS, et al. Dual oncostatin M (OSM) receptors. Cloning and characterization of an alternative signaling subunit conferring OSM-specific receptor activation. J Biol Chem. 1996 Dec 20;271(51):32635–43.

134. Zarling JM, Shoyab M, Marquardt H, Hanson MB, Lioubin MN, Todaro GJ. Oncostatin M: a growth regulator produced by differentiated histiocytic lymphoma cells. Proc Natl Acad Sci. 1986 Dec 1;83(24):9739–43.

135. Pan CM, Wang ML, Chiou SH, Chen HY, Wu CW. Oncostatin M suppresses metastasis of lung adenocarcinoma by inhibiting SLUG expression through coordination of STATs and PIASs signalings. Oncotarget. 2016 Sep 13;7(37):60395–406.

136. Lim SY, Ahn SH, Park H, Lee J, Choi K, Choi C, et al. Transcriptional regulation of adrenomedullin by oncostatin M in human astroglioma cells: Implications for tumor invasion and migration. Sci Rep. 2014 Sep 23;4:6444.

137. Repovic P, Fears CY, Gladson CL, Benveniste EN. Oncostatin-M induction of vascular endothelial growth factor expression in astroglioma cells. Oncogene. 2003 Nov 6;22(50):8117–24.

138. Kucia-Tran JA, Tulkki V, Smith S, Scarpini CG, Hughes K, Araujo AM, et al. Overexpression of the oncostatin-M receptor in cervical squamous cell carcinoma is associated with epithelial–mesenchymal transition and poor overall survival. Br J Cancer. 2016 Jul 12;115(2):212–22.

139. Caffarel MM, Coleman N. Oncostatin M receptor is a novel therapeutic target in cervical squamous cell carcinoma. J Pathol. 2014 Mar;232(4):386–90.

140. Douglas AM, Goss GA, Sutherland RL, Hilton DJ, Berndt MC, Nicola NA, et al. Expression and function of members of the cytokine receptor superfamily on breast cancer cells. Oncogene. 1997 Feb 13;14(6):661–9.

141. Zhang F, Li C, Halfter H, Liu J. Delineating an oncostatin M-activated STAT3 signaling pathway that coordinates the expression of genes involved in cell cycle regulation and extracellular matrix deposition of MCF-7 cells. Oncogene. 2003 Feb;22(6):894–905.

142. Hutt JA, DeWille JW. Oncostatin M Induces Growth Arrest of Mammary Epithelium via a CCAAT/enhancer-binding Protein δ-dependent Pathway 1 Supported in part by NIH Grant RR00136CA (to J. A. H.) and NIH Grants CA 57607 and P30CA16058 from the National Cancer Institute (to J. W. D.).1. Mol Cancer Ther. 2002 Jun 1;1(8):601–10.

143. Covert H, Mellor LF, Wolf CL, Ankenbrandt N, Emathinger JM, Tawara K, et al. OSM-induced CD44 contributes to breast cancer metastatic potential through cell detachment but not epithelial-mesenchymal transition. Cancer Manag Res. 2019;11:7721–37.

144. Chen M, Ren R, Lin W, Xiang L, Zhao Z, Shao B. Exploring the oncostatin M (OSM) feed-forward signaling of glioblastoma via STAT3 in pan-cancer analysis. Cancer Cell Int. 2021 Oct 26;21(1):565.

145. Kaposi's sarcoma - Overview - Mayo Clinic [Internet]. [cited 2022 Feb 15]. Available from: https://www.mayoclinic.org/diseases-conditions/kaposis-sarcoma/cdc-20387726

146. Miles SA, Martínez-Maza O, Rezai A, Magpantay L, Kishimoto T, Nakamura S, et al. Oncostatin M as a potent mitogen for AIDS-Kaposi's sarcoma-derived cells. Science. 1992 Mar 13;255(5050):1432–4.

147. Amaral MC, Miles S, Kumar G, Nel AE. Oncostatin-M stimulates tyrosine protein phosphorylation in parallel with the activation of p42MAPK/ERK-2 in Kaposi's cells. Evidence that this pathway is important in Kaposi cell growth. J Clin Invest. 1993 Aug;92(2):848–57.

148. Bernard C, Merval R, Lebret M, Delerive P, Dusanter-Fourt I, Lehoux S, et al. Oncostatin M Induces Interleukin-6 and Cyclooxygenase-2 Expression in Human Vascular Smooth Muscle Cells. Circ Res. 1999 Dec 3;85(12):1124–31.

149. Barrott JJ, Kafchinski LA, Jin H, Potter JW, Kannan SD, Kennedy R, et al. Modeling synovial sarcoma metastasis in the mouse: PI3′-lipid signaling and inflammation. J Exp Med. 2016 Nov 9;213(13):2989–3005.

150. Carter D. 9 synovial sarcoma questions, answered [Internet]. MD Anderson Cancer Center. [cited 2022 Jun 14]. Available from: https://www.mdanderson.org/cancerwise/synovial-sarcoma.h00-159068712.html

151. Radiology (ACR) RS of NA (RSNA) and AC of. Radioimmunotherapy (RIT) [Internet]. Radiologyinfo.org. [cited 2022 Feb 16]. Available from: https://www.radiologyinfo.org/en/info/radio-immuno

152. Fact Sheet: What is Radioimmunotherapy? - SNMMI [Internet]. [cited 2022 Feb 16]. Available from: https://www.snmmi.org/AboutSNMMI/Content.aspx?ItemNumber=29736

153. First Radioimmunotherapy Approved by FDA. 2002 Mar 31 [cited 2022 Feb 16]; Available from: https://www.cancernetwork.com/view/first-radioimmunotherapy-approved-fda

154. Non-Hodgkin's lymphoma - Symptoms and causes - Mayo Clinic [Internet]. [cited 2022 Feb 16]. Available from: https://www.mayoclinic.org/diseases-conditions/non-hodgkins-lymphoma/symptoms-causes/syc-20375680

155. BEXXAR - Drug Information - Chemocare [Internet]. [cited 2022 Feb 18]. Available from: https://chemocare.com/chemotherapy/drug-info/bexxar.aspx

156. GlaxoSmithKline LLC; Withdrawal of Approval of the Indication for Treatment of Patients With Relapsed or Refractory, Low Grade, Follicular, or Transformed CD20 Positive Non-Hodgkin's Lymphoma Who Have Not Received Prior Rituximab; BEXXAR [Internet]. Federal Register. 2013 [cited 2022 Feb 18]. Available from: https://www.federalregister.gov/documents/2013/10/23/2013-24840/glaxosmithkline-llc-withdrawal-of-approval-of-the-indication-for-treatment-of-patients-with-relapsed

157. Memorial Sloan Kettering Cancer Center. Phase II Trial of 131 I-Omburtamab in Combination With External Beam Radiotherapy for Desmoplastic Small Round Cell Tumors and Other Solid Tumors Involving the Peritoneum [Internet]. clinicaltrials.gov; 2022 Feb [cited 2022 Mar 8]. Report No.: NCT04022213. Available from: https://clinicaltrials.gov/ct2/show/NCT04022213

158. A Phase II Study of 131I-Omburtamab plus Radiotherapy in People with Desmoplastic Small Round Cell Tumors and Other Solid Tumors in the Peritoneum | Memorial Sloan Kettering Cancer Center [Internet]. [cited 2022 Mar 9]. Available from: https://www.mskcc.org/cancer-care/clinical-trials/19-182

159. Modak S, Zanzonico P, Grkovski M, Slotkin EK, Carrasquillo JA, Lyashchenko SK, et al. B7H3-Directed Intraperitoneal Radioimmunotherapy With Radioiodinated Omburtamab for Desmoplastic Small Round Cell Tumor and Other Peritoneal Tumors: Results of a Phase I Study. J Clin Oncol Off J Am Soc Clin Oncol. 2020 Dec 20;38(36):4283–91.

160. MacroGenics. A Phase 1, Open-label, Dose Escalation Study of MGA271 in Pediatric Patients With B7-H3-Expressing Relapsed or Refractory Solid Tumors [Internet]. clinicaltrials.gov; 2022 Feb [cited 2022 Mar 8]. Report No.: NCT02982941. Available from: https://clinicaltrials.gov/ct2/show/NCT02982941

161. Memorial Sloan Kettering Cancer Center. Phase II Study of Intrathecal I-3F8 in Patients With GD2-Expressing Central Nervous System and Leptomeningeal Neoplasms [Internet]. clinicaltrials.gov; 2021 Oct [cited 2022 Mar 8]. Report No.: NCT00445965. Available from: https://clinicaltrials.gov/ct2/show/NCT00445965

162. Kramer K, Pandit-Taskar N, Humm JL, Zanzonico PB, Haque S, Dunkel IJ, et al. A phase II study of radioimmunotherapy with intraventricular 131 I-3F8 for medulloblastoma. Pediatr Blood Cancer. 2018 Jan;65(1).

163. Chang HR, Cordon-Cardo C, Houghton AN, Cheung NK, Brennan MF. Expression of disialogangliosides GD2 and GD3 on human soft tissue sarcomas. Cancer. 1992 Aug 1;70(3):633–8.

164. HER2+ Cancer Treatment Option | Herceptin® (trastuzumab) [Internet]. herceptin. [cited 2022 Mar 9]. Available from: https://www.herceptin.com/

165. Bhusari P, Vatsa R, Singh G, Parmar M, Bal A, Dhawan DK, et al. Development of Lu-177-trastuzumab for radioimmunotherapy of HER2 expressing breast cancer and its feasibility assessment in breast cancer patients. Int J Cancer. 2017 Feb 15;140(4):938–47.

166. Sahlmann CO, Homayounfar K, Niessner M, Dyczkowski J, Conradi LC, Braulke F, et al. Repeated adjuvant anti-CEA radioimmunotherapy after resection of colorectal liver metastases: Safety, feasibility, and long-term efficacy results of a prospective phase 2 study. Cancer. 2017 Feb 15;123(4):638–49.

167. Pancreatic Cancer Prognosis [Internet]. [cited 2022 Mar 10]. Available from: https://www.hopkinsmedicine.org/health/conditions-and-diseases/pancreatic-cancer/pancreatic-cancer-prognosis

168. Picozzi VJ, Ramanathan RK, Lowery MA, Ocean AJ, Mitchel EP, O'Neil BH, et al. (90)Y-clivatuzumab tetraxetan with or without low-dose gemcitabine: A phase Ib study in patients with metastatic pancreatic cancer after two or more prior therapies. Eur J Cancer Oxf Engl 1990. 2015 Sep;51(14):1857–64.

169. Kasten BB, Arend RC, Katre AA, Kim H, Fan J, Ferrone S, et al. B7-H3-targeted 212Pb radioimmunotherapy of ovarian cancer in preclinical models. Nucl Med Biol. 2017 Apr;47:23–30.

170. Quelven I, Monteil J, Sage M, Saidi A, Mounier J, Bayout A, et al. 212Pb α-Radioimmunotherapy Targeting CD38 in Multiple Myeloma: A Preclinical Study. J Nucl Med. 2020 Jul 1;61(7):1058–65.

171. Hao G, Mastren T, Silvers W, Hassan G, Öz OK, Sun X. Copper-67 radioimmunotheranostics for simultaneous immunotherapy and immuno-SPECT. Sci Rep. 2021 Feb 11;11(1):3622.

172. Zaheer J, Kim H, Lee YJ, Kim JS, Lim SM. Combination Radioimmunotherapy Strategies for Solid Tumors. Int J Mol Sci. 2019 Nov 8;20(22):5579.

173. Huhalov A, Chester KA. Engineered single chain antibody fragments for radioimmunotherapy. Q J Nucl Med Mol Imaging Off Publ Ital Assoc Nucl Med AIMN Int Assoc Radiopharmacol IAR Sect Soc Of. 2004 Dec;48(4):279–88.

174. Xenaki KT, Oliveira S, van Bergen en Henegouwen PMP. Antibody or Antibody Fragments: Implications for Molecular Imaging and Targeted Therapy of Solid Tumors. Front Immunol. 2017 Oct 12;8:1287.

175. Lattuada L, Barge A, Cravotto G, Giovenzana GB, Tei L. The synthesis and application of polyamino polycarboxylic bifunctional chelating agents. Chem Soc Rev. 2011 Apr 18;40(5):3019–49.

176. White JM, Escorcia FE, Viola NT. Perspectives on metals-based radioimmunotherapy (RIT): moving forward. Theranostics. 2021 Apr 15;11(13):6293–314.

177. Cooper MS, Ma MT, Sunassee K, Shaw KP, Williams JD, Paul RL, et al. Comparison of 64Cu-complexing bifunctional chelators for radioimmunoconjugation: labeling efficiency, specific activity and in vitro/in vivo stability. Bioconjug Chem. 2012 May 16;23(5):1029–39.

178. Rondon A, Schmitt S, Briat A, Ty N, Maigne L, Quintana M, et al. Pretargeted radioimmunotherapy and SPECT imaging of peritoneal carcinomatosis using bioorthogonal click chemistry: probe selection and first proof-of-concept. Theranostics. 2019 Sep 19;9(22):6706–18.

179. Bargh JD, Walsh SJ, Isidro-Llobet A, Omarjee S, Carroll JS, Spring DR. Sulfatase-cleavable linkers for antibody-drug conjugates. Chem Sci. 2020 Mar 5;11(9):2375–80.

180. Radiometals for diagnostic imaging and theranostics [Internet]. Open Medscience. 2019 [cited 2022 Apr 14]. Available from: https://openmedscience.com/radiometals-for-diagnostic-imaging-and-theranostics/

181. Larson SM, Carrasquillo JA, Cheung NKV, Press O. Radioimmunotherapy of human tumours. Nat Rev Cancer. 2015 Jun;15(6):347–60.

182. Uenomachi M, Takahashi M, Shimazoe K, Takahashi H, Kamada K, Orita T, et al. Simultaneous in vivo imaging with PET and SPECT tracers using a Compton-PET hybrid camera. Sci Rep. 2021 Sep 9;11(1):17933.

183. Schoffelen R, van der Graaf WTA, Sharkey RM, Franssen GM, McBride WJ, Chang CH, et al. Quantitative immuno-SPECT monitoring of pretargeted radioimmunotherapy with a bispecific antibody in an intraperitoneal nude mouse model of human colon cancer. J Nucl Med Off Publ Soc Nucl Med. 2012 Dec;53(12):1926–32.

184. Bouchelouche K, Tagawa ST, Goldsmith SJ, Turkbey B, Capala J, Choyke P. PET/CT Imaging and Radioimmunotherapy of Prostate Cancer. Semin Nucl Med. 2011 Jan;41(1):29–44.

185. e5605c6d2607f5b521c46cdf7a23082c. Beta particles [Internet]. ARPANSA. ARPANSA; 2017 [cited 2022 Apr 14]. Available from: https://www.arpansa.gov.au/understanding-radiation/what-is-radiation/ionising-radiation/beta-particles

186. Couturier O, Supiot S, Degraef-Mougin M, Faivre-Chauvet A, Carlier T, Chatal JF, et al. Cancer radioimmunotherapy with alpha-emitting nuclides. Eur J Nucl Med Mol Imaging. 2005 May;32(5):601–14.

187. Gudkov SV, Shilyagina NYu, Vodeneev VA, Zvyagin AV. Targeted Radionuclide Therapy of Human Tumors. Int J Mol Sci. 2015 Dec 28;17(1):33.

188. Fisher R, Pusztai L, Swanton C. Cancer heterogeneity: implications for targeted therapeutics. Br J Cancer. 2013 Feb 19;108(3):479–85.

189. Yang Q, Parker CL, McCallen JD, Lai SK. Addressing challenges of heterogeneous tumor treatment through bispecific protein-mediated pretargeted drug delivery. J Control Release Off J Control Release Soc. 2015 Dec 28;220(0 0):715–26.

190. Fleuren EDG, Versleijen-Jonkers YMH, Heskamp S, van Herpen CML, Oyen WJG, van der Graaf WTA, et al. Theranostic applications of antibodies in oncology. Mol Oncol. 2014 Jun;8(4):799–812.

191. Alpha Emitter Radium-223 and Survival in Metastatic Prostate Cancer | NEJM [Internet]. [cited 2022 Apr 15]. Available from: https://www.nejm.org/doi/full/10.1056/nejmoa1213755

192. Horning SJ, Younes A, Jain V, Kroll S, Lucas J, Podoloff D, et al. Efficacy and Safety of Tositumomab and Iodine-131 Tositumomab (Bexxar) in B-Cell Lymphoma, Progressive After Rituximab. J Clin Oncol. 2005 Feb;23(4):712–9.

193. Biogen. A Prospectively Randomized, Phase III, Multicenter, Controlled Trial to Evaluate the Safety and Efficacy of the Zevalin Therapeutic Regimen Plus Rituxan Compared With Rituxan Alone in Patients With Relapsed or Refractory Follicular NHL [Internet]. clinicaltrials.gov; 2006 Sep [cited 2022 Apr 14]. Report No.: NCT00057343. Available from: https://clinicaltrials.gov/ct2/show/NCT00057343

194. PharmD K de F. Risks and Side Effects of Biologics [Internet]. Arthritis-health. [cited 2022 May 11]. Available from: https://www.arthritis-health.com/treatment/medications/risks-and-side-effects-biologics

195. Festa RA, Thiele DJ. Copper: An essential metal in biology. Curr Biol. 2011 Nov 8;21(21):R877–83.

196. Audi G, Bersillon O, Blachot J, Wapstra AH. The Nubase evaluation of nuclear and decay properties. Nucl Phys A. 2003 Dec 22;729(1):3–128.

197. copper | Uses, Properties, & Facts | Britannica [Internet]. [cited 2022 May 12]. Available from: https://www.britannica.com/science/copper

198. Table of Isotopes decay data [Internet]. [cited 2022 May 13]. Available from: http://nucleardata.nuclear.lu.se/toi/nuclide.asp?iZA=290067

199. Goeckermann RH, Perlman I. Characteristics of Bismuth Fission with High Energy Particles. Phys Rev. 1948 May 1;73(9):1127–8.

200. Lancashire R. Inorganic Chemistry Lecture Material [Internet]. The University of the West Indies, Mona, JAMAICA; 2000 [cited 2022 May 18]. Available from: http://wwwchem.uwimona.edu.jm/courses/copper.html

201. PubChem. Copper (I) oxide [Internet]. [cited 2022 May 18]. Available from: https://pubchem.ncbi.nlm.nih.gov/compound/10313194

202. copper - Principal compounds | Britannica [Internet]. [cited 2022 May 18]. Available from: https://www.britannica.com/science/copper/Principal-compounds

203. Kubíček V, Böhmová Z, Ševčíková R, Vaněk J, Lubal P, Poláková Z, et al. NOTA Complexes with Copper(II) and Divalent Metal Ions: Kinetic and Thermodynamic Studies. Inorg Chem. 2018 Mar 19;57(6):3061–72.

204. Husain N, Mahmood R. Copper(II) generates ROS and RNS, impairs antioxidant system and damages membrane and DNA in human blood cells. Environ Sci Pollut Res Int. 2019 Jul;26(20):20654–68.

205. He M, Abro B, Kaushal M, Chen L, Chen T, Gondim M, et al. Tumor mutation burden and checkpoint immunotherapy markers in primary and metastatic synovial sarcoma. Hum Pathol. 2020 Jun;100:15–23.

206. Haldar M, Hancock JD, Coffin CM, Lessnick SL, Capecchi MR. A Conditional Mouse Model of Synovial Sarcoma: Insights into a Myogenic Origin. Cancer Cell. 2007 Apr 10;11(4):375–88.

207. Hanahan D, Weinberg RA. Hallmarks of Cancer: The Next Generation. Cell. 2011 Mar 4;144(5):646–74.

208. Radons J. Inflammatory stress and sarcomagenesis: a vicious interplay. Cell Stress Chaperones. 2014 Jan;19(1):1–13.

209. Stacchiotti S, Van Tine BA. Synovial Sarcoma: Current Concepts and Future Perspectives. J Clin Oncol. 2018 Jan 10;36(2):180–7.

210. Doxorubicin: MedlinePlus Drug Information [Internet]. [cited 2022 Apr 20]. Available from: https://medlineplus.gov/druginfo/meds/a682221.html

211. Radiopharmaceuticals Emerging as New Cancer Therapy - National Cancer Institute [Internet]. 2020 [cited 2022 Apr 5]. Available from: https://www.cancer.gov/news-events/cancer-currents-blog/2020/radiopharmaceuticals-cancer-radiation-therapy

212. Buchmann I, Meyer RG, Mier W, Haberkorn U. Myeloablative radioimmunotherapy in conditioning prior to haematological stem cell transplantation: closing the gap between benefit and toxicity? Eur J Nucl Med Mol Imaging. 2009 Mar 1;36(3):484–98.

213. Lhuillier C, Rudqvist NP, Elemento O, Formenti SC, Demaria S. Radiation therapy and anti-tumor immunity: exposing immunogenic mutations to the immune system. Genome Med. 2019 Jun 20;11(1):40.

214. Gai Y, Sun L, Hui W, Ouyang Q, Anderson CJ, Xiang G, et al. New Bifunctional Chelator p-SCN-PhPr-NE3TA for Copper-64: Synthesis, Peptidomimetic Conjugation, Radiolabeling, and Evaluation for PET Imaging. Inorg Chem. 2016 Jul 18;55(14):6892–901.

215. Soft Tissue Sarcoma: Your Chances of Recovery (Prognosis) [Internet]. Saint Luke's Health System. [cited 2022 May 25]. Available from: http://www.saintlukeskc.org/health-library/soft-tissue-sarcoma-your-chances-recovery-prognosis

216. What is the lifetime or cumulative dose for Adriamycin? [Internet]. Drugs.com. [cited 2022 May 25]. Available from: https://www.drugs.com/medical-answers/lifetime-cumulative-dose-adriamycin-3537856/

217. Nagao K, Ito H, Yoshida H. Chromosomal translocation t(X;18) in human synovial sarcomas analyzed by fluorescence in situ hybridization using paraffin-embedded tissue. Am J Pathol. 1996 Feb;148(2):601–9.

218. Lai JP, Rosenberg AZ, Miettinen MM, Lee CCR. NY-ESO-1 expression in sarcomas. Oncoimmunology. 2012 Nov 1;1(8):1409–10.

219. CTAG1B cancer/testis antigen 1B [Homo sapiens (human)] - Gene - NCBI [Internet]. [cited 2022 Jun 14]. Available from: https://www.ncbi.nlm.nih.gov/gene/1485

220. Vasquez KO, Peterson JD. Early Detection of Acute Drug-Induced Liver Injury in Mice by Noninvasive Near-Infrared Fluorescence Imaging. J Pharmacol Exp Ther. 2017 Apr;361(1):87–98.

221. Zhao L, Zhang B. Doxorubicin induces cardiotoxicity through upregulation of death receptors mediated apoptosis in cardiomyocytes. Sci Rep. 2017 Mar 16;7(1):44735.

222. Detectnet (Copper Cu 64 dotatate Injection, for Intravenous Use): Uses, Dosage, Side Effects, Interactions, Warning [Internet]. RxList. [cited 2022 Jun 14]. Available from: https://www.rxlist.com/detectnet-drug.htm

223. Indium 111 Oxyquinoline | Memorial Sloan Kettering Cancer Center [Internet]. [cited 2022 Jun 14]. Available from: https://www.mskcc.org/cancer-care/patient-education/indium-111-oxyquinoline

224. Commissioner O of the. FDA approves new diagnostic imaging agent to detect rare neuroendocrine tumors [Internet]. FDA. FDA; 2020 [cited 2022 Jun 14]. Available from: https://www.fda.gov/news-events/press-announcements/fda-approves-new-diagnostic-imaging-agent-detect-rare-neuroendocrine-tumors

225. Axup JY, Bajjuri KM, Ritland M, Hutchins BM, Kim CH, Kazane SA, et al. Synthesis of site-specific antibody-drug conjugates using unnatural amino acids. Proc Natl Acad Sci. 2012 Oct 2;109(40):16101–6.